AD_____

Award Number: DAMD17-99-1-9481

TITLE: Protein Kinase Pathways that Regulate Neuronal Survival and Death

PRINCIPAL INVESTIGATOR: Kim A. Heidenreich, Ph.D.

CONTRACTING ORGANIZATION: University of Colorado Health Sciences Center
Denver, Colorado 80291-0238

REPORT DATE: August 2001

TYPE OF REPORT: Annual

PREPARED FOR: U.S. Army Medical Research and Materiel Command
Fort Detrick, Maryland 21702-5012

REPORT DOCUMENTATION PAGE

Form Approved
OMB No. 074-0188

1. AGENCY USE ONLY (Leave blank)	2. REPORT DATE	3. REPORT TYPE AND DATES COVERED
	August 2001	Annual (1 Aug 00 - 31 Jul 01)

4. TITLE AND SUBTITLE
Protein Kinase Pathways that Regulate Neuronal Survival and Death

5. FUNDING NUMBERS
DAMD17-99-1-9481

6. AUTHOR(S)
Kim A. Heidenreich, Ph.D.

7. PERFORMING ORGANIZATION NAME(S) AND ADDRESS(ES)
University of Colorado Health Sciences Center
Denver, Colorado 80291-0238

E-Mail: **Kim.heidenreich@uchsc.edu**

8. PERFORMING ORGANIZATION REPORT NUMBER

9. SPONSORING / MONITORING AGENCY NAME(S) AND ADDRESS(ES)
U.S. Army Medical Research and Materiel Command
Fort Detrick, Maryland 21702-5012

10. SPONSORING / MONITORING AGENCY REPORT NUMBER

11. SUPPLEMENTARY NOTES

20020124 210

12a. DISTRIBUTION / AVAILABILITY STATEMENT
Approved for Public Release; Distribution Unlimited

12b. DISTRIBUTION CODE

13. Abstract ***(Maximum 200 Words)*** *(abstract should contain no proprietary or confidential information)*
Loss of post-mitotic neurons from the adult brain underlies the pathology of neurodegenerative diseases and neurotoxin exposure. Neuronal cell death occurs by two mechanisms: necrosis and apoptosis. Apoptosis is a process whereby developmental cues and environmental stimuli activate a genetic program to implement a series of steps that culminate in cell death. An important aspect of apoptosis is that it can be halted and such interventions may rescue dying neurons. The overall goal of this project is to identify key protein kinases that regulate neuronal survival and apoptosis. The aims, as described in the Statement of Work, are to: 1) Define key protein kinase cascades regulated by neurotrophic factors, 2) Modulate the protein kinase cascades regulated by neurotrophic factors and determine the consequence on neuronal survival and death, and 3) Examine the cross-talk between pro-apoptotic and anti-apoptotic protein kinase pathways. Our key research accomplishments over the last year lie in several areas. One is identifying transcription factors downstream of the protein kinases that regulate neuronal survival and death. The second area is defining the role of Rho/Rac GTPases in regulating neuronal cell death. The third area is understanding how various pathways known to regulate neuronal apoptosis operate together to direct the fate of neurons. The progress made in these areas has resulted in 4 manuscripts (1 article under revision) and 8 abstracts presented at national and international meetings this past year.

14. SUBJECT TERMS	15. NUMBER OF PAGES
Neurodegeneration, apoptosis, neurons, p38 MAP kinase, JNK, MEF2D, FKHD	50
	16. PRICE CODE

17. SECURITY CLASSIFICATION OF REPORT	18. SECURITY CLASSIFICATION OF THIS PAGE	19. SECURITY CLASSIFICATION OF ABSTRACT	20. LIMITATION OF ABSTRACT
Unclassified	Unclassified	Unclassified	Unlimited

Table of Contents

Cover..... 1

SF 298..... 2

Table of Contents..... 3

Introduction..... 4

Body..... 4-6

Key Research Accomplishments..... 6

Reportable Outcomes..... 7,8

Conclusions..... 8

References.....

Appendices..... 9

INTRODUCTION

Loss of post-mitotic neurons from the adult brain underlies the pathology of neurodegenerative diseases and neurotoxin exposure. Neuronal cell death occurs by two mechanisms: necrosis and apoptosis. Apoptosis is a process whereby developmental cues and environmental stimuli activate a genetic program to implement a series of steps that culminate in cell death. An important aspect of apoptosis is that it can be halted and such interventions may rescue dying neurons. The overall goal of this project is to identify key protein kinases involved in regulating neuronal survival and apoptosis. The aims for the this year of funding as described in the Statement of Work were to: 1) Continue studies on protein kinase cascades that regulate neuronal survival, 2) Modulate the protein kinase cascades regulated by neurotrophic factors and determine the consequence on neuronal survival and death, and 3) Begin studies examining the cross-talk in pro-apoptotic and anti-apoptotic protein kinase signaling cascades. The progress made in these areas, described below, has resulted in 4 published manuscripts (plus 1 article under revision) and 8 abstracts presented at national and international scientific meetings.

Task #1. The first task is to identify protein kinase cascades that regulate neuronal survival.

As described in our progress report last year, we have identified a number of protein kinase cascades that either inhibit or initiate neuronal apoptosis. This year we have extended those previous studies by identifying a transcription factor downstream of a calcium-regulated protein kinase/phosphatase pathway that controls neuronal survival. The results of these studies have been published in the Journal of Neuroscience this year and are described in the attached **Appendix #1**.

We have also examined the role of upstream Rho/Rac GTPases in neuronal survival. We have shown that inhibition of Rac/Cdc42 function induces apoptosis of cerebellar granule neurons via a c-jun signaling pathway. These results were published in the Journal of Biological Chemistry and are described in **Appendix #2**.

Task #2 The second task is to determine whether activation or inhibition of the neurotrophin- regulated kinases is necessary or sufficient to influence neuronal survival.

Over the last year we finished up work demonstrating that inhibitors of p38 MAP kinase, a protein kinase activated when neurons die by apoptosis, increase the survival of transplanted dopamine neurons. Fetal cell transplantation therapies are being developed for the treatment of a

number of neurodegenerative disorders including Parkinson's disease. Massive apoptotic cell death is a major limiting factor for the success of neurotransplantation. We showed that inhibitors of stress-activated protein kinases improve the outcome of cell transplantation by preventing apoptosis of neurons after grafting. These inhibitors offer advantages over other approaches to block neuronal apoptosis because they are small organic molecules that are orally active and cross the blood-brain barrier. These results were published in Brain Research this year (**Appendix#3**).

In collaboration with Dr. Curt Freed, we completed studies on the effects of growth factors on survival of human dopamine neurons transplanted into Parkinsonian rats. We showed that *in vitro* preincubation of human fetal tissue strands with IGF-I and bFGF improves dopamine cell survival and the behavioral outcome of transplants. These results were published in Experimental Neurology and are described in more detail in **Appendix #4**.

Task #3 The third task is to determine whether there is cross-talk between pro-apoptotic and anti-apoptotic signaling pathways.

We have recently discovered that convergence of glycogen synthase kinase-3β and c-jun pro-apoptotic signals appear to be required upstream of myocyte enhancer factor 2D degradation during neuronal apoptosis. Cerebellar granule neurons undergo apoptosis when deprived of serum and depolarizing K^+. The pro-survival transcription factor, myocyte enhancer factor 2D (MEF2D), is rapidly hyperphosphorylated and cleaved by caspases in apoptotic cerebellar granule neurons. MEF2D degradation occurs prior to activation of the executioner caspase-3, and therefore, may play a critical role in the commitment of cerebellar granule neurons to apoptosis. We also know that the pro-apoptotic proteins, GSK-3 β and c-Jun turn on apoptosis in granule neurons, however, the precise targets of their action are currently unknown. Over the last year, we investigated whether either GSK-3β or c-Jun facilitate MEF2D processing during apoptosis. We utilized the neurotrophin, insulin-like growth factor-I (IGF-I), to selectively inhibit GSK-3β activation, and the p38/JNK inhibitor, SB203580, to selectively block c-Jun induction. Neither IGF-I nor SB203580 had any significant effect on MEF2D hyperphosphorylation, the decreased DNA binding of MEF2 proteins, or the initial loss of MEF2-dependent transcriptional activity observed in trophic factor-deprived CGNs. However, incubation with either IGF-I or SB203580 significantly blocked degradation of MEF2D and the corresponding formation of a NH_2-terminal truncated MEF2 fragment that has previously been shown to act as a dominant-negative transcription factor. Moreover, inclusion of either IGF-I or

SB203580 during acute trophic factor withdrawal significantly enhanced recovery of MEF2-dependent transcriptional activity in cerebellar granule neurons following the re-addition of depolarizing K^+. The results demonstrate that GSK-3β and c-Jun are both required upstream of MEF2D degradation, suggesting that these pro-apoptotic molecules act in a coordinated manner very early in the apoptotic cascade. This work will be presented at the Society for Neuroscience meetings in November 2001 (**Appendix #5**).

Another area that we've made progress in is understanding how neurotrophin signaling pathways impact on the intrinsic death machinery in neurons. Over the last year, we identified the intrinsic (mitochondrial) death pathway as a principal target of IGF-I action. In cerebellar granule neurons undergoing apoptosis, IGF-I blocked activation of both the executioner caspase-3 and the mitochondrial-dependent initiator caspase-9. Upstream of caspase-9, IGF-I inhibited redistribution of cytochrome C from mitochondria to focal complexes localized in neuronal processes. IGF-I had no effect on mitochondrial swelling or mitochondrial membrane depolarization, but significantly attenuated induction of the pro-apoptotic Bcl-2 family member Bim. Although the transcription factor c-Jun has previously been shown to regulate Bim, IGF-I failed to block c-Jun phosphorylation in trophic factor-deprived granule neurons. In contrast, IGF-I significantly inhibited dephosphorylation and nuclear localization of the forkhead transcription factor (FKHR), suggesting a role for FKHR in the regulation of Bim expression. Moreover, Bim induction, cytochrome C release and caspase activation were blocked by cycloheximide, indicating that *de novo* synthesis of Bim is required for apoptosis. Thus, IGF-I rescues cerebellar granule neurons from apoptosis by blocking intrinsic death signaling at the level of FKHR regulation of Bim. A manuscript describing thes results in under preparation.

KEY RESEARCH ACCOMPLISHMENTS

Our key research accomplishments over the last year lie in several areas. One is defining transcription factors downstream of identified protein kinases that regulate neuronal survival and death. We have also opened up a relatively new area of investigation examining the role of Rho/Rac GTPases (upstream of protein kinases)in regulating neuronal cell death. The third area is understanding how various pathways known to regulate neuronal apoptosis operate together to direct the fate of neurons.

REPORTABLE OUTCOMES

Manuscripts (2001)

1. Zawada WM, MK Meintzer, C Sable, CR Freed, and **KA Heidenreich**. Inhibitors of p38 MAP kinase increase the survival of transplanted dopamine neurons. Brain Res. 891:185-196, 2001.

2. Clarkson, ED, WM Zawada, KP Bell, JE Esplen, PK Choi, **KA Heidenreich**, and CR Freed. IGF-I and bFGF improve dopamine neuron survival and behavioral outcome in parkinsonian rats receiving cultured human feat tissue strands. Exp. Neurology 168:183-191, 2001

3. Linseman DA, **KA Heidenreich**, and SK Fisher. Fyn tyrosine kinase links muscarinic receptor stimulation to phosphorylation of the CdC42 effector ACK-1. J. Biol. Chem. 276: 5622-5628, 2001.

4. Li M, , DA Linseman, MP Allen, MK Meintzer, X Wang, T Laessig, ME Wierman, and **KA Heidenreich**. MEFA and MEF2D undergo phosphorylation and caspase-mediated degradation during apoptosis of cultured rat cerebellar granule neurons. J. Neuroscience 21 (17): 6544-6552, 2001.

5. Linseman DA, TA Laessig, M McClure, MK Meintzer, H Barth, K Aktories, and **KA Heidenreich.** Inhibition of Rac/Cdc42 function induces apoptosis of cerebellar granule neurons via a c-jun signaling pathway. J. Biol. Chem. 276: ____-___, 2001.

6. Allen, MP, DA Linseman, H Udo, M Xu, B Varnum, ER Kandel, **KA Heidenreich**, and ME Wierman. A novel mechanism for GnRH neuron migration involving Gas6/Ark signaling to p39 MAP kinase. (under revision, Mol. Cell. Biol.).

7. Linseman, DA, ML McClure, RJ Bouchard, TA Laessig, D Brenner, and **KA Heidenreich**. Suppression of death receptor signaling in cerebellar Purkinje neurons protects neighboring granule neurons form apoptosis. (submitted, Cell Death and Differentiation).

Abstracts (2001)

1. Linseman, DA, M Li, MK Meintzer, T Laessig, and **KA Heidenreich**. IGF-I suppresses caspase activation and degradation of myocyte-enhancer factor-2D (MEF2-D) during apoptosis of cerebellar granule neurons. Endocrine Society 2001.

2. Allen, MP, DA Linseman, M Xu, **KA Heidenreich**, and ME Wierman. Cytoskeletal remodeling and migration of immortalized GnRH neurons is mediated by an adhesion related kinase (ARK)>RAC>p38 MAPK signaling pathway. Endocrine Society 2001.

3. Linseman, DA, T Laessig, MK Meintzer, M McClure, H, Barth, K Aktories, **KA Heidenreich.** Rac/Cdc42 function is required for cerebellar granule neuron survival. Gordon Conference, Oxford, UK, 2001

4. Allen, MP, DA Linseman, M Xu, **KA Heidenreich**, and ME Wierman. PI-3 kinase couples the adhesion related kinase (Ark) receptor to a Rac/p38 dependent migratory pathway in GnRH neurons. Society for Neuroscience, 2001.

5. Ahmadi, F, S Doolin, NR Zahniser, MP Grogan, **KA Heidenreich**, and WM Zawada. HNT-neurons are resistant to serum withdrawal and MPP+. Society for Neuroscience, 2001.

6. Linseman, DA, M Li, MK Meintzer, T Laessig, **KA Heidenreich**. Convergence of GSK-3 beta and c-jun signaling during apoptosis of cerebellar granule neurons. Society for Neuroscience, 2001.

7. ML McClure, Linseman, DA, RJ Bouchard, TA Laessig, D Brenner, and **KA Heidenreich**. Suppression of death receptor signaling in cerebellar Purkinje neurons protects neighboring granule neurons form apoptosis. Society for Neuroscience, 2001.

8. ML McClure, Linseman, DA, RJ Bouchard, TA Laessig, D Brenner, and **KA Heidenreich**. Suppression of death receptor signaling in cerebellar Purkinje neurons protects neighboring granule neurons form apoptosis. UCHSC Student Research Forum, October 12, 2001.

Invited talks and national committees

2001 Organizing committee for the 8th International Meeting on Neural Transplantation and Repair
2001 Department of Defense Sponsored Parkinson's Related Research, panel discussion
2001 Chairperson, Plenary Symposium on AKT and MAPK, The Endocrine Society
2001 VA Merit Review, Neurobiology D study section
2001 Ad hoc grant reviewer, Virginia Center on Aging

PATENT: Use of protein kinase inhibitors to treat neurodegenerative diseases **#09/469,980.** Issued 09/01.

CONCLUSIONS

The scope of research over the last year has been to extend our studies outlined in Task#1 and Task#2 of our research proposal. Towards this goal, we have identified a number protein kinase cascades and some of the downstream effectors that regulate neuronal survival. The discovery that the MEF2 transcription fators regulate neuronal survival is important for identifying genes that promote neuronal survival. Experiments are planned to continue studying the regulation of MEF2s in neurons and identify the genes that are transcriptionally modified by this family of transcription factors. We have been able to translate some of findings from our *in vitro* studies to more clinically relevant research. We have shown that treatment of dopamine neurons with either growth factors or inhibitors of p38 MAP kinase increases the survival of transplanted dopamine neurons. Although other laboratories have shown that inhibitors of apoptosis (i.e.

peptide caspase inhibitors) improve transplantation, the practicality of using peptide inhibitors clinically is hampered by their poor entry into brain. The advantages that the p38 MAP kinase inhibitors (pyridinyl compounds) have over growth factors and caspase inhibitors for preventing apoptosis include their small size, organic nature, and ability to cross the blood-brain barrier. Finally, we have begun studies examining how different pro-apoptotic and anti-apoptotic pathways interact with each other (Task#3). These studies are important for the identification of good cellular targets for therapeutic intervention.

REFERENCES none

APPENDICES: 4 MANUSCRIPTS attached

1 ABSTRACTS attached

The Journal of Neuroscience, September 1, 2001, 21(17):6544–6552

Myocyte Enhancer Factor 2A and 2D Undergo Phosphorylation and Caspase-Mediated Degradation during Apoptosis of Rat Cerebellar Granule Neurons

Mingtao Li,[1] Daniel A. Linseman,[1] Melissa P. Allen,[2] Mary Kay Meintzer,[1] Xiaomin Wang,[1] Tracey Laessig,[1] Margaret E. Wierman,[2] and Kim A. Heidenreich[1]

Departments of [1]Pharmacology and [2]Medicine, University of Colorado Health Sciences Center and the Denver Veterans Affairs Medical Center, Denver, Colorado 80262

Myocyte enhancer factor 2 (MEF2) proteins are important regulators of gene expression during the development of skeletal, cardiac, and smooth muscle. MEF2 proteins are also present in brain and recently have been implicated in neuronal survival and differentiation. In this study we examined the cellular mechanisms regulating the activity of MEF2s during apoptosis of cultured cerebellar granule neurons, an established *in vitro* model for studying depolarization-dependent neuronal survival. All four MEF2 isoforms (A, B, C, and D) were detected by immunoblot analysis in cerebellar granule neurons. Endogenous MEF2A and MEF2D, but not MEF2B or MEF2C, were phosphorylated with the induction of apoptosis. The putative sites that were phosphorylated during apoptosis are functionally distinct from those previously reported to enhance MEF2 transcription. The increased phosphorylation of MEF2A and MEF2D was followed by decreased DNA binding, reduced transcriptional activity, and caspase-dependent cleavage to fragments containing N-terminal DNA binding domains and C-terminal transactivation domains. Expression of the highly homologous N terminus of MEF2A (1–131 amino acids) antagonized the transcriptional activity and prosurvival effects of a constitutively active mutant of MEF2D (MEF2D-VP16). We conclude that MEF2A and MEF2D are prosurvival factors with high transcriptional activity in postmitotic cerebellar granule neurons. When these neurons are induced to undergo apoptosis by lowering extracellular potassium, MEF2A and MEF2D are phosphorylated, followed by decreased DNA binding and cleavage by a caspase-sensitive pathway to N-terminal fragments lacking the transactivation domains. The degradation of MEF2D and MEF2A and the generation of MEF2 fragments that have the potential to act as dominant-inactive transcription factors lead to apoptotic cell death.

Key words: MEF2; neurons; apoptosis; transcription; caspase; cerebellum

Myocyte enhancer factor 2 (MEF2) transcription factors are members of the MADS (MCM1-agamous-deficiens-serum response factor) family of transcription factors (Yu et al., 1992; Naya and Olson, 1999). A hallmark of MADS-box proteins is their combinational association with other MADS domain factors, as well as other heterologous classes of transcriptional regulators (Shore and Sharrocks, 1995). Mammalian MEF2 proteins are encoded by four genes (MEF2A, MEF2B, MEF2C, and MEF2D), each of which gives rise to alternatively spliced transcripts (Yu et al., 1992; Leifer et al., 1993; Martin et al., 1994). The MEF2 family of genes is highly expressed in cells of muscle lineage, where they have been shown to be important regulators of gene expression during the development of skeletal, cardiac, and smooth muscle (McDermott et al., 1993; Martin et al., 1994; Molkentin et al., 1996). In these tissues the MEF2 proteins interact with myogenic basic helix–loop–helix transcription factors such as MyoD to activate myogenesis (Molkentin and Olson, 1996; Ornatsky et al., 1997).

Received Feb. 9, 2001; revised June 15, 2001; accepted June 21, 2001.

This research was supported by United States Army Medical Research and Materiel Command Grant DAMD17-99-1-9481, by National Institutes of Health Grant NS38619-01A1, and by a Veterans Affairs Merit Award and Research Enhancement Award Program Award to KA.H.

M.L. and D.A.L. contributed equally to this manuscript.

Correspondence should be addressed to Dr. Kim A. Heidenreich, Denver Veterans Affairs Medical Center-111H, 1055 Clermont Street, Denver, CO 80220. E-mail: kim.heidenreich@uchsc.edu.

All MEF2 family members also are highly expressed in neurons of the CNS (Leifer et al., 1993, 1994; McDermott et al., 1993; Ikeshima et al., 1995; Lyons et al., 1995; Mao et al., 1999). Recent *in vitro* findings support the hypothesis that MEF2 transcription factors regulate neuronal survival and development. In cultures of cerebral cortical neurons in which proliferating precursor cells and postmitotic differentiating neurons can be distinguished, MEF2C is expressed selectively in newly generated postmitotic neurons and is not detectable in BrdU-positive precursor cells (Mao et al., 1999). Transfection of postmitotic cortical neurons with different MEF2C mutants demonstrated that MEF2C is required for the survival of these neurons. In postnatal day 19 (P19) neuronal precursor cells, the expression of MEF2 induces a mixed neuronal/myogenic phenotype (Okamoto et al., 2000). During retinoic acid-induced neurogenesis of these cells, a dominant-negative form of MEF2C enhances apoptosis but does not affect cell division. On the other hand, P19 cells induced to undergo apoptosis can be rescued from cell death by the expression of constitutively active MEF2C. In addition, overexpression of MEF2C in P19 cells results in induction of neurofilament protein, the nuclear antigen NeuN, and MASH-1, a neural-specific transcription factor known to interact with MEF2s (Skerjanc and Wilton, 2000). These data suggest that MEF2 proteins regulate neuronal development by promoting survival and inducing differentiation.

In the present study we examined the mechanisms regulating the activity of MEF2 proteins during apoptosis of cultured rat

cerebellar granule neurons, a well established model of depolarization-dependent neuronal survival. We provide evidence that MEF2A and MEF2D are prosurvival factors with high DNA binding and transcriptional activity in postmitotic cerebellar granule neurons. When these neurons are induced to undergo apoptosis by lowering extracellular potassium, MEF2A and MEF2D are phosphorylated. The phosphorylation of MEF2D and MEF2A is followed by decreased DNA binding and cleavage by a caspase-sensitive pathway to N-terminal MEF2 fragments that lack the transactivation domain. The decreased DNA binding of MEF2s and the formation of MEF2 fragments that can act as dominant-inactive transcription factors are sufficient to block the prosurvival effects of MEF2s and induce apoptosis in mature cerebellar granule neurons.

MATERIALS AND METHODS

Materials. The MEF2A antibody is an affinity-purified rabbit polyclonal antibody that was raised to a peptide corresponding to codons 487–507 of human MEF2A purchased from Santa Cruz Biotechnology (Santa Cruz, CA). According to the manufacturer, this antibody may cross-react to a small extent with MEF2C. The affinity-purified rabbit polyclonal MEF2C antibody, a gift from John Schwarz (University of Texas Medical School, Houston, TX), was raised against an isoform-specific peptide representing codons 300–316 of human MEF2C and is specific for MEF2C (Firulli et al., 1996). The rabbit polyclonal antibody to MEF2B was raised against a polyhistidine fusion protein corresponding to codons 234–365 of human MEF2B and was kindly provided by Dr. Ron Prywes (Columbia University, NY). Antibody to MEF2D is a monoclonal antibody raised against a peptide corresponding to codons 346–511 of mouse MEF2D purchased from Transduction Laboratories (Lexington, KY). The dominant-inactive MEF2 mutant pcDNA3-MEF2A131 was kindly provided by Dr. Prywes. The dominant-active MEF2 mutant pCMV-MEF2D-VP16 was a gift from Dr. John C. McDermott (York University, Toronto, Ontario, Canada). The pGL2-MEF2-Luc reporter plasmid (Lemercier et al., 2000) was provided by Dr. Saadi Khochbin (INSERM, France). The caspase-3 antibody was purchased from Santa Cruz Biotechnology, and the polyclonal anti-β-galactosidase (β-gal) antibody was purchased from 5 Prime→3 Prime (Boulder, CO). Cy3-conjugated goat antibody to rabbit IgG was purchased from Chemicon (Temecula, CA). The caspase inhibitors YVAD-CHO, DEVD-FMK, and ZVAD-FMK were obtained from Calbiochem (La Jolla, CA). [α-^{32}P]CTP (3000 Ci/mmol) was purchased from Amersham Pharmacia Biotechnology (Piscataway, NJ).

Neuronal cell culture. Rat cerebellar granule neurons were prepared from 7- to 8-d-old Sprague Dawley rat pups (15–19 gm) as described previously (Li et al., 2000). Briefly, neurons were seeded at a density of 2.0×10^6 cells/ml in basal modified Eagle's (BME) medium containing 10% fetal bovine serum, 25 mM KCl, 2 mM glutamine, and penicillin (100 U/ml)/streptomycin (100 μg/ml). Cytosine arabinoside (10 μM) was added to the culture medium 24 hr after plating to limit the growth of non-neuronal cells. With the use of this protocol, 95–99% of the cultured cells were granule neurons. Transfections were performed at day 5–6 in culture, and experiments were performed after 7 d in culture. Apoptosis was induced by removing the serum and reducing the extracellular potassium concentration from 25 to 5 mM. Control cultures were treated identically but were maintained in serum-free medium supplemented with 25 mM KCl.

Western blot analysis. Western blot analysis was performed as described previously (Li et al., 2000). Briefly, neurons were lysed by adding SDS sample buffer [62.5 mM Tris-HCl, pH 6.8, 2% (w/v) SDS, 10% glycerol, 50 mM DTT, and 0.1% (w/v) bromphenol blue]. The samples were resolved by SDS-PAGE with the use of either 7.5 or 12% acrylamide gels, as indicated in the legends. Proteins were transferred to Hybond-P membranes (polyvinylidene difluoride). The membranes were incubated with anti-MEF2A (1:5000), anti-MEF2D (1:1000), anti-MEF2C (1:1000), and anti-MEF2B (1:500). After incubation with the primary antibodies the filters were washed and then incubated with the respective horseradish peroxidase (HRP)-conjugated anti-rabbit or anti-mouse antibody (Amersham Pharmacia Biotech). Then the blots were washed and subsequently were developed with an enhanced chemiluminescence system (Amersham Pharmacia Biotech) and exposed to Kodak autoradiographic film. Quantitation was performed with the Bio-Rad Quantity One software (Hercules, CA).

Preparation of nuclear extracts from cerebellar granule neurons. After 7 d in culture the cerebellar granule neurons were rinsed two times in serum-free BME containing 25 mM KCl and then maintained in 25 or 5 mM KCl medium in the absence or presence of caspase inhibitors. Neurons that did not receive inhibitors received the control vehicle dimethyl sulfoxide (DMSO). After the indicated times the neurons (100 mm dishes) were washed with ice-cold PBS and detached from culture dishes by a cell scraper in 0.5 ml of buffer A [0.25 M sucrose and (in mM) 15 Tris, pH 7.9, 60 KCl, 2 EDTA, pH 8.0, 0.5 EGTA, 15 NaCl, 1.0 Na_3VO_4, 50 NaF, 0.5 spermidine, 1 DTT, 1 benzamidine, and 0.5 PMSF plus 20 μg/ml leupeptin, 0.76 μg/ml pepstatin, and 2 μM aprotinin]. The cells were centrifuged at 250 × *g* for 5 min. The pellets were washed twice in buffer A and then homogenized with 15 strokes of a tight-fitting Dounce homogenizer to release the nuclei. Then the homogenate was centrifuged at 14,000 × *g* for 15 sec to pellet the nuclei. The supernatants were removed, and the pellets were resuspended in buffer C [(in mM) 20 HEPES, pH 7.9, 500 KCl, 1.5 $MgCl_2$, 1 EDTA, pH 8.0, 1.0 Na_3VO_4, 50 NaF, 1.0 DTT, 1 benzamidine, and 0.5 PMSF plus 20 μg/ml leupeptin, 0.76 μg/ml pepstatin, 25% glycerol, and 10 μM aprotinin]. Nuclear proteins were extracted at 4°C for 45 min, and insoluble nuclei were precipitated by centrifugation at 14000 × *g* for 15 min. Supernatants were dialyzed against a buffer containing 10% glycerol and (in mM) 10 Tris, pH 7.9, 5 $MgCl_2$, 50 KCl, 1 EDTA, pH 8.0, 1.0 Na_3VO_4, 50 NaF, 1 DTT, 1 PMSF, and 1 benzamidine for 3 hr at 4°C. The extracts were quantified for protein content by the BCA method (Pierce, Rockford, IL) and frozen in small aliquots at −70°C.

Electrophoretic mobility shift assays. Nuclear extracts from cerebellar granule neurons (10 μg) were incubated with double-stranded oligonucleotides corresponding to the muscle creatine kinase MEF2 site 5′-CGGATCGCTCTAAA*A*ATAACCCTGTCG-3′ (Amacher et al., 1993) or to a mutant oligonucleotide containing C→G and A→C substitutions at the two italicized residues. The oligomers were end-labeled with the Klenow fragment of DNA polymerase I (Life Technologies, Gaithersburg, MD) and [α-^{32}P]CTP to a specific activity of 10,000–30,000 cpm/ng. Binding reactions were performed for 20 min at 4°C in 1 mM dithiothreitol, 2.5 mM $MgCl_2$, 10% glycerol, 0.1 mg/ml bovine serum albumin, 30 ng/μl of poly(dI-dC), 20 mM HEPES, pH 7.9, and 50–100,000 cpm of oligomer in a total volume of 20 μl. For the supershift analysis, 1 μl of specific antisera or preimmune serum was added to the nuclear extracts for 20 min at 4°C, followed by another 20 min in the presence of labeled oligomers. The protein–DNA complexes were analyzed on 5% nondenaturing polyacrylamide gels containing 3% glycerol and 0.25× TBE (90 M Tris borate, 1 mM EDTA) in the cold room. After electrophoresis the gels were dried and exposed to film at −70°C.

Transfection assays and reporter gene expression. Cerebellar granule neurons were transfected by a calcium phosphate coprecipitation method described previously (Li et al., 2000). Neurons were transfected with 1 μg of MEF2-luciferase expression plasmids (pGL2-MEF2-luc) and/or 1–3 μg of MEF2D expression plasmids (pCMV-MEF2D-VP16, pcDNA3-MEF2A131) and 1 μg of pCMV-β-gal as an internal control for transfection efficiency. The total amount of DNA for each transfection was kept constant (7 μg/ml) by using the empty vector pcDNA3. Neurons were kept in conditioned medium after transfection for 2 hr; then the medium was replaced with BME containing 25 or 5 mM KCl. After 4 hr the cell extracts were prepared with reporter lysis buffer (Promega, Madison, WI), and the activities of luciferase and β-galactosidase were measured with the Luciferase Assay System (Promega) and the β-galactosidase Enzyme Assay System (Promega), respectively.

Quantitation of apoptosis in transfected neurons. Neurons were transfected as described previously (Li et al., 2000). Plasmids (pCMV-MEF2D-VP16, pCMV-MEF2D-VP16 plus pcDNA3-MEF2A131, and pCMV-LacZ) were added to the transfection media at a final concentration of 4–5 μg/ml. The total amount of DNA for each transfection was kept constant by using the empty vector pcDNA3. After transfection the neurons were switched to a medium containing 25 or 5 mM KCl. Then 16 hr later the cells were immunostained with a polyclonal antibody to β-galactosidase (1:500 dilution), followed by a Cy3-conjugated goat antibody to rabbit IgG (1:500) to identify cells expressing β-galactosidase. To visualize the nuclei of transfected neurons, we included the DNA dye Hoechst 33258 (5.0 μg/ml) in the wash after the secondary antibody incubation. Apoptosis was quantified by scoring the percentage of cells in the β-galactosidase-expressing cell population with condensed or fragmented nuclei. So that we could obtain unbiased counting, cells (~500)

were scored blindly without knowledge of their previous treatment. Experiments were performed in triplicate.

RESULTS

MEF2 protein expression and phosphorylation state in control and apoptotic cerebellar granule neurons

Primary cerebellar granule neurons represent a widely used *in vitro* model system that mimics the trophic action of neuronal activity that is seen in the developing nervous system (D'Mello et al., 1993; Miller et al., 1997). Thus, elevated levels of extracellular potassium promote neuronal survival by opening L-type voltage-sensitive calcium channels, leading to an influx of calcium into neurons. Lowering of extracellular potassium decreases calcium influx and promotes neuronal cell death by an apoptotic mechanism.

Western analysis indicated that all four members of the MEF2 superfamily of transcription factors were present in cerebellar granule cells (Fig. 1*A*). When neurons were induced to undergo apoptosis by lowering extracellular potassium, there were selective shifts in the mobility of MEF2A (Fig. 1*A*, *top*) and MEF2D (Fig. 1*A*, *bottom*) on SDS gels. The mobility shifts were detected in neuronal cell lysates as early as 30 min and sustained to 8 hr. The shifts in mobility of MEF2A and MEF2D were enhanced when the samples were electrophoresed for longer times through higher resolution gels (Fig. 1*B*). Treatment of neuronal protein extracts with calf intestinal alkaline phosphatase before electrophoresis reversed the mobility shift of MEF2A and MEF2D seen in the low potassium conditions, confirming that the shifts in mobility of MEF2A and MEF2D were attributable to enhanced serine/threonine phosphorylation (Fig. 1*C*). The phosphorylation sites responsible for the increase in phosphorylation seen on lowering intracellular calcium are functionally different from those previously reported to enhance transcription. Both a p38 inhibitor (10 μM SB203580) and a MEK inhibitor (10 μM PD98059) failed to block the increase in phosphorylation seen with the induction of apoptosis (data not shown). The relative intensities of the slower-migrating MEF2A and MEF2D proteins decreased after 4 and 8 hr in low potassium medium (Fig. 1*A*, *lanes 6, 8*), whereas the faster-migrating MEF2 proteins observed under depolarizing conditions remained constant, suggesting a link between MEF2 phosphorylation and degradation.

MEF2D transcriptional activity is regulated by extracellular potassium

The transcriptional activity of MEF2 proteins in cerebellar granule neurons was measured with a luciferase reporter plasmid that contains two MEF2 consensus sites, followed by the luciferase reporter gene (Lemercier et al., 2000). Cerebellar granule neurons grown in the presence of depolarizing potassium (25 mM) demonstrated high endogenous MEF2-driven luciferase activity (Fig. 2*A*). After the potassium was lowered to 5 mM for 4–8 hr, the transcriptional activity of the MEF2 reporter was decreased by ~90% ($p < 0.05$) (Figure 2*A*). Incubation in 5 mM potassium for 4 hr, followed by the readdition of 25 mM potassium for an additional 4 hr, restored ~50% of the MEF2 transcriptional activity (Fig. 2*A*). Similarly, the readdition of 25 mM potassium also reversed the mobility shift in MEF2D (Fig. 2*B*), suggesting that phosphorylation of MEF2D during apoptosis is associated with the observed decrease in MEF2 transcriptional activity. The fact that only a partial recovery of MEF2-driven luciferase activity was observed in the above experiment could be accounted for by the significant degradation of MEF2D that had occurred after

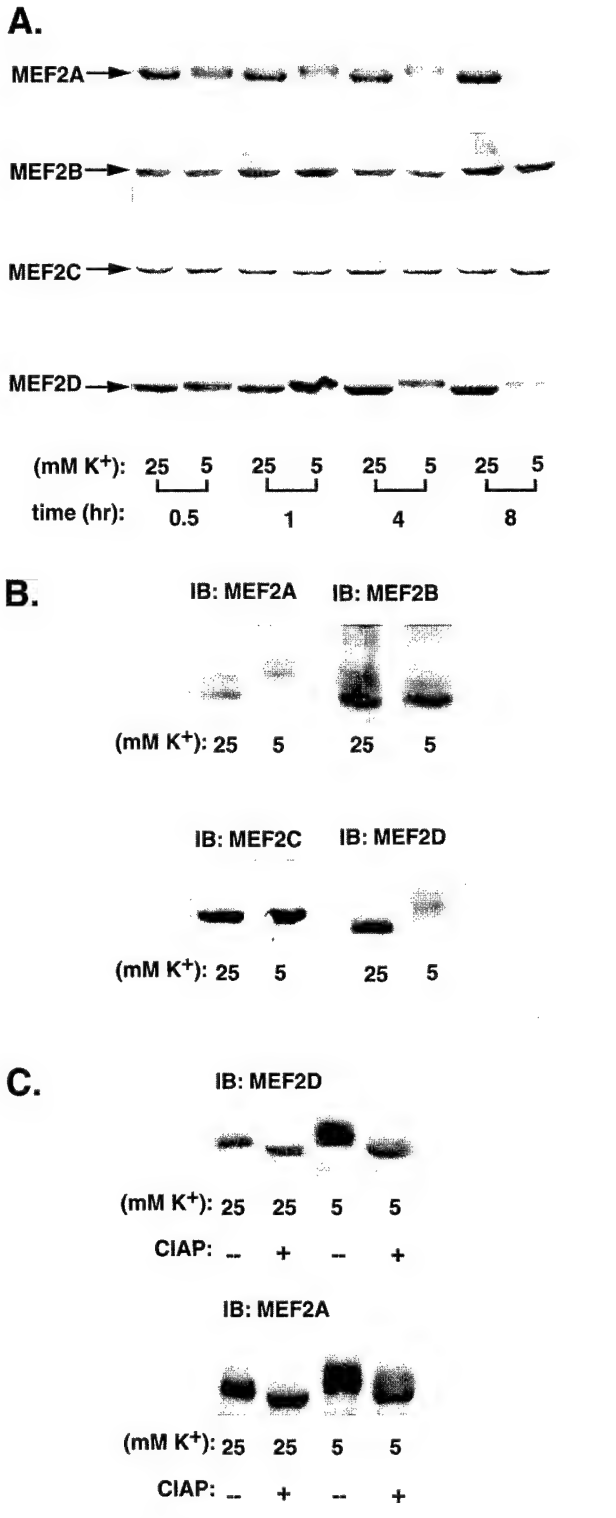

Figure 1. MEF2D and MEF2A, but not MEF2B and MEF2C, are phosphorylated and degraded during the apoptosis of cerebellar granule neurons. *A*, Cerebellar granule neurons (day 7) were placed in serum-free medium containing 25 or 5 mM KCl for the indicated times. Neuronal cell lysates were resolved on 7.5% SDS-acrylamide gels and subjected to Western analysis with the use of specific antibodies to MEF2A, MEF2B, MEF2C, and MEF2D. Data are representative of three separate experiments. *B*, Cell extracts were prepared as described above and analyzed on higher resolution gels. *C*, Cell extracts were incubated in the absence or presence of calf intestinal alkaline phosphatase (*CIAP*; 10 U/ml) before gel electrophoresis.

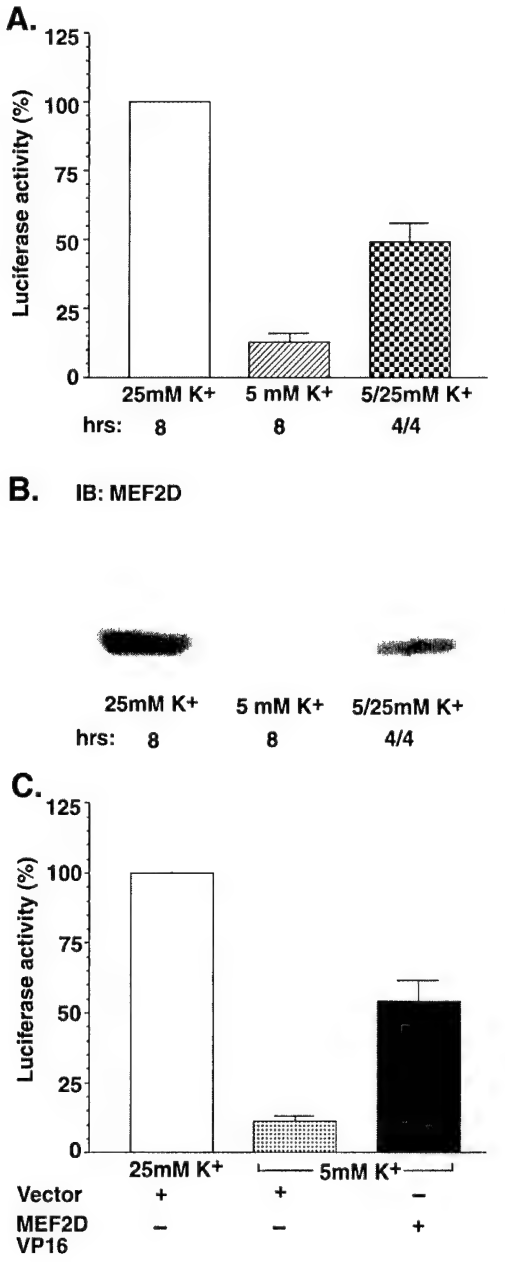

Figure 2. Neurons switched to 5 mM KCl show enhanced MEF2D phosphorylation and decreased MEF2 transcriptional activity; the readdition of 25 mM KCl promotes the dephosphorylation of MEF2D and the partial recovery of MEF2 transcriptional activity. *A*, Cerebellar granule neurons (day 6) were transfected with a MEF2-responsive luciferase reporter and pCMV-β-gal. After transfection (2 hr) the neurons were placed in serum-free medium containing either 25 or 5 mM KCl for 8 hr. In addition, some cells were incubated for 4 hr in 5 mM KCl, followed by the readdition of 25 mM KCl for an additional 4 hr. Then luciferase and β-galactosidase activities were determined as described in Materials and Methods. *B*, Cerebellar granule neurons were incubated as described in *A*, and the phosphorylation status and relative quantity of MEF2D were determined by immunoblot (*IB*) analysis. *C*, Cerebellar granule neurons were transfected with a MEF2-responsive luciferase reporter and pCMV-β-gal in the absence or presence of pCMV-MEF2D-VP16. After 4 hr the luciferase and β-galactosidase activities were determined. Data are expressed as a percentage of control neurons grown in 25 mM KCl and are the mean ± SEM (n = 3).

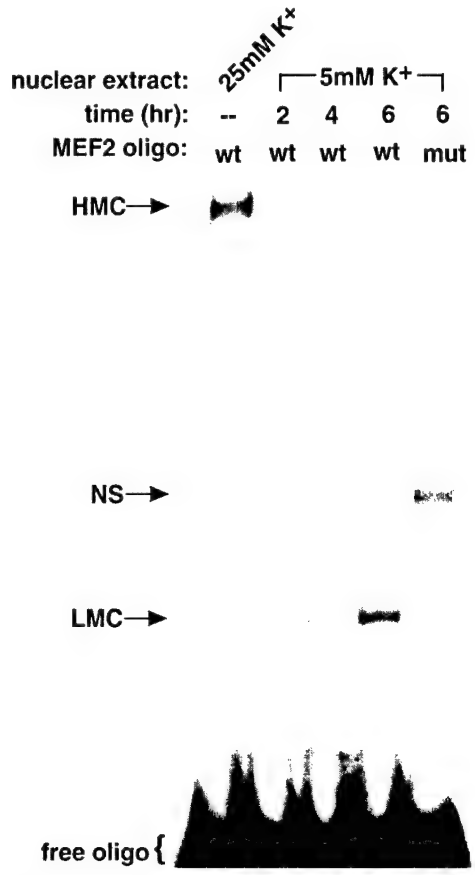

Figure 3. MEF2 DNA binding activity is decreased in apoptotic neurons. Cerebellar granule neurons (day 7) were placed in serum-free medium containing 25 or 5 mM KCl. After the indicated times, nuclear extracts were prepared, and gel mobility shift assays were performed with a double-stranded ^{32}P-labeled consensus (*wt*) or mutant (*mut*) MEF2 oligomer. *NS*, Nonspecific protein/DNA complex; *HMC*, high-mobility complex; *LMC*, low-mobility complex.

4 hr in 5 mM potassium (Fig. 2*B*, *lane 1* vs *lane 3*). Finally, transfection of neurons with MEF2D-VP16, a constitutively active mutant of MEF2D, attenuated the decline of MEF2 luciferase activity during potassium withdrawal (Fig. 2*C*). The decrease in MEF2 transcriptional activity was not attributable to a nonselective effect of cell death, because the transcriptional activity of AP-1 measured with an AP-1 luciferase reporter construct was increased by 30% under the same conditions by which the MEF2 transcriptional activity decreased (data not shown).

DNA binding of MEF2A and MEF2D is regulated by extracellular potassium

To determine whether the DNA binding activity of MEF2 proteins was regulated during induction of the apoptosis of cerebellar granule neurons, we performed electrophoretic mobility shift assays (EMSAs) by using wild-type and mutant MEF2 double-stranded oligonucleotides. Nuclear extracts from cerebellar granule neurons cultured in medium containing 25 mM KCl demonstrated one specific high-mobility protein–DNA complex, HMC (Fig. 3). Extracts from neurons cultured in 5 mM KCl revealed a decrease in the HMC that was detected as early as 2 hr after the potassium was lowered. In addition to the decrease in the HMC associated with the apoptotic response, a new lower-mobility MEF2–DNA binding complex, LMC, was detected in extracts

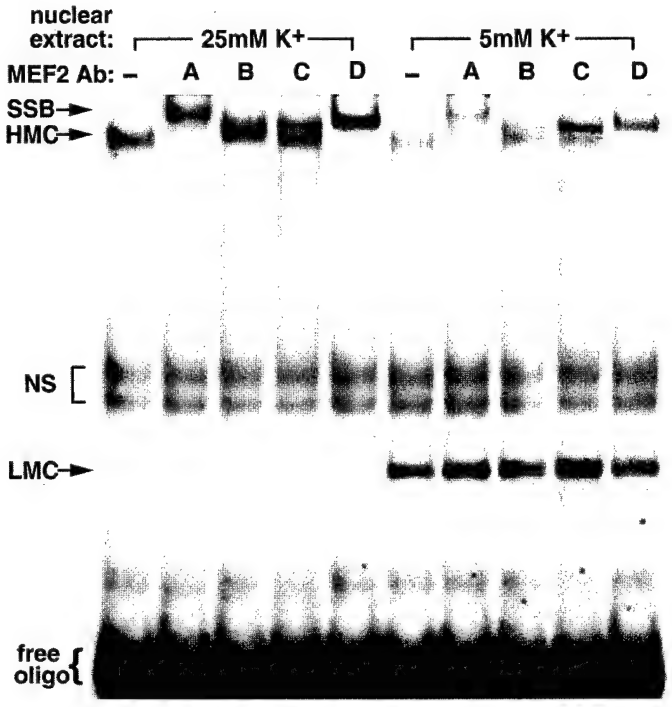

Figure 4. MEF2A and MEF2D are the major MEF2s in the high-molecular-weight DNA binding complex. Cerebellar granule neurons (day 7) were placed in serum-free medium containing 25 or 5 mM KCl. After 4 hr, nuclear extracts were prepared, and supershift gel mobility shift assays were performed with a double-stranded ^{32}P-labeled consensus MEF2 oligomer in the absence or presence of MEF2 antibodies. Note that the lower-molecular-weight complex did not shift with MEF2 antibodies. *SSB*, Supershifted band; *HMC*, high-mobility complex; *LMC*, low-mobility complex; *NS*, nonspecific protein/DNA complex.

isolated 4 and 6 hr after the media change. Neither the HMC nor the LMC was detected by using a mutant MEF2 oligonucleotide.

EMSAs that used antibodies against MEF2A, B, C, and D proteins were performed to determine which MEF2 proteins were bound to DNA under control and apoptotic conditions (Fig. 4). In control neurons, antibodies against MEF2A and MEF2D shifted the HMC to a slower migrating band (SSB), whereas antibodies against MEF2B and MEF2C had little effect on the MEF2–DNA complex. Similar results were obtained in apoptotic neurons, although the amount of high-mobility complex was significantly lower than that present in healthy neurons. Interestingly, the LMC was not shifted by any of the MEF2 antibodies. Because each of the antibodies was raised against the C terminus, but not the N terminus DNA binding domain of MEF2 proteins (Fig. 5*A*), we questioned whether MEF2A and MEF2D were degraded during apoptosis to yield MEF2 fragments that bound DNA but did not interact with the antibodies.

Degradation of MEF2A and MEF2D during apoptosis of cerebellar granule neurons

To test the hypothesis that MEF2 proteins were degraded during apoptosis, we performed Western analysis and exposed the transferred proteins to film for longer periods of time than in previous experiments. The results showed that, within 1 hr of inducing apoptosis, MEF2D was phosphorylated, as shown previously, and a smaller-molecular-weight MEF2D fragment appeared (Fig. 5*B*). The fragment, usually a broad band, had an apparent molecular weight of 40–45 kDa, ~15 kDa less than full-length MEF2D.

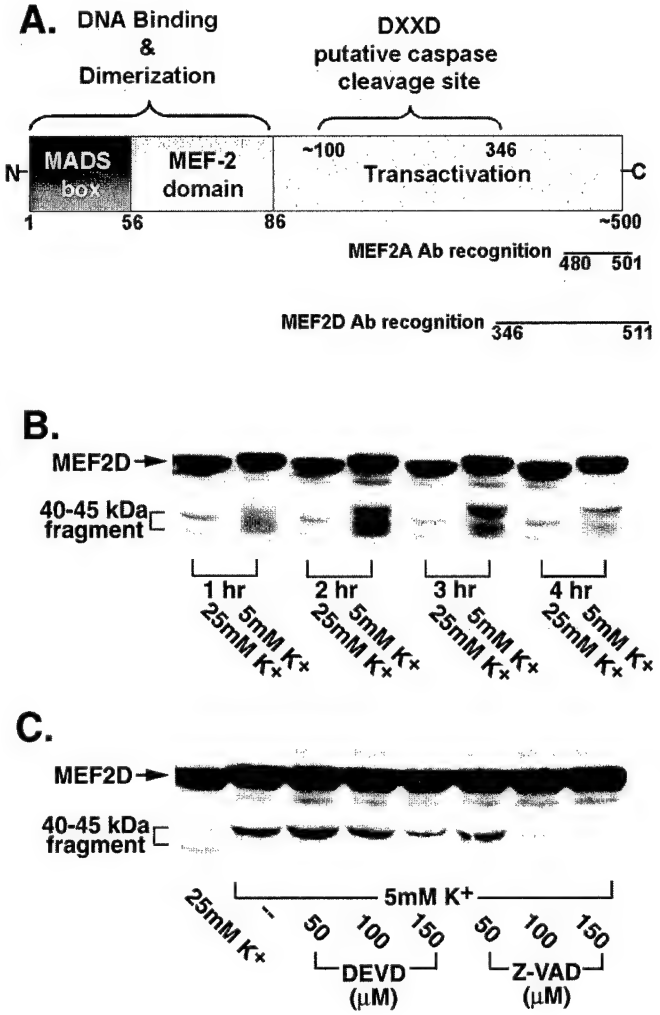

Figure 5. MEF2D is cleaved by a caspase-mediated pathway during apoptosis. *A*, Domain structure of the MEF2 proteins, including the MEF2A and MEF2D antibody recognition motifs and the putative caspase cleavage region. *B*, Cerebellar granule neurons (day 7) were placed in serum-free medium containing 25 or 5 mM KCl. At the indicated times, Western analysis was performed with 12% SDS-acrylamide gels and specific MEF2D antibodies. *C*, Neurons were placed in serum-free medium containing 25 or 5 mM KCl (4 hr) in the absence or presence of various concentrations of the caspase-3-specific inhibitor DEVD or the pan-caspase inhibitor Z-VAD. *Brackets* indicate a lower-molecular-weight cleavage product recognized by the C-terminal MEF2D antibody.

Analysis of various MEF2 sequences (rat MEF2D and mouse MEF2D1a and MEF2A) revealed several putative caspase cleavage sites (DXXD) between the DNA binding domain and the antibody recognition domain (amino acids 100–346) (Fig. 5*A*). To determine whether the MEF2 fragment that was generated during apoptosis resulted from caspase cleavage, we performed experiments to assess whether caspase inhibitors blocked formation of the MEF2D fragment. DEVD, a caspase-3-specific inhibitor, and Z-VAD, a nonselective caspase inhibitor, blocked the formation of the MEF2D fragment in a dose-dependent manner (Fig. 5*C*). Z-VAD was much more effective and potent than DEVD in preventing cleavage of MEF2D, suggesting that an upstream caspase rather than the downstream caspase-3 might be involved in cleaving MEF2D. Consistent with this idea was the finding that the cleavage of MEF2D occurred much earlier than the activation

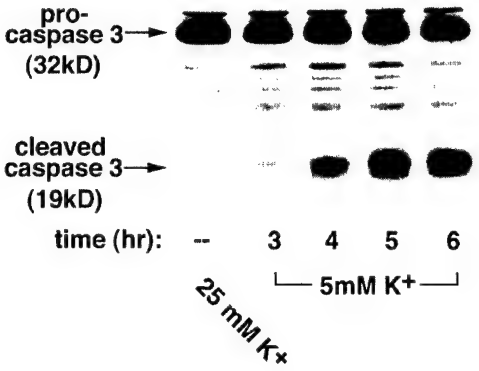

Figure 6. Caspase-3 activation in rat cerebellar granule neurons. Cerebellar granule neurons (day 7) were placed in serum-free medium containing 25 or 5 mM potassium. At the indicated times, Western analysis was performed with 15% SDS-acrylamide gels and an antibody that detects pro-caspase-3 and an active caspase-3 cleavage product.

of caspase-3, which was maximal at 5–6 hr after the induction of apoptosis (Fig. 6).

Caspase inhibitor blocks formation of the low-mobility protein–DNA complex

Blockade of MEF2D cleavage by caspase inhibitors supported the hypothesis that during apoptosis MEF2D is cleaved to generate a N-terminal DNA binding fragment, which is not recognized by antibodies directed against the regulatory domain, and a C-terminal fragment that is recognized by Western blotting. To test this hypothesis directly, we treated neurons with and without a caspase inhibitor before the EMSAs (Fig. 7). As shown previously in nuclear extracts from control neurons grown in 25 mM KCl, the LMC was very low (Fig. 7, *lane 1*). After 4 hr of apoptosis induced by lowering the extracellular potassium to 5 mM, the LMC was abundant (Fig. 7, *lane 2*). The caspase inhibitor Z-VAD, added at the time of the medium change, prevented the formation of the lower-molecular-weight complex (Fig. 7, *lane 3*). In addition, DVED and YVAD (a caspase-1-selective inhibitor) were only partially effective at inhibiting the formation of the low-molecular-weight complex (data not shown). Together, these data suggest that MEF2D and MEF2A are cleaved by a caspase-sensitive pathway to generate N-terminal fragments that bind to DNA but are not recognized by antibodies directed to the C terminus of each of these proteins.

The N-terminal MEF2 fragment can act as a dominant-negative transcription factor

Cleavage of MEF2 between the DNA binding domain and the antibody recognition domain would separate the DNA binding domain from the transactivation domain. To test the possibility that the N-terminal truncated fragment could act in a dominant-negative manner to block both the DNA binding and transcriptional activity of MEF2, we transfected neurons with MEF2D-VP16 in the absence or presence of increasing amounts of truncated MEF2A131. The expression plasmid MEF2D-VP16 encodes the DNA binding domain of mouse MEF2D (amino acids 1–92) fused to the transcriptional activation domain of VP16 (amino acids 412–490) under control of a CMV promoter. Its use as a constitutively active transcription factor has been reported previously (Han and Prywes, 1995). MEF2A131 encodes mouse MEF2A that is truncated at position 131, leaving the DNA binding domain intact, and is highly homologous to the corresponding region of MEF2D. After cotransfection of these

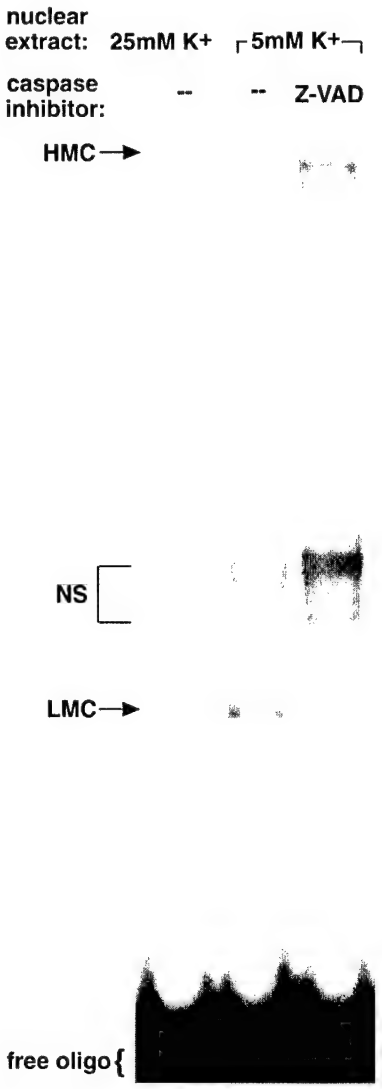

Figure 7. Formation of the lower-molecular-weight protein/DNA binding complex is prevented by caspase inhibition. Cerebellar granule neurons (day 7) were placed in serum-free medium containing 25 or 5 mM KCl in the absence or presence of 100 μM pan-caspase inhibitor (*Z-VAD*). After 4 hr, nuclear extracts were prepared, and gel mobility shift assays were performed with a double-stranded ^{32}P-labeled consensus MEF2 oligomer. *HMC*, High-mobility complex; *LMC*, low-mobility complex; *NS*, nonspecific protein/DNA complex.

two expression plasmids, transcriptional activity was determined with the MEF2 luciferase reporter plasmid (Fig. 8*A*). As observed previously, neurons incubated in 5 mM potassium had low MEF2 transcriptional activity. However, the expression of a constitutively active mutant of MEF2D (MEF2D-VP16) maintained high MEF2 transcriptional activity even in the presence of 5 mM potassium. When the VP16 mutant of MEF2D (1 μg) was expressed in the presence of increasing concentrations of truncated MEF2A131 (1–3 μg of DNA), the N-terminal MEF2 fragment blocked MEF2 luciferase activity in a dose-dependent manner (Fig. 8*A*). These data indicate that a truncated MEF2 can block the DNA binding and activity of MEF2 competitively. The consequence of the expression of truncated MEF2 on neuronal apoptosis is seen in Figure 8*B*. In these experiments, neurons were transfected with the control vector, MEF2D-VP16, or MEF2D-VP16 in the presence of increasing amounts of trun-

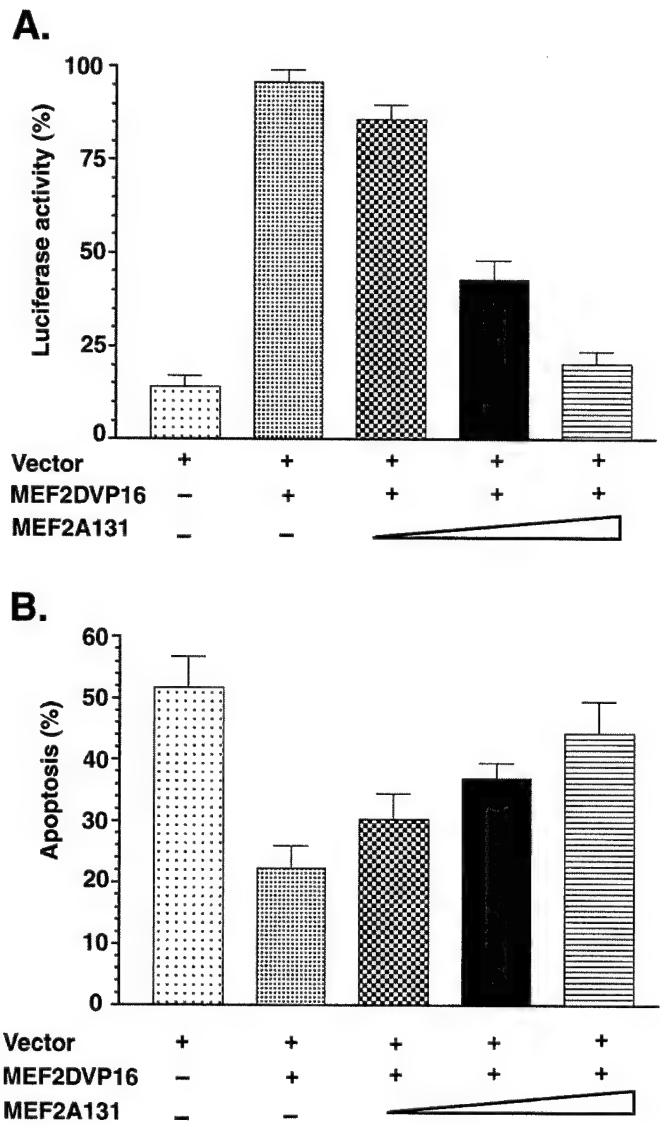

Figure 8. The N terminus of MEF2 antagonizes MEF2 activity and MEF2-mediated neuronal survival. *A*, Cerebellar granule neurons (day 6) were transfected with a MEF2-responsive luciferase reporter and pCMV-β-gal in the absence or presence of 1 μg of MEF2D-VP16 and MEF2A131 (1–3 μg). After transfection (2 hr) the neurons were placed in serum-free medium containing 5 mM KCl. After 4 hr, luciferase and β-galactosidase activities were determined. Luciferase activity was normalized with respect to that of β-galactosidase. Data are expressed as percentage of control neurons grown in 25 mM potassium. Data are the mean ± SEM (n = 3). *B*, Cerebellar granule neurons (day 5) were cotransfected with pCMV-β-gal and the indicated expression vector at the concentrations given in *A*. After transfection the neurons were placed in serum-free medium containing 5 mM KCl for 16 hr and then fixed and immunostained with a β-gal antibody. The neurons also were stained with Hoechst 33258. Apoptosis was quantified by scoring the percentage of transfected neurons with condensed or fragmented nuclei. Data are the mean ± SEM (n = 3). *Vector*, Empty pcDNA vector.

cated MEF2A131. In neurons maintained in 5 mM potassium for 16 hr the level of apoptosis was 56%. Transfection of the neurons with MEF2D-VP16 reduced the amount of apoptosis to ~22%. When the truncated MEF2A131 mutant (1–3 μg of DNA) was introduced with MEF2D-VP16 into neurons, the ability of MEF2D-VP16 to block apoptosis was attenuated in a dose-dependent manner. These data indicate that the MEF2 N-terminal fragment can act as a dominant-negative transcription factor and antagonize the prosurvival function of MEF2D.

DISCUSSION

Examination of the temporal and spatial localization of MEF2 proteins in brain has revealed that MEF2 expression coincides with the initiation of postmitotic neuronal maturation (Leifer et al., 1993, 1994; McDermott et al., 1993; Ikeshima et al., 1995; Lyons et al., 1995; Mao et al., 1999). For example, in the developing cerebral cortex, MEF2C immunoreactivity is present in the cortical plate and is not found in the intermediate zone or ventricular zone (Mao et al., 1999). At 14 weeks of gestation, MEF2C immunoreactivity is present in cell nuclei throughout the cortical plate. Subsequently, MEF2C immunoreactivity develops a bilaminate and then a trilaminate distribution and ultimately is expressed preferentially in layers II, IV, and VI of mature neocortex (Leifer et al., 1994). These findings suggest a role for MEF2C in postmitotic neuronal differentiation, in particular in the development of certain cortical layers.

In the cerebellum, MEF2A and MEF2D mRNA levels dramatically increase at ~P9, reach a peak at P15–P18, and stay high in adults (Leifer et al., 1994; Ikeshima et al., 1995; Lin et al., 1996; Mao and Wiedmann, 1999). This time course of MEF2 expression coincides with the expression of the $GABA_A$ receptor α6 subunit mRNA, a marker for the differentiation of mature cerebellar granule neurons. Immunohistochemical staining reveals that MEF2 protein expression occurs primarily in the internal granule cell layer of the cerebellum (Ikeshima et al., 1995). During postnatal development, differentiated granule neurons generated in the external germinal layer migrate to the internal granule layer where they are innervated by mossy fiber axons. There is considerable loss of granule neurons during this process and it is thought that the survival of granule neurons is regulated by depolarization-induced mechanisms during this time period.

Postmitotic granule neurons derived from neonatal rat can be maintained readily *in vitro* in their fully differentiated state if they are depolarized with a high extracellular concentration of potassium (D'Mello et al., 1993; Miller et al., 1997). If the extracellular potassium concentration is reduced, granule neurons undergo programmed cell death with classic morphological and biochemical features of apoptosis. These characteristics, along with the abundance and high degree of homogeneity, make cultured granule neurons an excellent model to examine the role of MEF2 proteins in depolarization-dependent neuronal survival.

In this report we have defined a novel mechanism by which the activity and levels of MEF2 proteins are regulated during apoptosis of cerebellar granule neurons. We also have shown that MEF2 proteins are regulated in an isotype-specific manner. All four MEF2 isoforms (A, B, C, and D) were detected by immunoblot analysis in rat cerebellar granule neurons. However, in agreement with results from immunocytochemistry and *in situ* hybridization (Ikeshima et al., 1995; Lyons et al., 1995), MEF2A and MEF2D were the most prominent MEF2 proteins detected in the cultured cerebellar granule neurons when equal amounts of total protein were analyzed by Westerns (data not shown). MEF2A and MEF2D appear to be responsible for most, if not all, of the MEF2 DNA binding activity in viable cerebellar granule neurons. When granule neurons are induced to undergo apoptosis by lowering potassium, endogenous MEF2A and MEF2D, but not MEF2B and MEF2C, are phosphorylated. Phosphorylation is accompanied by a decrease in MEF2 transcriptional activity, and both effects are reversed by the readdition of depolarizing potas-

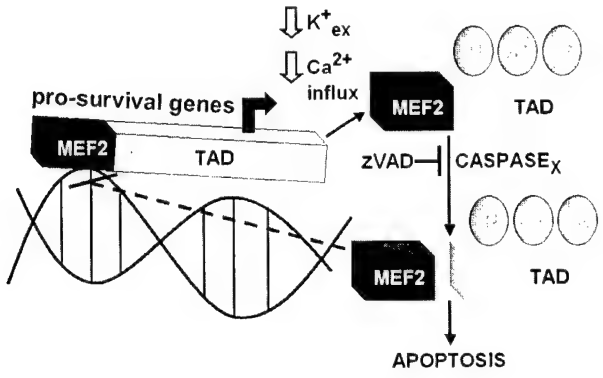

Figure 9. The regulation of MEF2 proteins during apoptosis of rat cerebellar granule neurons. When granule neurons are induced to undergo apoptosis by lowering extracellular potassium to 5 mM, endogenous MEF2D and MEF2A (data not shown) are phosphorylated. Phosphorylation of MEF2D induced by decreasing calcium influx not only leads to decreased DNA binding but also is associated with a caspase-dependent cleavage of MEF2D. The caspase involved in cleaving MEF2D remains to be identified. The cleavage of MEF2D results in an N-terminal fragment (~100 amino acids long) that retains its DNA binding capacity, is not recognized by C-terminal antibodies, and lacks the transactivation domain. The MEF2 N-terminal fragment is capable of blocking the activity of MEF2D, thus acting as a dominant-negative transcription factor. The decline in MEF2 activity because of decreased DNA binding and formation of a dominant-inactive MEF2 fragment leads to apoptosis.

sium. The most novel findings of the present study show that the phosphorylation of MEF2D that is induced by decreasing calcium influx not only correlates with decreased DNA binding but also is associated with a direct or indirect caspase-dependent cleavage of MEF2D (Fig. 9). The cleavage of MEF2D results in a N-terminal fragment (~100 amino acids long) that retains its DNA binding capacity, is not recognized by C-terminal antibodies, and lacks the transactivation domain. The MEF2 N-terminal fragment is capable of blocking the activity of MEF2D, thus acting as a dominant-negative transcription factor. The decline in MEF2 activity resulting from decreased DNA binding and formation of a dominant-inactive MEF2 fragment appears to be sufficient to mediate execution of the apoptotic process. Overexpression of a constitutively active MEF2D that does not get cleaved prevents the loss in MEF2 transcriptional activity during apoptosis and protects against apoptosis that is induced by lowering membrane depolarization and calcium influx.

The signaling pathways responsible for the changes in the phosphorylation state of MEF2 could involve an increase in the activity of a calcium-sensitive kinase, a decrease in the activity of a calcium-sensitive phosphatase, or both. Mao and Wiedman (1999) recently reported similar data that MEF2A is hyperphosphorylated when calcium influx is decreased or when the protein phosphatase calcineurin is inhibited in cerebellar granule neurons. Although other isoforms were not examined in the previous study, the data suggest that enhanced phosphorylation of MEF2A and MEF2D seen on lowering extracellular potassium is likely to be attributable to decreased activity of the calcium-dependent phosphatase calcineurin. Furthermore, because MEF2B and MEF2C did not undergo hyperphosphorylation in response to lowering extracellular potassium, the data indicate that MEF2A and MEF2D are regulated post-translationally in an isotype-specific manner in cerebellar granule neurons.

The putative phosphorylation sites described in this study are functionally distinct from the previously described phosphorylation sites that enhance MEF2 transcriptional activity. Some MEF2 isoforms directly interact with p38 MAP kinase and ERK5/BMK1 and are phosphorylated by both protein kinases (Kato et al., 1997; Yang et al., 1998; Ornatsky et al., 1999; Zhao et al., 1999). Phosphorylation of MEF2 proteins by p38 MAP kinase and ERK5 stimulates transcriptional activity. The increased transcriptional activity could involve changes in protein conformation that enhance interaction with the transcriptional machinery. Alternatively, phosphorylation might be required for the recruitment of an essential transcriptional cofactor or release of a repressor. In support of the latter mechanism, histone deacetylases (HDACs) have been shown to repress the transcriptional activity of MEF2s (Miska et al., 1999; Lemercier et al., 2000; Lu et al., 2000a,b; Youn et al., 2000). Phosphorylation of HDACs by the calcium-sensitive protein kinase CaMK results in the dissociation of HDACs and the unmasking of transcriptional activity.

Other studies in T-cells have mapped a calcineurin-dependent induction of the nur77 promoter to a putative MEF2 DNA binding site (Youn et al., 1999). Although the transcriptional activity of MEF2 in activated T-cells requires calcium signals, its DNA binding activity seems to be constitutive and insensitive to changes in calcium. Again, the data are in contrast to the results of this study in which decreases in intracellular calcium signaling resulted in decreased DNA binding and transcriptional activity. The antibodies used in T-cells examining nur77 promoter activity did not distinguish between MEF2 isoforms. This raises the possibility that the discrepancy may be attributable to differential regulation of the various MEF2 isoforms and/or the presence of cell type-specific accessory proteins.

In summary, the complexities in MEF2-regulated gene expression have been advanced primarily from studies in muscle and T-cells. In the present study we have delineated a novel phosphorylation signaling pathway associated with DNA binding, transcriptional activity, and degradation of neuronal MEF2 proteins. The data in this study also support the hypothesis that MEF2A and MEF2D regulate neuronal survival in the cerebellum, particularly in response to depolarization-induced signals that are important during development.

REFERENCES

Amacher SL, Buskin JN, Hauschka SD (1993) Multiple regulatory elements contribute differentially to muscle creatine kinase enhancer activity in skeletal and cardiac muscle. Mol Cell Biol 13:2753–2764.

D'Mello SR, Galli C, Ciotti T, Calissano P (1993) Induction of apoptosis in cerebellar granule neurons by low potassium: inhibition of death by insulin-like growth factor I and cAMP. Proc Natl Acad Sci USA 23:10989–10993.

Firulli AB, Miano JM, Bi W, Johnson AD, Casscells W, Olson EN, Schwarz JJ (1996) Myocyte enhancer binding factor-2 expression and activity in vascular smooth muscle cells. Association with the activated phenotype. Circ Res 78:196–204.

Han TH, Prywes R (1995) Regulatory role of MEF2D in serum induction of the c-*jun* promoter. Mol Cell Biol 15:2907–2915.

Ikeshima H, Imai S, Shimoda K, Hata J, Takano T (1995) Expression of a MADS-box gene, MEF2D, in neurons of the mouse central nervous system: implication of its binary function in myogenic and neurogenic cell lineages. Neurosci Lett 200:117–120.

Kato Y, Kravchenko VV, Tapping RI, Han J, Ulevitch RJ, Lee JD (1997) BMK1/ERK5 regulates serum-induced early gene expression through transcription factor MEF2C. EMBO J 16:7054–7066.

Leifer D, Krainc D, Yu YT, McDermott J, Breitbart RE, Heng J, Neve RL, Kosofsky B, Nadal-Ginard B, Lipton SA (1993) MEF2C, a MADS/MEF2-family transcription factor expressed in a laminar distribution in cerebral cortex. Proc Natl Acad Sci USA 90:1546–1550.

Leifer D, Golden J, Kowall NW (1994) Myocyte-specific enhancer binding factor 2C expression in human brain development. Neuroscience 63:1067–1079.

Lemercier C, Verdel A, Galloo B, Curtet S, Brocard MP, Khochbin S

(2000) mHDA1/HDAC5 histone deacetylase interacts with and represses MEF2A transcriptional activity. J Biol Chem 275:15594–15599.
Li M, Wang X, Meintzer MK, Laessig T, Birnbaum MJ, Heidenreich KA (2000) Cyclic AMP promotes neuronal survival by phosphorylation of glycogen synthase kinase 3β. Mol Cell Biol 20:9356–9363.
Lin X, Shah S, Bulleit RF (1996) The expression of MEF2 genes is implicated in CNS neuronal differentiation. Brain Res Mol Brain Res 42:307–316.
Lu J, McKinsey TA, Nicol RL, Olson EN (2000a) Signal-dependent activation of the MEF2 transcription factor by dissociation from histone deacetylases. Proc Natl Acad Sci USA 97:4070–4075.
Lu J, McKinsey TA, Zhang CL, Olson EN (2000b) Regulation of skeletal myogenesis by association of the MEF2 transcription factor with class II histone deacetylases. Mol Cell 6:233–244.
Lyons GE, Micales BK, Schwarz J, Martin JF, Olson EN (1995) Expression of *mef2* genes in the mouse central nervous system suggests a role in neuronal maturation. J Neurosci 15:5727–5738.
Mao Z, Wiedmann M (1999) Calcineurin enhances MEF2 DNA binding activity in calcium-dependent survival of cerebellar granule neurons. J Biol Chem 274:31102–31107.
Mao Z, Bonni A, Xia F, Nadal-Vicens M, Greenberg ME (1999) Neuronal activity-dependent cell survival mediated by transcription factor MEF2. Science 286:785–790.
Martin JF, Miano JM, Hustad CM, Copeland NG, Jenkins NA, Olson EN (1994) A MEF2 gene that generates a muscle-specific isoform via alternative mRNA splicing. Mol Cell Biol 14:1647–1656.
McDermott JC, Cardoso MC, Yu YT, Andres V, Leifer D, Krainc D, Lipton SA, Nadal-Ginard B (1993) hMEF2C gene encodes skeletal muscle- and brain-specific transcription factors. Mol Cell Biol 13:2564–2577.
Miller TM, Tansey MG, Johnson Jr EM, Creedon DJ (1997) Inhibition of phosphatidylinositol 3-kinase activity blocks depolarization and insulin-like growth factor I-mediated survival of cerebellar granule cells. J Biol Chem 272:9847–9853.
Miska EA, Karlsson C, Langley E, Nielsen SJ, Pines J, Kouzarides T (1999) HDAC4 deacetylase associates with and represses the MEF2 transcription factor. EMBO J 18:5099–5107.
Molkentin JD, Olson EN (1996) Combinatorial control of muscle development by basic helix–loop–helix and MADS-box transcription factors. Proc Natl Acad Sci USA 93:9366–9373.
Molkentin JD, Firulli AB, Black BL, Martin JF, Hustad CM, Copeland N, Jenkins N, Lyons G, Olson EN (1996) MEF2B is a potent transactivator expressed in early myogenic lineages. Mol Cell Biol 16:3814–3824.
Naya FS, Olson E (1999) MEF2: a transcriptional target for signaling pathways controlling skeletal muscle growth and differentiation. Curr Opin Cell Biol 11:683–688.
Okamoto S, Krainc D, Sherman K, Lipton SA (2000) Antiapoptotic role of the p38 mitogen-activated protein kinase–myocyte enhancer factor 2 transcription factor pathway during neuronal differentiation. Proc Natl Acad Sci USA 97:7561–7566.
Ornatsky OI, Andreucci JJ, McDermott JC (1997) A dominant-negative form of transcription factor MEF2 inhibits myogenesis. J Biol Chem 272:33271–33278.
Ornatsky OI, Cox DM, Tangirala P, Andreucci JJ, Quinn ZA, Wrana JL, Prywes R, Yu YT, McDermott JC (1999) Post-translational control of the MEF2A transcriptional regulatory protein. Nucleic Acids Res 27:2646–2654.
Shore P, Sharrocks AD (1995) The MADS-box family of transcription factors. Eur J Biochem 229:1–13.
Skerjanc IS, Wilton S (2000) Myocyte enhancer factor 2C upregulates MASH-1 expression and induces neurogenesis in P19 cells. FEBS Lett 472:53–56.
Yang CC, Ornatsky OI, McDermott JC, Cruz TF, Prody CA (1998) Interaction of myocyte enhancer factor 2 (MEF2) with a mitogen-activated protein kinase, ERK5/BMK1. Nucleic Acids Res 26:4771–4777.
Youn HD, Sun L, Prywes R, Liu JO (1999) Apoptosis of T-cells mediated by Ca^{2+}-induced release of the transcription factor MEF2. Science 286:790–793.
Youn HD, Grozinger CM, Liu JO (2000) Calcium regulates transcriptional repression of myocyte enhancer factor 2 by histone deacetylase 4. J Biol Chem 275:22563–22567.
Yu YT, Breitbart RE, Smoot LB, Lee Y, Mahdavi V, Nadal-Ginard B (1992) Human myocyte-specific enhancer factor 2 comprises a group of tissue-restricted MADS-box transcription factors. Genes Dev 6:1783–1798.
Zhao M, New L, Kravchenko VV, Kato Y, Gram H, di Padova F, Olson EN, Ulevitch RJ, Han J (1999) Regulation of the MEF2 family of transcription factors by p38. Mol Cell Biol 19:21–30.

balt3/bc-bc/bc-bc/bc4201/bc4881-01a eichelbt S=4 11/9/01 18:20 4/Color Figure(s) 5 ARTNO: M103959200

THE JOURNAL OF BIOLOGICAL CHEMISTRY

Vol. 276, No. ??, Issue of ???? ??, pp. 1–xxx, 2001
Printed in U.S.A.

An Essential Role for Rac/Cdc42 GTPases in Cerebellar Granule Neuron Survival*

Received for publication, May 2, 2001
Published, JBC Papers in Press, August 16, 2001, DOI 10.1074/jbc.M103959200

Daniel A. Linseman‡§, Tracey Laessig‡, Mary Kay Meintzer‡, Maria McClure‡, Holger Barth¶, Klaus Aktories¶, and Kim A. Heidenreich‡

From the ‡Department of Pharmacology, University of Colorado Health Sciences Center and the Denver Veterans Affairs Medical Center, Denver, Colorado 80220 and the ¶Institüt fur Pharmakologie and Toxikologie, Universität Freiburg, Freiburg [redacted], Germany

AQ: A

AQ: B

Rho family GTPases are critical molecular switches that regulate the actin cytoskeleton and cell function. In the current study, we investigated the involvement of Rho GTPases in regulating neuronal survival using primary cerebellar granule neurons. *Clostridium difficile* toxin B, a specific inhibitor of Rho, Rac, and Cdc42, induced apoptosis of granule neurons characterized by c-Jun phosphorylation, caspase-3 activation, and nuclear condensation. Serum and depolarization-dependent survival signals could not compensate for the loss of GTPase function. Unlike trophic factor withdrawal, toxin B did not affect the antiapoptotic kinase Akt or its target glycogen synthase kinase-3β. The proapoptotic effects of toxin B were mimicked by *Clostridium sordellii* lethal toxin, a selective inhibitor of Rac/Cdc42. Although Rac/Cdc42 GTPase inhibition led to F-actin disruption, direct cytoskeletal disassembly with *Clostridium botulinum* C2 toxin was insufficient to induce c-Jun phosphorylation or apoptosis. Granule neurons expressed high basal JNK and low p38 mitogen-activated protein kinase activities that were unaffected by toxin B. However, pyridyl imidazole inhibitors of JNK/p38 attenuated c-Jun phosphorylation. Moreover, both pyridyl imidazoles and adenoviral dominant-negative c-Jun attenuated apoptosis, suggesting that JNK/c-Jun signaling was required for cell death. The results indicate that Rac/Cdc42 GTPases, in addition to trophic factors, are critical for survival of cerebellar granule neurons.

Rho GTPases belong to the Ras superfamily of monomeric G proteins. The three most studied Rho GTPases, RhoA, Rac1, and Cdc42Hs, are best known as regulators of actin cytoskeletal dynamics (1). However, Rho GTPases also modulate other critical cell functions including cell cycle progression (2), gene transcription (3), and cell-cell or cell-matrix adhesion (4, 5). Recently, Rho GTPases have also been shown to influence cell survival. For example, Rho GTPases up-regulate expression of prosurvival Bcl-2 family members in T cells and epithelial cells (6, 7). Constitutive activation of Rho GTPases with cytotoxic necrotizing factor protects epithelial cells from UV-induced apoptosis (8). Similarly, constitutively active Rac inhibits apoptosis induced by various stimuli in Rat1 fibroblasts, epithelial cells, and hematopoietic cells (9–11). However, the prosurvival effects of Rho GTPases are cell type- and paradigm-specific. For example, overexpression of Rac sensitizes NIH-3T3 fibroblasts to serum withdrawal-induced apoptosis (12). Furthermore, constitutively active Rho GTPase mutants enhance susceptibility of CHO cells expressing a chimeric CD4-Fas receptor to Fas-induced apoptosis (13). Thus, in non-neuronal cells Rho GTPases can display either prosurvival or proapoptotic functions.

In contrast to non-neuronal cells, comparatively few studies have investigated a role for Rho GTPases in neuronal survival. Furthermore, the available data suggest that neuronal cell type-specific responses may exist. For example, dominant-negative mutants of Rac and Cdc42 protect sympathetic neurons from nerve growth factor withdrawal-induced apoptosis by suppressing activation of apoptosis signal-regulated kinase and c-Jun-NH_2-terminal kinase (JNK)[1] (14, 15), suggesting that Rho GTPases can function as upstream activators of stress-activated protein kinase cascades during neuronal apoptosis. On the other hand, recent data obtained from primary cortical neurons suggest that Rho GTPases may also mediate prosurvival signaling in some neuronal cell types. Inhibitors of 3-hydroxy-3-methylglutaryl-CoA reductase (statins) decrease the plasma membrane localization of Rho GTPases and induce cortical neuron apoptosis (16). Similar results utilizing statins to induce apoptosis were also reported recently for rat brain neuroblasts (17). These latter findings provide *indirect* evidence that Rho GTPases may play a prosurvival function in some types of neurons.

AQ: C

Fn1

In the current study, we utilized clostridial toxins, enzymes that covalently modify and inactivate Rho family GTPases in a highly specific manner (18), to investigate if Rho GTPases regulate the survival of primary rat cerebellar granule neurons (CGNs). Clostridial toxins provide a distinct advantage over statins in that they directly modify Rho GTPases rather than affecting mevalonate synthesis, a precursor required for the isoprenylation of many cellular proteins besides Rho GTPases. CGNs isolated from early postnatal rats provide a well characterized *in vitro* model to study neuronal apoptosis in that their survival requires serum-derived and activity-dependent (membrane depolarization) signals (19, 20). The results show that inhibition of Rho GTPases, specifically Rac/Cdc42, promotes apoptosis of CGNs maintained in culture medium containing

AQ: D

* This work was supported by a Department of Veterans Affairs merit award (to K. A. H.) and by the Research Enhancement Award Program (to K. A. H. and D. A. L.). The costs of publication of this article were defrayed in part by the payment of page charges. This article must therefore be hereby marked "*advertisement*" in accordance with 18 U.S.C. Section 1734 solely to indicate this fact.

§ To whom correspondence should be addressed: Denver VAMC-111H, 1055 Clermont St., Denver, CO 80220. Tel.: 303-399-8020 (ext. 5264); Fax: 303-393-5271; E-mail: Dan.Linseman@UCHSC.edu.

AQ: K

[1] The abbreviations used are: JNK, c-Jun NH_2-terminal kinase; CGN(s), cerebellar granule neuron(s); DAPI, 4,6-diamidino-2-phenylindole; CMV, cytomegalovirus; DN, dominant-negative; GSK3β, glycogen synthase kinase-3β; MAP, mitogen-activated protein; BSA, bovine serum albumin; PBS, phosphate-buffered saline; PAGE, polyacrylamide gel electrophoresis.

serum and depolarizing potassium, indicating that serum-derived and calcium-dependent survival signals cannot compensate for the loss of GTPase function. Moreover, apoptosis occurs independently of actin cytoskeletal disruption and requires phosphorylation of the transcription factor c-Jun. The data are the first to establish clearly a prosurvival function for Rho GTPases in a primary neuronal cell model.

EXPERIMENTAL PROCEDURES

Materials—*Clostridium difficile* toxin B (21), *Clostridium sordellii* lethal toxin (22), *Clostridium botulinum* C2 toxin (23), and *C. botulinum* C3 fusion toxin (C2IN-C3) (24) were isolated and prepared as described previously. SB203580 (4-(4-fluorophenyl)-2-(4-methyl-sulfinyl-phenyl)-5-(4-pyridyl)-1H-imid-azole), cytochalasin D, anisomycin, actinomycin D, and cycloheximide were from Calbiochem. PD169316 (4-(4-fluorophenyl)-2-(4-nitrophenyl)-5-(4-pyridyl)-1H-imidazole) was provided by Dr. Alan Saltiel (Warner-Lambert/Parke-Davis, Ann Arbor, MI). RWJ67657 (4-(4-(4-fluorophenyl)-1-(3-phenylpropyl)-5-(4-pyridinyl)-1H-imidazol-2-yl)-3-butyn-1-ol) was obtained from Dr. Scott Wadsworth (R. W. Johnson Pharmaceutical Research Institute, Raritan, NJ). Hoechst dye 33258 and DAPI (4,6-diamidino-2-phenylindole) were from Sigma. Latrunculin A and rhodamine-conjugated phalloidin were from Molecular Probes (Eugene, OR). Adenoviral-CMV was obtained from Dr. Jerry Schaack, University of Colorado Health Sciences Center (Denver). Adenoviral-*Crm*A was obtained from the University of North Carolina Vector Core (Chapel Hill). Adenoviral dominant-negative (DN)-c-Jun (TAM67) was kindly provided by Dr. Jong Sung Park, Medical College of Virginia (Richmond). Polyclonal antibodies to c-Jun and caspase-3 were purchased from Santa Cruz Biotechnology (Santa Cruz, CA). Y27632 was from Upstate Biotechnology (Lake Placid, NY). Polyclonal, phospho-specific antibodies to c-Jun (Ser-63), Akt (Ser-473), glycogen synthase kinase-3β (GSK3β) (Ser-9), JNK (Thr-183/Tyr-185), and p38 MAP kinase (Thr-180/Tyr-182) were obtained from Cell Signaling Technology/New England Biolabs (Beverly, MA). AQ: E

Cell Culture—Rat CGNs were isolated from 7–8-day-old Sprague-Dawley rat pups (15–19 g) as described previously (25). Briefly, neurons were plated at a density of 2.0×10^6 cells/ml in basal modified Eagle's medium containing 10% fetal bovine serum, 25 mM KCl, 2 mM L-glutamine, and penicillin (100 units/ml)-streptomycin (100 μg/ml) (Life Technologies, Inc.). Cytosine arabinoside (10 μM) was added to the culture medium 24 h after plating to limit the growth of non-neuronal cells. Using this protocol, the cultures were ~95–99% pure for granule neurons. In general, experiments were performed after 7 days in culture. Apoptosis was induced by either removing serum and decreasing the extracellular potassium concentration from 25 mM to 5 mM or by the direct addition of clostridial toxins to complete medium containing serum and 25 mM potassium.

Quantitation of Apoptosis—After induction of apoptosis as described above, CGNs were fixed with paraformaldehyde, and nuclei were stained with either Hoechst dye or DAPI. Cells were considered apoptotic if their nuclei were either condensed or fragmented. In general, ~500 cells from at least two fields of a 35-mm well were counted. Data are presented as the percentage of cells in a given treatment group which were scored as apoptotic. Experiments were performed in triplicate.

Adenoviral Infection—On day 5 in culture, CGNs were infected with either control adenovirus (adenoviral-CMV), adenoviral-*Crm*A, or adenoviral-DN-c-Jun each at an multiplicity of infection of 5–10. After infection, cells were returned to the incubator for 48 h at 37 °C and 10% CO_2. On day 7, the cells were then incubated for an additional 24 h with either vehicle (1 mg/ml BSA in PBS) or 500 pg/ml *C. difficile* toxin B. Apoptosis was quantified as described above. AQ: F

Preparation of CGN Cell Extracts—After incubation with clostridial toxins for the indicated times specified in the text, the treatment medium was aspirated, CGNs were washed once with 2 ml of ice-cold PBS (pH 7.4), and cells were then placed on ice and scraped into lysis buffer (200 μl/35-mm well) containing 20 mM HEPES (pH 7.4), 1% Triton X-100, 50 mM NaCl, 1 mM EGTA, 5 mM β-glycerophosphate, 30 mM sodium pyrophosphate, 100 μM sodium orthovanadate, 1 mM phenylmethylsulfonyl fluoride, 10 μg/ml leupeptin, and 10 μg/ml aprotinin. Cell debris was removed by centrifugation at 6,000 × *g* for 3 min, and the protein concentration of the supernatant was determined using a commercially available protein assay kit (Pierce Chemical Co.). Aliquots (~150 μg) of supernatant protein were diluted to a final concentration of 1 × SDS-polyacrylamide gel electrophoresis (PAGE) sample buffer, boiled for 5 min, and electrophoresed through 10–15% polyacrylamide gels. Proteins were transferred to polyvinylidene fluoride membranes (Millipore Corp., Bedford, MA) and processed for immunoblot analysis. AQ: G

Immunoblot Analysis—Nonspecific binding sites were blocked in PBS (pH 7.4) containing 0.1% Tween 20 (PBS-T) and 1% BSA for 1 h at room temperature. Primary antibodies were diluted in blocking solution (final dilution of 1:250–1:1,000) and incubated with the membranes for 1 h. Excess primary antibody was removed by washing the membranes three times in PBS-T. The blots were then incubated with the appropriate peroxidase-conjugated secondary antibody diluted in PBS-T (final dilution of 1:5,000–1:10,000) for 1 h and subsequently washed three times in PBS-T. Immunoreactive proteins were detected by enhanced chemiluminescence (Amersham Pharmacia Biotech). In some experiments, membranes were reprobed after stripping in 0.1 M Tris-HCl (pH 8.0), 2% SDS, and 100 mM β-mercaptoethanol for 30 min at 52 °C. The blots were rinsed twice in PBS-T and processed as above with a different primary antibody. Autoluminograms shown are representative of at least three independent experiments.

Phospho-c-Jun Immunocytochemistry—CGNs were cultured on polyethyleneimine-coated glass coverslips and were incubated with clostridial toxins ± pyridyl imidazole inhibitors as described in the text. After incubation, CGNs were fixed with paraformaldehyde and then permeabilized and blocked with PBS (pH 7.4) containing 0.1% Triton X-100 and 5% BSA. Cells were then incubated for ~16 h at 4 °C with rabbit polyclonal anti-phospho-c-Jun (Ser-63) at a dilution of 1:1,000 in PBS containing 0.1% Triton X-100 and 2% BSA. The primary antibody was aspirated, and the cells were washed five times with PBS. The cells were then incubated with rhodamine-conjugated donkey anti-rabbit secondary antibody (1:500) for 1 h at room temperature. CGNs were then washed five more times with PBS, and coverslips were adhered to glass slides in mounting medium (0.1% *p*-phenylenediamine in 75% glycerol in PBS). Fluorescent images were captured using a 63 × oil immersion objective on a Zeiss Axioplan 2 microscope equipped with a Cooke sensicam deep-cooled CCD camera and a Slidebook software analysis program (Intelligent Imaging Innovations Inc., Denver).

F-actin Staining—CGNs cultured on polyethyleneimine-coated glass coverslips were incubated for ~24 h with either vehicle (BSA in PBS), toxin B, lethal toxin, or C2 toxin. After incubation, cells were fixed with paraformaldehye, permeabilized with Triton X-100, and incubated for 1 h with rhodamine-conjugated phalloidin and DAPI to stain F-actin and nuclei, respectively. Fluorescent images were captured under 63 × oil as described above.

Data Analysis—Results shown represent the means ± S.E. for the number (n) of independent experiments performed. Statistical differences between the means of unpaired sets of data were evaluated using one-way analysis of variance followed by a *post hoc* Dunnett's test. A p value of < 0.05 was considered statistically significant.

RESULTS

Inhibition of Rho, Rac, and Cdc42 with C. difficile Toxin B Induces Apoptosis of CGNs—Primary rat CGNs require survival signals derived from depolarization-induced calcium influx, and to a lesser extent serum, to be maintained in culture (19, 20). To determine if signals originating from Rho family GTPases are also required for CGN survival, the function of these G proteins was compromised by incubation with clostridial toxins that covalently modify and inhibit specific Rho family members (18). Toxin B from *C. difficile* is a monoglucosyltransferase that glucosylates a critical threonine residue within the Rho, Rac, and Cdc42 GTPases (26). Covalent modification of this site interferes with the ability of these G proteins to interact with their downstream effector proteins. Toxin B exhibits a very high degree of substrate specificity in that it glucosylates Rho, Rac, and Cdc42, but not other small molecular weight GTPases such as Ras, Rab, or Arf (26).

Incubation of CGNs for ~24 h with very low concentrations of toxin B (50–500 pg/ml) resulted in significant alterations in nuclear morphology with hallmarks of apoptotic cell death. Whereas cells incubated in the presence of vehicle displayed large intact nuclei, toxin B induced significant nuclear condensation and fragmentation (Fig. 1*A*). Identification of apoptotic nuclei by staining with Hoechst dye revealed a time- and concentrationdependent apoptotic mode of cell death after treatment with toxin B (Fig. 1*B*). Primary cultures of rat CGNs were F1

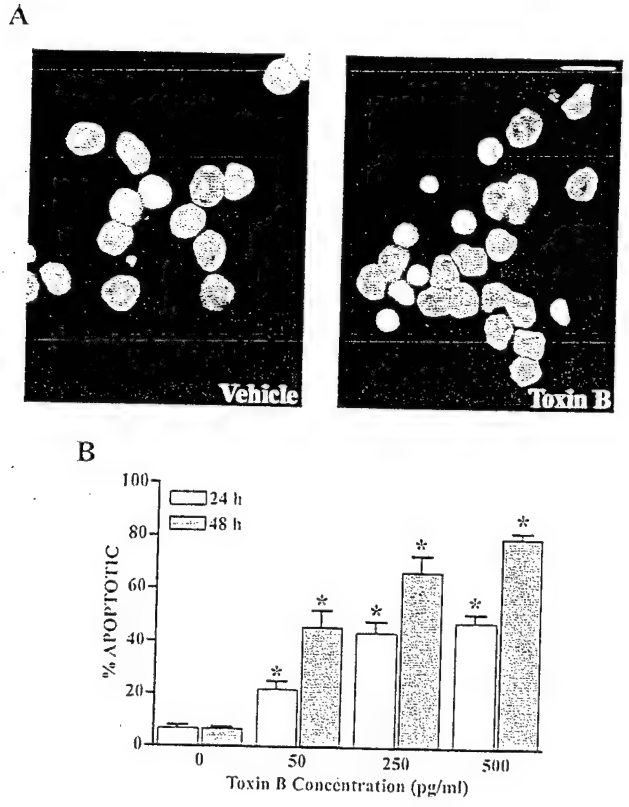

FIG. 1. **Inhibition of Rho, Rac, and Cdc42 function with *C. difficile* toxin B induces apoptosis of rat CGNs: cell death is dependent on *de novo* RNA and protein synthesis.** *A*, CGNs were cultured in medium containing serum and a depolarizing concentration of potassium. On culture day 7, either vehicle (1 mg/ml BSA in PBS, *left panel*) or 500 pg/ml toxin B (*right panel*) was added directly to the culture medium, and nuclei were stained 24 h later with DAPI. Apoptotic nuclei appear bright, condensed, and sometimes fragmented. *Scale bar* = 20 μm. *B*, neurons were incubated with varying concentrations of toxin B for 24 or 48 h, and apoptosis was quantitated by nuclear staining with Hoechst dye. *Asterisks* indicate a significant difference from the control ($p < 0.01$, $n = 3$). *C*, cells were incubated with either vehicle (*Veh*) or 500 pg/ml toxin B (*ToxB*) alone or in combination with either 10 μg/ml cycloheximide (*CHX*) or 2 μg/ml actinomycin D (*ActD*), and apoptosis was assessed as described in *B*. *Asterisks* indicate a significant difference from toxin B alone ($p < 0.01$, $n = 3$).

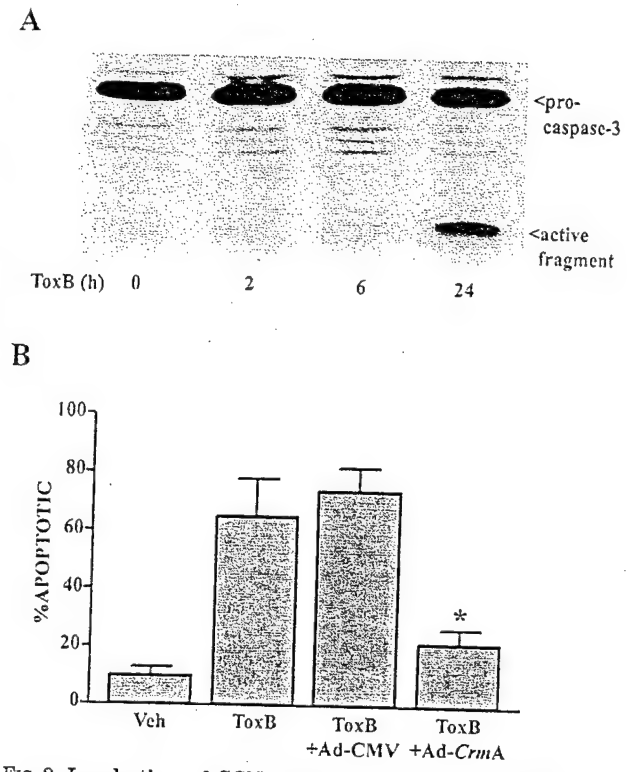

FIG. 2. **Incubation of CGNs with toxin B elicits activation of caspase-3: apoptosis is attenuated by inhibition of caspase function.** *A*, neurons were incubated with 500 pg/ml toxin B (*ToxB*) for varying times, and cell lysates were prepared for SDS-PAGE as described under "Experimental Procedures." Caspase-3 cleavage was assessed by immunoblotting with a polyclonal antibody that recognizes both pro-caspase-3 (~32 kDa) and an active fragment (~19 kDa). *B*, after 5 days in culture, granule neurons were infected with either control adenovirus (*Ad-CMV*) or adenoviral-*Crm*A (each at a multiplicity of infection of 5). On day 7, neurons were incubated with either PBS/BSA vehicle (*Veh*) or 500 pg/ml toxin B for a further 24 h, and the degree of apoptosis was compared in uninfected *versus* infected cells by Hoechst staining. The *asterisk* indicates a significant difference from toxin B in the uninfected control ($p < 0.01$, $n = 4$). AQ: L

remarkably sensitive to Rho GTPase inhibition with ~80% of the cells undergoing apoptosis after 48 h of incubation with 500 pg/ml toxin B. This latter observation is particularly striking given that cell death occurred in the presence of serum and a depolarizing concentration of potassium. Consistent with previous results that indicate that CGN apoptosis induced by withdrawal of serum and potassium is blocked by inhibitors of RNA or protein synthesis (19), toxin B-induced apoptosis was similarly prevented by coincubation with either cycloheximide or actinomycin D (Fig. 1*C*). Thus, apoptosis of CGNs after inhibition of Rho family GTPases apparently requires the synthesis of proapoptotic proteins.

Apoptotic cell death is orchestrated by the activation of a caspase cascade, proteases that cleave target proteins, including other caspases, at postaspartate residues (for review, see Ref. 27). Of the caspase family members, caspase-3 is commonly regarded as an "executioner" caspase because its cleavage from an inactive promolecule to an active protease by upstream caspases usually signifies commitment to apoptosis (28, 29). Caspase-3 activation is a key component of CGN apoptosis induced after the withdrawal of serum and potassium (30). In a like manner, prolonged inhibition of Rho GTPase function with toxin B led to a significant activation of caspase-3 (Fig. 2*A*). Moreover, adenoviral infection of CGNs with the known caspase inhibitor, *Crm*A (31), significantly attenuated toxin B-induced apoptosis (Fig. 2*B*). Collectively, these results indicate that inhibition of Rho family GTPases in CGNs evokes the activation of a caspase cascade that ultimately leads to apoptotic cell death. F2 AQ: H

Toxin B Elicits an Acute Increase in the Phosphorylation and Expression of c-Jun—Previous work has demonstrated that apoptosis of CGNs after withdrawal of serum and potassium requires the activity of the transcription factor c-Jun (32). Indeed, deprivation of serum and potassium for 4 h resulted in a substantial accumulation of phosphorylated c-Jun in the nu-

balt3/bc-bc/bc-bc/bc4201/bc4881-01a eichelbt S=4 11/9/01 18:21 4/Color Figure(s) 5 ARTNO: M103959200

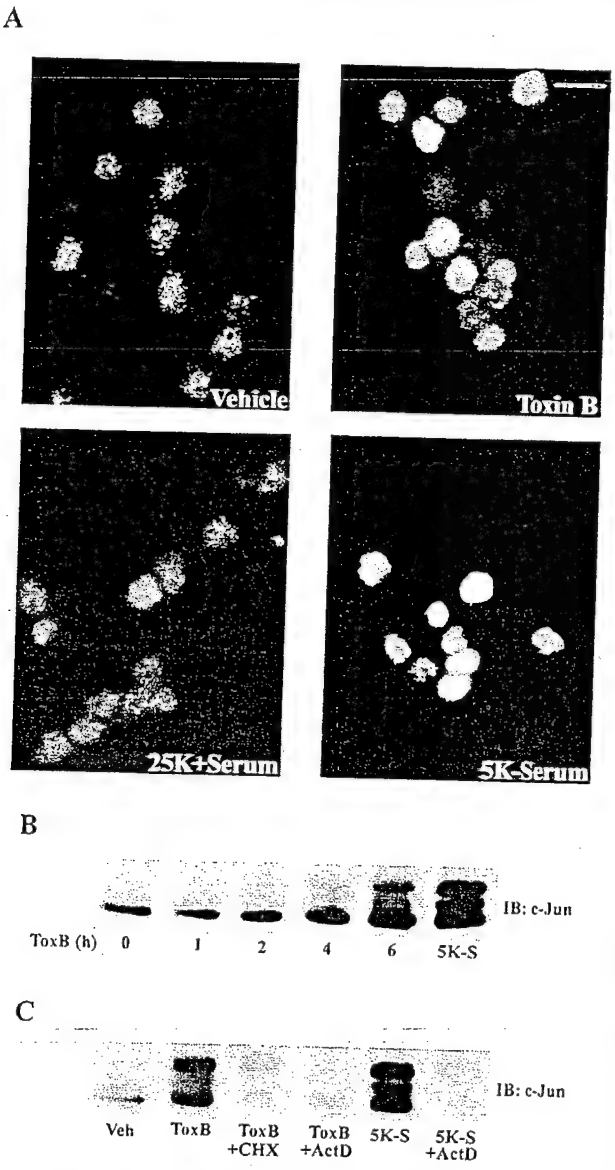

FIG. 3. **Toxin B stimulates an acute increase in c-Jun phosphorylation and expression which is dependent on RNA and protein synthesis.** *A*, granule neurons were incubated for 6 h with either vehicle (PBS containing 1 mg/ml BSA) or 500 pg/ml toxin B (*upper panels*). Alternatively, cells were incubated for 4 h in either high potassium medium containing serum (*25K+Serum*) or were deprived of serum and potassium (*5K−Serum*) (*lower panels*). After treatment, cells were fixed, and nuclear accumulation of phosphorylated c-Jun was analyzed by staining with a phospho-specific antibody that recognizes c-Jun phosphorylated on Ser-63, as described under "Experimental Procedures." *Scale bar* = 20 μm. *B*, cells were incubated for varying times with 500 pg/ml toxin B (*ToxB*) or for 4 h in low potassium, serum-free medium (*5K−S*). Cell lysates were subjected to SDS-PAGE and immunoblotted (*IB*) for total c-Jun. *C*, neurons were incubated for either 6 h with vehicle (*Veh*) or 500 pg/ml toxin B or for 4 h in 5K−S medium in the absence or presence of either 10 μg/ml cycloheximide (*CHX*) or 2 μg/ml actinomycin D (*ActD*). Total c-Jun was assessed by immunoblotting as described under "Experimental Procedures."

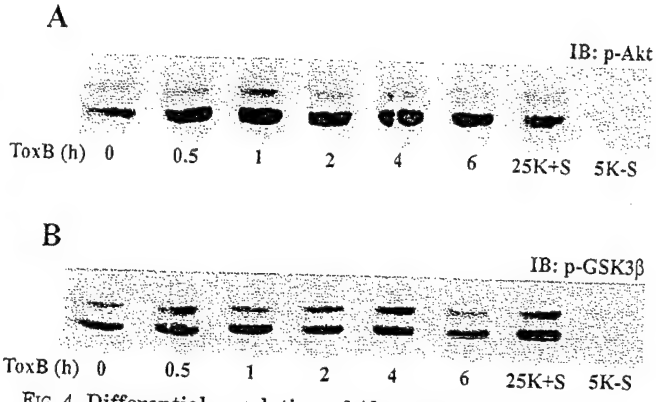

FIG. 4. **Differential regulation of Akt and GSK3β during apoptosis induced by either toxin B or withdrawal of serum and potassium.** CGNs were incubated for varying times with 500 pg/ml toxin B (*ToxB*). Alternatively, cells were incubated for 6 h in either high potassium medium containing serum (*25K+S*) or in low potassium, serum-free medium (*5K−S*). *A*, cell lysates were subjected to SDS-PAGE, transferred to polyvinylidene fluoride, and membranes were probed for active phosphorylated Akt (*p-Akt*) using an antibody that recognizes Akt phosphorylated on Ser-473. *B*, inactive phosphorylated GSK3β (*p-GSK3β*) was detected by immunoblotting (*IB*) with an antibody that recognizes GSK3β phosphorylated on Ser-9.

clei of CGNs (Fig. 3*A*, *lower panels*) and an overall increase in total c-Jun (including several distinct phosphorylation variants with differing apparent mobilities) in cell lysates (Fig. 3*B*, *first lane versus sixth lane*). Inhibition of Rho, Rac, and Cdc42 with toxin B for 6 h also resulted in significant increases in nuclear phospho-c-Jun (Fig. 3*A*, *upper panels*) and in total c-Jun detected in cell lysates (Fig. 3*B*). Furthermore, in accordance with the data presented in Fig. 1*C*, inhibitors of either protein or RNA synthesis essentially abolished the increase in c-Jun expression elicited by either toxin B or deprivation of serum and potassium (Fig. 3*C*). Thus, apoptosis induced after either an inhibition of Rho family GTPase function or removal of trophic factors is associated with enhanced phosphorylation and expression of the proapoptotic transcription factor c-Jun.

Akt and GSK3β Are Regulated Differentially during Apoptosis Induced by Toxin B or Withdrawal of Serum and Potassium—Akt is a serine-threonine kinase that has been shown to be downstream of phosphatidylinositol 3-kinase in a prosurvival signaling pathway that is activated by both growth factors and integrins. The catalytic function of Akt is activated by phosphorylation on Ser-473 by upstream kinases (33, 34). GSK3β is a putative downstream substrate of activated Akt known to play a proapoptotic role in neurons (25, 35). Phosphorylation of GSK3β on Ser-9 by Akt effectively inactivates the kinase activity of GSK3β and thereby inhibits its proapoptotic function (25, 36). Although withdrawal of serum and potassium from CGNs for 6 h promoted the dephosphorylation (inactivation) of Akt (Fig. 4*A*, *last lane*) and corresponding dephosphorylation (activation) of GSK3β (Fig. 4*B*, *last lane*), incubation with toxin B had no significant effect on the phosphorylation (*i.e.*, activation) status of either kinase. These results indicate that Rho GTPases do not significantly regulate the phosphatidylinositol 3-kinase-Akt cell survival pathway in CGNs.

Selective Inhibition of Rac/Cdc42 Function with C. sordellii Lethal Toxin Mimics the Effects of Toxin B on c-Jun Phosphorylation and Apoptosis of CGNs: Dissociation of Actin Cytoskeletal Disruption and Cell Death—Lethal toxin from *C. sordellii* is similar to toxin B in that it also has monoglucosyltransferase activity; however, these two toxins differ in their substrate specificities. Whereas toxin B glucosylates all three Rho family members (Rho, Rac, and Cdc42), Rho is not a substrate for lethal toxin which selectively modifies Rac and to a lesser extent Cdc42, as well as some other Ras subfamily members (18, 22, 37). The glucosylation of Rac and Cdc42 catalyzed by lethal toxin occurs on the same threonine residue as that modified by toxin B.

An inevitable consequence of inhibiting Rho family GTPases is an eventual disruption of the actin cytoskeleton (26). Accordingly, phalloidin staining of CGNs after 24 h of incubation with either toxin B or lethal toxin revealed a significant disruption

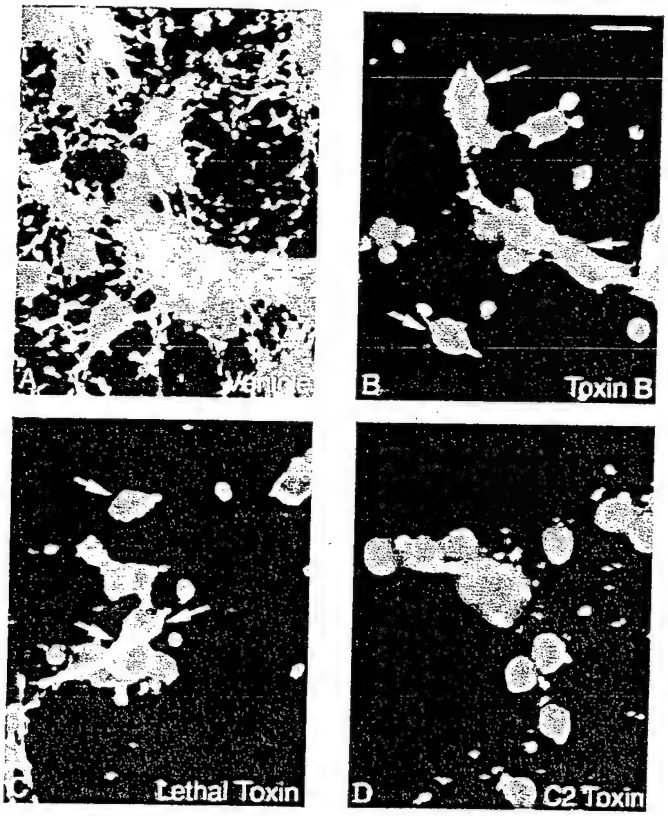

FIG. 5. **Incubation with *C. difficile* toxin B, *C. sordellii* lethal toxin, or *C. botulinum* C2 toxin induces disruption of the actin cytoskeleton in rat CGNs: differential effects on nuclear morphology.** Cells maintained in culture medium containing serum and a depolarizing concentration of potassium were exposed for 24 h to PBS/BSA vehicle (*A*), 500 pg/ml toxin B (*B*), 200 ng/ml lethal toxin (*C*), or 200 ng/ml C2 (*C2IIa+C2I*) toxin (*D*). After fixation, F-actin was visualized with rhodamine-conjugated phalloidin (shown in *white*), and nuclei were stained with DAPI (shown in *blue*). *Scale bar* = 20 μm. Cytoskeletal rounding and/or perinuclear accumulation of F-actin aggregates is indicated by the *arrows* in *B* and *C*. Note that although each toxin resulted in significant disruption of the actin cytoskeleton, a significant number of condensed nuclei were observed only in cells incubated with either toxin B or lethal toxin.

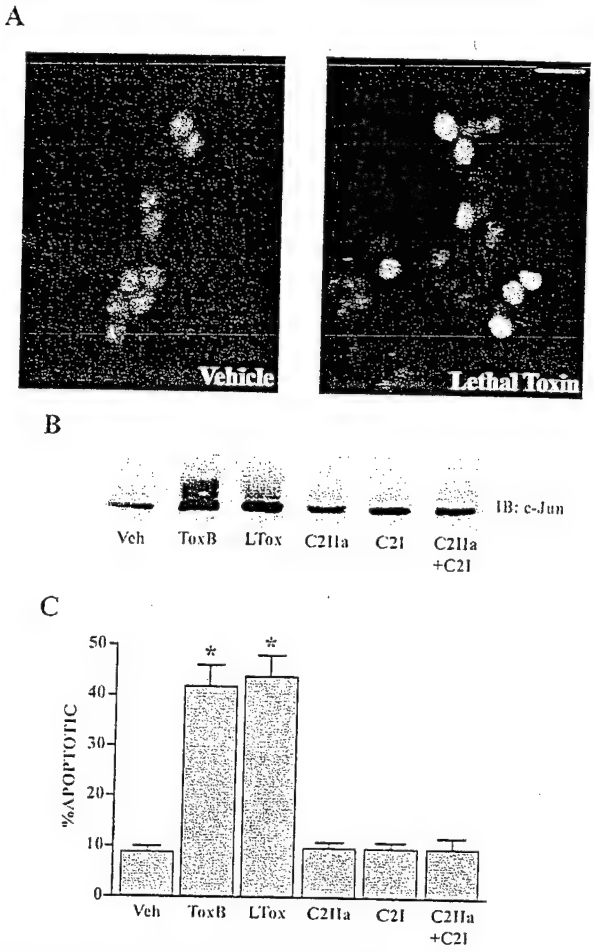

FIG. 6. **Selective inhibition of Rac/Cdc42 function with *C. sordellii* lethal toxin mimics the effects of toxin B on c-Jun phosphorylation/expression and neuronal apoptosis: direct ADP-ribosylation of F-actin with C2 toxin is insufficient to induce cell death.** *A*, granule neurons were incubated for 6 h with either vehicle (PBS containing 1 mg/ml BSA, *left panel*) or 200 ng/ml lethal toxin (*right panel*). After incubation, cells were fixed, and nuclear phospho-c-Jun was analyzed by staining with an antibody that specifically recognizes c-Jun phosphorylated on Ser-63, as described under "Experimental Procedures." *Scale bar* = 20 μm. *B*, cells were incubated for 6 h with either vehicle (*Veh*), 500 pg/ml toxin B (*ToxB*), 200 ng/ml lethal toxin (*LTox*), 200 ng/ml activated binding component of C2 toxin (*C2IIa*), 200 ng/ml catalytic component of C2 toxin (*C2I*), or complete C2 toxin (*C2IIa+C2I*). After treatment, cell lysates were resolved by SDS-PAGE, transferred to polyvinylidene fluoride, and membranes were probed for total c-Jun. *C*, neurons were incubated as described in *B* for 24 h. Apoptotic cells were quantified by nuclear staining with Hoechst dye. *Asterisks* indicate a significant difference from the vehicle control ($p < 0.01$, $n = 4$).

F5 of the cytoskeleton characterized by cell rounding and a perinuclear accumulation of F-actin aggregates (Fig. 5, *A–C*). Similarly, incubation with *C. botulinum* C2 toxin, an ADP-ribosyltransferase that directly modifies F-actin (23), resulted in a nearly complete loss of F-actin staining (Fig. 5*D*). Interestingly, although incubation of CGNs with each of the above three toxins led to disruption of the actin cytoskeleton, a significant number of condensed nuclei were only observed with toxin B or lethal toxin, but not C2 toxin (Fig. 5).

In a manner analogous to toxin B, selective inhibition of Rac/Cdc42 with lethal toxin elicited acute increases in both F6 nuclear staining for phospho-c-Jun (Fig. 6*A*) and total c-Jun detected in cell lysates (Fig. 6*B*). Lethal toxin also induced caspase-3 cleavage (data not shown), and prolonged incubation of CGNs with either toxin B or lethal toxin resulted in a similar degree of apoptosis (~45% apoptosis after 24 h) (Fig. 6*C*). In contrast, specific inhibition of either Rho (with *C. botulinum* C3 fusion toxin (24)) or Rho kinase (with Y27632 (38)) did not enhance c-Jun phosphorylation or induce CGN apoptosis (data not shown). Furthermore, direct disruption of F-actin with either C2 toxin, cytochalasin D, or latrunculin A was also insufficient to induce either c-Jun phosphorylation/expression (Fig. 6*B* and data not shown) or apoptosis (Fig. 6*C* and data not shown). These results indicate that a selective inhibition of Rac/Cdc42 function is entirely sufficient to evoke CGN apoptosis independently of Rho inactivation. Furthermore, the apoptosis induced after inhibition of Rac/Cdc42 also occurs independently of actin cytoskeletal disruption.

CGNs Possess High Intrinsic JNK Activity and Low Basal p38 MAP Kinase Activity That Are Unaffected by Toxin B—To determine if the increase in c-Jun phosphorylation observed after acute inhibition of Rho family GTPases was caused by an enhancement of stress-activated protein kinase activity, the degree of JNK and p38 MAP kinase activation was assessed in CGNs. CGNs exhibited high basal JNK activity indicated by significant amounts of dually phosphorylated 46-kDa and 54-kDa isoforms of JNK which were only slightly increased by anisomycin exposure (Fig. 7*A*, *first lane versus sixth lane*). F7 Incubation with toxin B for up to 6 h did not significantly increase the high basal JNK activity detected in CGNs (Fig.

balt3/bc-bc/bc-bc/bc4201/bc4881-01a eichelbt S=4 11/9/01 18:23 4/Color Figure(s) 5 ARTNO: M103959200

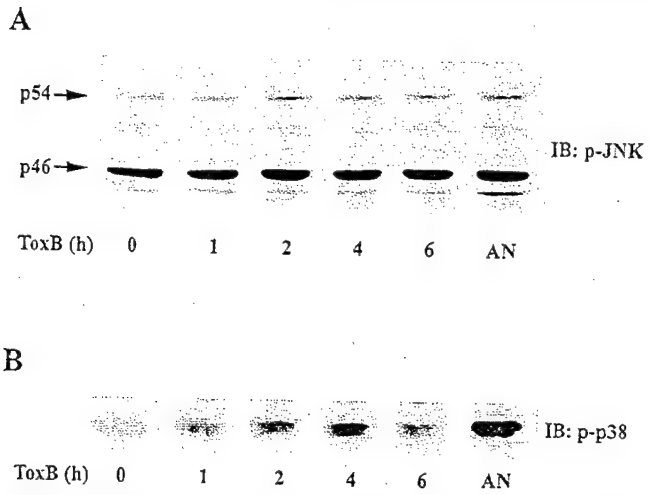

FIG. 7. **Primary cultures of rat CGNs exhibit high basal JNK activity and low basal p38 MAP kinase activity, neither of which is affected by incubation with toxin B.** Granule neurons were incubated for varying times with 500 pg/ml toxin B (*ToxB*) or for 1 h with 10 μM anisomycin (*AN*). After incubation, cell lysates were subjected to SDS-PAGE, transferred to polyvinylidene fluoride, and probed for either active JNK (*p-JNK*) (*A*) or active p38 (*p-p38*) (*B*) with antibodies that specifically recognize the Tyr/Thr dually phosphorylated forms of the enzymes.

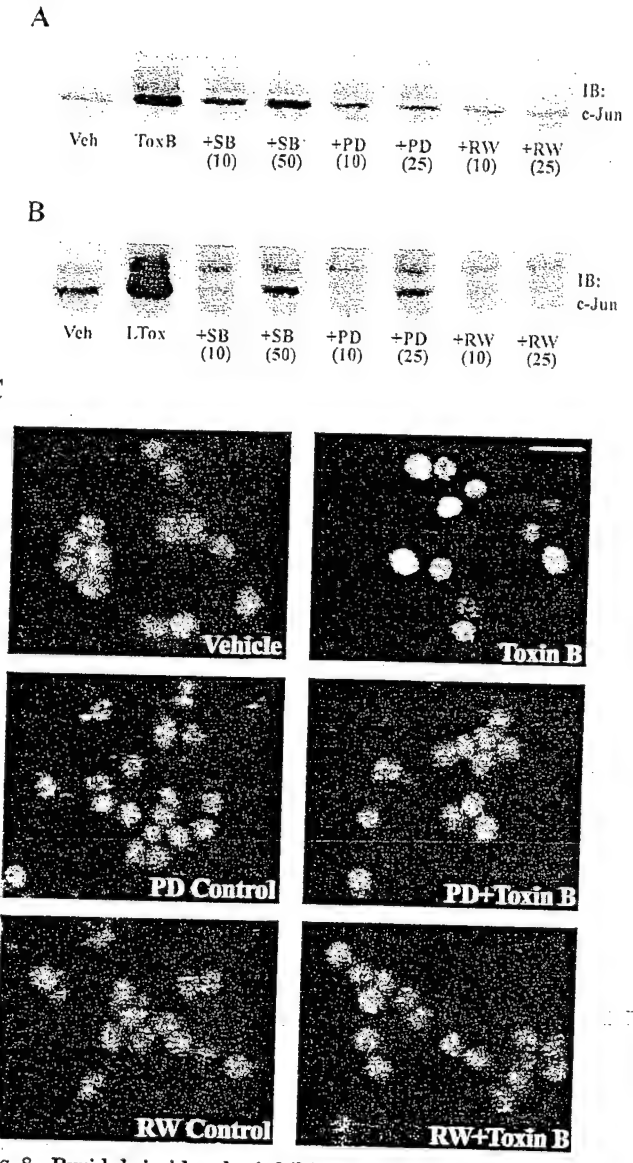

FIG. 8. **Pyridyl imidazole inhibitors of p38/JNK signaling block the increase in c-Jun phosphorylation/expression induced by both toxin B and lethal toxin.** Neurons were incubated for 6 h with either 500 pg/ml toxin B (*ToxB*) (*A*) or 200 ng/ml lethal toxin (*LTox*) (*B*) alone or in combination with 10 or 50 μM SB203580 (*SB*), 10 or 25 μM PD169316 (*PD*), or 10 or 25 μM RWJ67657 (*RW*). After incubation, cell lysates were immunoblotted for total c-Jun. *C*, cells were incubated as described above with toxin B alone or in combination with either 25 μM PD169316 or 25 μM RWJ67657. Nuclear accumulation of c-Jun phosphorylated on Ser-63 was assessed as described under "Experimental Procedures." *Scale bar* = 20 μm.

7*A*). Relative to JNK activity, the basal p38 MAP kinase activity of CGNs was low as demonstrated by a substantial increase after anisomycin exposure (Fig. 7*B*, *first lane versus sixth lane*). Yet, incubation of CGNs with toxin B did not result in a significant increase in the activation of p38 MAP kinase (Fig. 7*B*). Thus, inhibition of Rho family GTPases does not promote a detectable activation of stress-activated protein kinases in CGNs.

Pyridyl Imidazole Inhibitors of p38/JNK Signaling and Adenoviral DN-c-Jun Attenuate CGN Apoptosis Induced after Inhibition of Rac/Cdc42 Function—Recently, others have reported that CGNs exhibit high basal JNK activity that is largely unaltered by withdrawal of serum and potassium (32). However, Coffey *et al.* (39) have demonstrated that a small pool of active JNK may translocate from the cytoplasm to the nucleus in response to stress, where it can then phosphorylate c-Jun. To determine if the high basal JNK activity detected in CGNs was required for the enhanced phosphorylation of c-Jun after inhibition of Rac/Cdc42, we utilized several pyridyl imidazole compounds to inhibit JNK and p38 activities in CGNs. Although this class of compounds has previously been thought to inhibit p38 MAP kinase specifically, a recent report demonstrated that pyridyl imidazoles are also capable of blocking JNK activity in CGNs (40). Coincubation of CGNs with any one of three different pyridyl imidazole compounds (SB203580 (40), PD169316 (41), or RWJ67657 (42)) significantly attenuated the increase in total c-Jun induced by either toxin B (Fig. 8*A*) or lethal toxin (Fig. 8*B*). The two more potent compounds, PD169316 and RWJ67657, were also very effective at inhibiting the nuclear accumulation of phosphorylated c-Jun elicited by toxin B (Fig. 8*C*). In agreement with c-Jun playing a causative role in CGN apoptosis resulting from inhibition of Rac/Cdc42, the pyridyl imidazoles significantly blunted apoptosis in cells incubated with either toxin B (Fig. 9*A*) or lethal toxin (Fig. 9*B*). Moreover, adenoviral DN-c-Jun also significantly attenuated toxin B-induced apoptosis (Fig. 9*C*). Thus, an enhanced phosphorylation and expression of the transcription factor, c-Jun, are required for CGN apoptosis induced by inhibition of Rac/Cdc42 function.

DISCUSSION

Primary rat CGNs are a widely studied model of activity-dependent (depolarization-mediated) neuronal survival. Membrane depolarization elicits Ca^{2+} influx through L-type voltage-gated channels, and inhibitors of Ca^{2+} entry induce apoptosis of CGNs (20). Recently, one Ca^{2+}-dependent survival factor was identified as the transcription factor, myocyte-enhancer factor-2 (43). Transfection of CGNs with a constitutively active mutant of myocyte-enhancer factor-2 attenuates apoptosis induced by lowering extracellular potassium (43). In addition to Ca^{2+}-dependent survival signals, growth factors such as insulin-like growth factor-I are also known to protect CGNs from apoptosis induced by withdrawal of serum and potassium (19, 20). The principal sur-

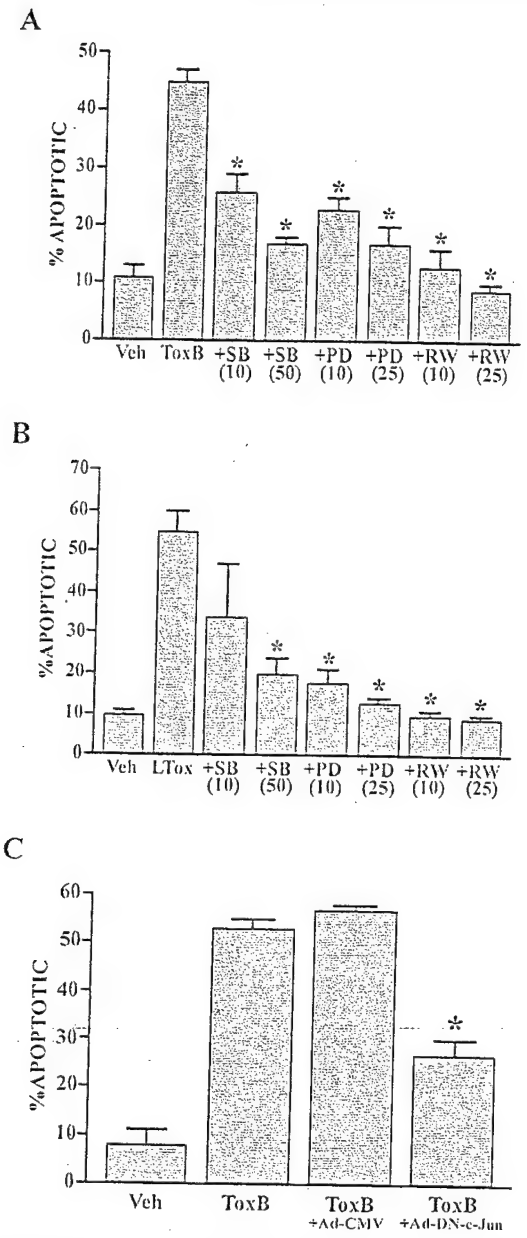

FIG. 9. **Pyridyl imidazoles and adenoviral DN-c-Jun attenuate apoptosis of CGNs induced by either toxin B or lethal toxin.** Granule neurons were incubated for 24 h with 500 pg/ml toxin B (*ToxB*) (*A*) or 200 ng/ml lethal toxin (*LTox*) (*B*) alone or in combination with pyridyl imidazole inhibitors of p38/JNK as described in the legend to Fig. 8. Apoptosis was quantitated by nuclear staining with Hoechst dye. *Asterisks* indicate a significant difference from either toxin B (*A*) or lethal toxin (*B*) alone ($p < 0.01$, $n = 3$). *C*, cells were infected with either control adenovirus (*Ad-CMV*) or Ad-DN-c-Jun (each at a multiplicity of infection of 10) followed by incubation with toxin B; apoptosis was quantified by Hoechst staining. *Asterisks* indicate a significant difference from toxin B in the uninfected control ($p < 0.01$, $n = 3$).

vival signaling pathway stimulated by growth factors is a phosphatidylinositol 3-kinase-dependent activation of the antiapoptotic kinase Akt (25, 34, 44). Thus, CGN survival is promoted by signals originating from both Ca^{2+} influx and growth factor receptors.

In the present study, we have identified a novel prosurvival signaling pathway in CGNs which requires the function of Rho family GTPases. Incubation of CGNs with either *C. difficile* toxin B (an inhibitor of Rho, Rac, and Cdc42) or *C. sordellii* lethal toxin (a selective inhibitor of Rac and to a lesser extent Cdc42) induced cell death with biochemical and morphological hallmarks of apoptosis. Inhibition of Rac/Cdc42 function promoted activation of caspase-3 and induced nuclear condensation and fragmentation. These effects were not observed in CGNs incubated with specific inhibitors of either Rho (C3 fusion toxin) or the Rho effector, Rho kinase (Y27632). Like apoptosis evoked by withdrawal of serum and potassium (19, 30), cell death induced by either toxin B or lethal toxin was prevented by inhibitors of RNA or protein synthesis, as well as an inhibitor of caspases (*Crm*A). Surprisingly, inhibition of Rac/Cdc42 was able to induce apoptosis of CGNs incubated in medium containing both serum and a depolarizing concentration of potassium, suggesting that serum-derived and Ca^{2+}-dependent survival factors cannot compensate for the loss of GTPase function. These observations illustrate that the maintenance of Rac/Cdc42 function is obligatory for CGN survival. AQ: J

Previous work in other neuronal cell systems has yielded somewhat conflicting data on the role of Rho GTPases in neuronal survival. For example, Cdc42 and Rac facilitate apoptosis of primary sympathetic neurons during nerve growth factor withdrawal by activation of an apoptosis signal-regulated kinase/JNK signaling pathway (14, 15). However, in primary cortical neurons and rat brain neuroblasts the isoprenylation/plasma membrane localization of Rho GTPases correlates with neuronal survival (16, 17). Our data are the first to establish clearly a prosurvival function for Rho family GTPases in a neuronal cell model by utilizing highly selective inhibitors of Rho GTPase function (clostridial toxins). Collectively, these data indicate that as in non-neuronal cells, Rho GTPases can play either a prosurvival or proapoptotic role in neuronal cells depending on the type of neuron studied.

As mentioned above, growth factor-mediated survival of CGNs occurs primarily via a phosphatidylinositol 3-kinase-dependent activation of Akt (25, 34, 44). Akt, in turn, phosphorylates and inactivates several proapoptotic signaling molecules including GSK3β (36). Many studies have previously demonstrated a relationship between the Rac GTPase and phosphatidylinositol 3-kinase/Akt activity (45–47). Therefore, it was of interest to determine if inhibition of Rac function with *C. difficile* toxin B affected the activation status of either Akt or GSK3β in CGNs. In contrast to serum and potassium withdrawal, which led to an inactivation of Akt and a concurrent activation of GSK3β, toxin B had no effect on the activation status of either of these kinases. This result demonstrates that Rac does not influence phosphatidylinositol 3-kinase/Akt activity in CGNs significantly.

An inevitable downstream consequence of inhibiting Rho family GTPase function is the disruption of the actin cytoskeleton (26). In many non-neuronal cells, actin cytoskeletal disruption evokes apoptotic cell death (48–50). In the present study, apoptosis of CGNs induced by inhibition of Rho GTPases could be entirely dissociated from actin cytoskeletal disruption because agents that directly disassemble F-actin, *C. botulinum* C2 toxin, cytochalasin D, and latrunculin A, did not induce cell death within 24 h. Similar results were observed in intestinal epithelial cells that also undergo apoptosis after incubation with toxin B but not cytochalasin D (51). Our data indicate that the apoptosis observed in CGNs after blockade of Rac/Cdc42 function is likely the result of the inhibition of a specific downstream effector(s) of these GTPases rather than a global perturbation of CGN morphology. In this context, the serine/threonine kinase, p21-activated kinase, is a Rac/Cdc42 effector that has recently been shown to phosphorylate and inactivate proapoptotic signaling molecules such as the Bcl-2 family member Bad (52). Thus, future work will focus on the identification of Rac/Cdc42 effectors that promote survival of CGNs.

Inhibition of Rac/Cdc42 in CGNs induced a marked increase

in the phosphorylation, expression, and nuclear accumulation of the transcription factor c-Jun. c-Jun is a required proapoptotic factor in both nerve growth factor withdrawal-induced death of sympathetic neurons (53) and in CGN death after withdrawal of serum and potassium (32). In primary sympathetic neurons, nerve growth factor withdrawal is associated with an increase in the activity of the stress-activated protein kinase JNK (53). In contrast, CGNs have been reported to contain high basal JNK activity and low p38 MAP kinase activity that are unaffected by withdrawal of serum and potassium (32). The observation that inhibition of Rac/Cdc42 function enhanced c-Jun phosphorylation is somewhat paradoxical in that Cdc42 and Rac have been implicated upstream of JNK activation by several groups (14, 54, 55). In the present study, we observed high basal JNK activity and low p38 activity in control cultures of CGNs, neither of which was significantly increased after incubation with toxin B. Thus, inhibition of Rac/Cdc42 in CGNs increases c-Jun phosphorylation independently of activating stress-activated protein kinase cascades. Moreover, these data suggest that JNK activity in CGNs is regulated by a mechanism that is distinct from Rac/Cdc42 signaling. Similar Rac/Cdc42-independent regulation of JNK has been observed in fibroblasts and endothelial cells in response to platelet-derived growth factor and interleukin-1 (56).

Finally, pyridyl imidazole compounds that inhibit both p38 and JNK activities in CGNs (40) significantly attenuated both the increase in c-Jun phosphorylation and apoptosis induced after inhibition of Rac/Cdc42 with either toxin B or lethal toxin. These results are in agreement with previous data that showed that pyridyl imidazoles also inhibit apoptosis of CGNs evoked by withdrawal of serum and potassium (40) and improve the survival of transplanted neurons *in vivo* (41). In addition, CGN apoptosis induced by toxin B was also attenuated significantly by adenoviral DN-c-Jun. The above results suggest that the high basal JNK activity detected in CGNs is likely responsible for the enhanced phosphorylation of c-Jun after inhibition of Rac/Cdc42. Furthermore, c-Jun phosphorylation is required for apoptosis of CGNs in response to Rac/Cdc42 inhibition. The mechanism underlying the JNK-mediated phosphorylation of c-Jun in the absence of a detectable increase in JNK activity may involve translocation of a small pool of active JNK to the nucleus (39). Alternatively, modification of the association between JNK and the JNK-interacting protein JIP, which inhibits the JNK/c-Jun interaction, may also play a role (39). Interestingly, JIP has recently been shown to associate with a guanine nucleotide exchange factor for the Rho family GTPases (57). This latter observation suggests the possibility that active Rho GTPases may be required to maintain the JNK-JIP interaction, and therefore, inhibition of Rho GTPases may release active JNK from JIP, allowing for its interaction with and phosphorylation of c-Jun.

In summary, we have demonstrated that selective inhibition of Rac/Cdc42 with clostridial toxins induces apoptosis of CGNs. Cell death was observed in the presence of serum and depolarizing potassium, indicating that growth factor-mediated and Ca^{2+}-dependent survival signals could not compensate for the loss of GTPase function. Apoptosis occurred independently of actin cytoskeletal disruption but required signaling via the transcription factor c-Jun. These data indicate that specific effectors of Rac/Cdc42 GTPases promote the survival of CGNs.

Acknowledgments—We thank Ron Bouchard for assistance with the preparation of the manuscript.

REFERENCES

1. Nobes, C. D., and Hall, A. (1995) *Cell* **81**, 53–62
2. Olson, M. F., Ashworth, A., and Hall, A. (1995) *Science* **269**, 1270–1272
3. Hill, C. S., Wynne, J., and Treisman, R. (1995) *Cell* **81**, 1159–1170
4. Clark, E. A., King, W. G., Brugge, J. S., Symons, M., and Hynes, R. O. (1998) *J. Cell Biol.* **142**, 573–586
5. Fukata, M., Kuroda, S., Nakagawa, M., Kawajiri, A., Itoh, N., Shoji, I., Matsuura, Y., Yonehara, S., Fujisawa, H., Kikuchi, A., and Kaibuchi, K. (1999) *J. Biol. Chem.* **274**, 26044–26050
6. Gomez, J., Martinez, C., Giry, M., Garcia, A., and Rebollo, A. (1997) *Eur. J. Immunol.* **27**, 2793–2799
7. Fiorentini, C., Matarrese, P., Straface, E., Falzano, L., Fabbri, A., Donelli, G., Cossarizza, A., Boquet, P., and Malorni, W. (1998) *Exp. Cell Res.* **242**, 341–350
8. Fiorentini, C., Fabbri, A., Matarrese, P., Falzano, L., Boquet, P., and Malorni, W. (1997) *Biochem. Biophys. Res. Commun.* **241**, 341–346
9. Boehm, J. E., Chaika, O. V., and Lewis, R. E. (1999) *J. Biol. Chem.* **274**, 28632–28636
10. Joneson, T., and Bar-Sagi, D. (1999) *Mol. Cell. Biol.* **19**, 5892–5901
11. Nishida, K., Kaziro, Y., and Satoh, T. (1999) *Oncogene* **18**, 407–415
12. Embade, N., Valerón, P. F., Aznar, S., López-Collazo, E., and Lacal, J. C. (2000) *Mol. Biol. Cell* **11**, 4347–4358
13. Subauste, M. C., Von Herrath, M., Benard, V., Chamberlain, C. E., Chuang, T.-H., Chu, K., Bokoch, G. M., and Hahn, K. M. (2000) *J. Biol. Chem.* **275**, 9725–9733
14. Bazenet, C. E., Mota, M. A., and Rubin, L. L. (1998) *Proc. Natl. Acad. Sci. U. S. A.* **95**, 3984–3989
15. Kanamoto, T., Mota, M., Takeda, K., Rubin, L. L., Miyazono, K., Ichijo, H., and Bazenet, C. E. (2000) *Mol. Cell. Biol.* **20**, 196–204
16. Tanaka, T., Tatsuno, I., Uchida, D., Moroo, I., Morio, H., Nakamura, S., Noguchi, Y., Yasuda, T., Kitagawa, M., Saito, Y., and Hirai, A. (2000) *J. Neurosci.* **20**, 2852–2859
17. Garcia-Roman, N., Alvarez, A. M., Toro, M. J., Montes, A., and Lorenzo, M. J. (2001) *Mol. Cell. Neurosci.* **17**, 329–341
18. Busch, C., and Aktories, K. (2000) *Curr. Opin. Struct. Biol.* **10**, 528–535
19. D'Mello, S. R., Galli, C., Ciotti, T., and Calissano, P. (1993) *Proc. Natl. Acad. Sci. U. S. A.* **90**, 10989–10993
20. Galli, C., Meucci, O., Scorziello, A., Werge, T. M., Calissano, P., and Schettini, G. (1995) *J. Neurosci.* **15**, 1172–1179
21. Von Eichel-Streiber, C., Harperath, U., Bosse, D., and Hadding, U. (1987) *Microb. Pathog.* **2**, 307–318
22. Just, I., Selzer, J., Hofmann, F., Green, G. A., and Aktories, K. (1996) *J. Biol. Chem.* **271**, 10149–10153
23. Aktories, K., Bärmann, M., Ohishi, I., Tsuyama, S., Jakobs, K. H., and Habermann, E. (1986) *Nature* **322**, 390–392
24. Barth, H., Hofmann, F., Olenik, C., Just, I., and Aktories, K. (1998) *Infect. Immun.* **66**, 1364–1369
25. Li, M., Wang, X., Meintzer, M. K., Laessig, T., Birnbaum, M. J., and Heidenreich, K. A. (2000) *Mol. Cell. Biol.* **20**, 9356–9363
26. Just, I., Selzer, J., Wilm, M., Von Eichel-Streiber, C., Mann, M., and Aktories, K. (1995) *Nature* **375**, 500–503
27. Nunez, G., Benedict, M. A., Hu, Y., and Inohara, N. (1998) *Oncogene* **17**, 3237–3245
28. Kumar, S. (1997) *Int. J. Biochem. Cell Biol.* **29**, 393–396
29. Porter, A. G., and Janicke, R. U. (1999) *Cell Death Differ.* **6**, 99–104
30. Eldadah, B. A., Ren, R. F., and Faden, A. I. (2000) *J. Neurosci.* **20**, 179–186
31. Garcia-Calvo, M., Peterson, E. P., Leiting, B., Ruel, R., Nicholson, D. W., and Thornberry, N. A. (1998) *J. Biol. Chem.* **273**, 32608–32613
32. Watson, A., Eilers, A., Lallemand, D., Kyriakis, J., Rubin, L. L., and Ham, J. (1998) *J. Neurosci.* **18**, 751–762
33. Delcommenne, M., Tan, C., Gray, V., Rue, L., Woodgett, J., and Dedhar, S. (1998) *Proc. Natl. Acad. Sci. U. S. A.* **95**, 11211–11216
34. Downward, J. (1998) *Curr. Opin. Cell Biol.* **10**, 262–267
35. Hetman, M., Cavanaugh, J. E., Kimelman, D., and Xia, Z. (2000) *J. Neurosci.* **20**, 2567–2574
36. Shaw, M., Cohen, P., and Alessi, D. R. (1997) *FEBS Lett.* **416**, 307–311
37. Popoff, M. R., Chaves-Olarte, E., Lemichez, E., Von Eichel-Streiber, C., Thelestam, M., Chardin, P., Cussac, D., Antonny, B., Chavrier, P., Flatau, G., Giry, M., Gunzburg, J., and Boquet, P. (1996) *J. Biol. Chem.* **271**, 10217–10224
38. Uehata, M., Ishizaki, T., Satoh, H., Ono, T., Kawahara, T., Morishita, T., Tamakawa, H., Yamagami, K., Inui, J., Maekawa, M., and Narumiya, S. (1997) *Nature* **389**, 990–994
39. Coffey, E. T., Hongisto, V., Dickens, M., Davis, R. J., and Courtney, M. J. (2000) *J. Neurosci.* **20**, 7602–7613
40. Harada, J., and Sugimoto, M. (1999) *Jpn. J. Pharmacol.* **79**, 369–378
41. Zawada, W. M., Meintzer, M. K., Rao, P., Marotti, J., Wang, X., Esplen, J. E., Clarkson, E. D., Freed, C. R., and Heidenreich, K. A. (2001) *Brain Res.* **891**, 185–196
42. Wadsworth, S. A., Cavender, D. E., Beers, S. A., Lalan, P., Schafer, P. H., Malloy, E. A., Wu, W., Fahmy, B., Olini, G. C., Davis, J. E., Pellegrino-Gensey, J. L., Wachter, M. P., and Siekierka, J. J. (1999) *J. Pharmacol. Exp. Ther.* **291**, 680–687
43. Mao, Z., Bonni, A., Xia, F., Nadal-Vicens, M., and Greenberg, M. E. (1999) *Science* **286**, 785–790
44. Miller, T. M., Tansey, M. G., Johnson, E. M., Jr., and Creedon, D. J. (1997) *J. Biol. Chem.* **272**, 9487–9453
45. Carpenter, C. L. (1996) *Cell Dev. Biol.* **7**, 691–697
46. Ren, X.-D., and Schwartz, M. A. (1998) *Curr. Opin. Genet. Dev.* **8**, 63–67
47. Djouder, N., Schmidt, G., Frings, M., Cavalié, A., Thelen, M., and Aktories, K. (2001) *J. Immunol.* **166**, 1627–1634
48. Iimura, O., Vrtovsnik, F., Terzi, F., and Friedlander, G. (1997) *Kidney Int.* **52**, 962–972
49. Suria, H., Chau, L. A., Negrou, E., Kelvin, D. J., and Madrenas, J. (1999) *Life Sci.* **65**, 2697–2707
50. Yamazaki, Y., Tsuruga, M., Zhou, D., Fujita, Y., Shang, X., Dang, Y., Kawasaki, K., and Oka, S. (2000) *Exp. Cell Res.* **259**, 64–78
51. Fiorentini, C., Fabbri, A., Falzano, L., Fattorossi, A., Matarrese, P., Rivabene,

R., and Donelli, G. (1998) *Infect. Immun.* **66**, 2660–2665
52. Schurmann, A., Mooney, A. F., Sanders, L. C., Sells, M. A., Wang, H. G., Reed, J. C., and Bokoch, G. M. (2000) *Mol. Cell. Biol.* **20**, 453–461
53. Eilers, A., Whitfield, J., Babij, C., Rubin, L. L., and Ham, J. (1998) *J. Neurosci.* **18**, 1713–1724
54. Coso, O. A., Chiariello, M., Yu, J. C., Teramoto, H., Crespo, P., Xu, N., Miki, T., and Gutkind, J. S. (1995) *Cell* **81**, 1137–1146
55. Minden, A., Lin, A., Claret, F. X., Abo, A., and Karin, M. (1995) *Cell* **81**, 1147–1157
56. Davis, W., Stephens, L. R., Hawkins, P. T., and Saklatvala, J. (1999) *Biochem. J.* **338**, 387–392
57. Meyer, D., Liu, A., and Margolis, B. (1999) *J. Biol. Chem.* **274**, 35113–35118

ELSEVIER

Appendix 3

Brain Research 891 (2001) 185–196

BRAIN RESEARCH

www.elsevier.com/locate/bres

Research report

Inhibitors of p38 MAP kinase increase the survival of transplanted dopamine neurons

W. Michael Zawada,[a,c], Mary K. Meintzer[b,d], Pravin Rao[b,d], Jonathan Marotti[a], Xiaomin Wang[b,d], James E. Esplen[a], Edward D. Clarkson[a], Curt R. Freed[a,c], Kim A. Heidenreich[b,c,d,*]

[a]*Departments of Medicine and Pharmacology, Division of Clinical Pharmacology, University of Colorado School of Medicine, Denver, CO 80262, USA*

[b]*Department of Pharmacology, Denver, CO 80262, USA*

[c]*Neuroscience Training Program, University of Colorado School of Medicine, Denver, CO 80262, USA*

[d]*Denver Veterans Administration Medical Center, Denver, CO 80220, USA*

Accepted 12 September 2000

Abstract

Fetal cell transplantation therapies are being developed for the treatment of a number of neurodegenerative disorders including Parkinson's disease [10–12,21,22,24,36,43]. Massive apoptotic cell death is a major limiting factor for the success of neurotransplantation. We have explored a novel protein kinase pathway for its role in apoptosis of dopamine neurons. We have discovered that inhibitors of p38 MAP kinase (the pyridinyl imidazole compounds: PD169316, SB203580, and SB202190) improve survival of rat dopamine neurons in vitro and after transplantation into hemiparkinsonian rats. In embryonic rat ventral mesencephalic cultures, serum withdrawal led to 80% loss of dopamine neurons due to increased apoptosis. Incubation of the cultures with p38 MAP kinase inhibitors at the time of serum withdrawal prevented dopaminergic cell death by inhibiting apoptosis. In the hemiparkinsonian rat, preincubation of ventral mesencephalic tissue with PD169316 prior to transplantation accelerated behavioral recovery and doubled the survival of transplanted dopamine neurons. We conclude that inhibitors of stress-activated protein kinases improve the outcome of cell transplantation by preventing apoptosis of neurons after grafting.

Theme: Development and regeneration

Topic: Transplantation

Keywords: Pyridinyl imidazole; Apoptosis; Parkinson's disease; Neurodegeneration; Neurotransplantation; Dopamine neuron; p38 MAP kinase

1. Introduction

Parkinson's disease is a neurodegenerative disorder characterized by progressive deterioration of motor function resulting from the loss of nigrostriatal dopamine neurons and depletion of striatal dopamine [9]. Because L-dopa [6] therapy loses its effectiveness after 5 to 20 years of treatment, alternative therapeutic strategies such as neurotransplantation of fetal dopamine cells have been sought. Despite the success of neural transplants in some Parkinson patients, other patients improve only slightly or not at all. Data from animal [4] and human post-mortem studies [22] indicate that much of the variability in neurotransplantation results from poor survival of transplanted dopamine cells. Although some cells in the transplants probably die by necrosis from handling and shear forces created during implantation, the majority of the observed cell death is apoptotic [27,46]. The number of apoptotic cells observed in grafts of ventral mesencephalic tissue in parkinsonian rats is greatest during the first 24 h after transplantation and is dramatically reduced by the end of the first week [46]. These findings offer the exciting possibility that signaling pathways leading to the initiation

*Corresponding author. Tel.: +1-303-399-8020 ext. 3891; fax: +1-303-393-5271.

E-mail address: kim.heidenreich@uchsc.edu (K.A. Heidenreich).

0006-8993/01/$ – see front matter
PII: S0006-8993(00)02965-6

and execution of apoptosis can be blocked to prevent or reduce neuronal cell death.

Recent evidence from a number of laboratories indicates that the stress-activated MAP kinase, p38 MAP kinase, modulates cellular apoptosis. Effects of p38 MAP kinase are complex due to the existence of at least four isoforms, for review see [35]. The activity of p38 MAP kinase is stimulated by factors that induce apoptosis including trophic factor withdrawal [23,47], excitotoxic stimuli [20], and Fas activation [19]. Transfection of cells with constitutively-active upstream regulators of p38 MAP kinase induce apoptosis, whereas, dominant negative upstream kinases block cell death in response to apoptotic stimuli [17,18,42,47]. Peptide growth factors like insulin that support cell survival block the activity of p38 MAP kinase [15]. Finally, pyridinyl imidazole inhibitors of p38 MAP kinase block apoptosis in clonal cell lines [23] and embryonic chick neurons [16] in response to trophic factor withdrawal and in primary cerebellar granule neurons in response to cytotoxic stimuli [20]. In addition to its role in apoptosis, p38 MAP kinase plays a significant role in inflammation [2], control of the cell cycle, and differentiation of PC12 cells into neurons [32].

We have explored the p38 MAP kinase pathway for its role in apoptosis of dopamine neurons and found that inhibitors of p38 MAP kinase improve survival of dopamine neurons both in culture and after neurotransplantation in parkinsonian rats. These inhibitors offer advantages over other anti-apoptotic approaches because they are small organic molecules that are orally active [2,25] and cross the blood–brain barrier.

2. Methods

2.1. Culture of mesencephalic neurons and detection of apoptosis

E15 rat ventral mesencephalon was dissected as previously described [8]. Primary cultures of rat ventral mesencephalon were prepared in 1 ml of ice cold Ca^{2+}/Mg^{2+}-free Hanks' balanced salt solution (Mediatech) by mechanically dispersing tissue pieces using a sterile tip of a 1.0 ml Pipetman. Subsequently, cells were centrifuged at $200\times g$ for 5 min and resuspended in F12 medium (Irvine Sci.) with 5% human placental serum, 2 mM L-glutamine, 100 μg/ml streptomycin, 100 U/ml penicillin, 2.2 μg/ml ascorbic acid. Cells were seeded at a density of 6.0×10^4 viable cells/cm^2 in polyethylenimine-(Sigma) coated [3] 96-well plates in 0.1 ml of media. Cells were grown in a 95% air/5% CO_2 humidified atmosphere at 37°C in serum-containing medium for 24 h. At that time, medium was replaced with identical medium or medium lacking serum in the presence or absence of 0.01–100 μM PD169316 (4-[5-(4-Fluoro-phenyl)-2-(4-nitro-phenyl)-2H-imidazol-4-yl]-pyridine), obtained from Dr. Alan Saltiel of Parke-Davis Pharmaceuticals, Ann Arbor, MI or SB203580 and SB202190 (0.01–200 μM, commercially available from Calbiochem). Twenty h after media change cultures were fixed in 4% paraformaldehyde. Dopamine neurons were identified using polyclonal anti-rat TH antibody (1:100; Pel-Freez) followed by ABC staining kit (Vector) as described below. Cultures for the studies of apoptosis were fixed in 1% paraformaldehyde followed by 70% ethanol in glycine buffer 18 h after serum withdrawal. These cultures were sequentially incubated with a polyclonal anti-TH antibody (1:100) overnight, anti-rabbit FITC conjugate (1:40; Calbiochem) for 2 h and with 8 μg/ml of Hoechst 33258 DNA dye for 10 min. TH^+ cells (green fluorescence) were counted as apoptotic only if their nuclei (blue) contained one or more lobes of condensed nuclear chromatin. In the entire experiment, a total of 5066 TH^+ neurons were examined for nuclear chromatin condensation. Four groups were tested: (1) +serum (n=2595); (2) −serum (n=269); (3) −serum+10 μM PD169316 (n=1615); (4) −serum+10 μM SB203580 (n=587).

2.2. 6-hydroxydopamine lesion and behavioral recovery test

Forty seven male Sprague–Dawley rats (225–250 g) were anesthetized with equithesin (4 ml/kg) and placed in a stereotaxic frame. Unilateral lesions of the medial forebrain bundle were done by infusing 20 μg of 6-OHDA HBr (RBI), dissolved in 4 μl of sterile saline containing 0.2% ascorbate at 1 μl/min per site at 2 sites (AP: −2.1 mm posterior to bregma, LAT: 2.0 mm from the midline, VD: −7.8 mm below the dura; and AP: −4.3 mm posterior to bregma, LAT: 1.5 mm from the midline, VD: −7.8 mm below the dura). Animals were tested as previously described [37] for ipsilateral to the lesion turning (90 min) in response to methamphetamine (5.0 mg/kg injected i.p.) two weeks after receiving lesions. Lesioned animals were assigned to four groups of equal rotational rates: (1) vehicle only, (n=9, RPM=7.8±1.0); (2) tissue+vehicle (n=11, RPM=8.4±1.5); (3) tissue+PD169316 (n=14, RPM=8.2±0.9); (4) tissue+SB203580 (n=13, RPM=8.2±0.1). Only rats that rotated at three rpm or greater were included in this study. We have previously demonstrated [37] that in our drug-induced circling test performed in flat-bottomed Plexiglas cylinders circling above two rpm correlates with >95% dopamine depletion. In contrast, Ungerstedt and Arbuthnott demonstrated that, when methamphetamine-induced circling test is performed in hemispherical bowls instead of cylinders, higher circling rates (4–6 rpm) predict >95% dopamine depletion [41].

2.3. Neurotransplantation

E15 rat ventral mesencephalon was dissected according to previously published methods [8]. For transplantation,

half of a ventral mesencephalon was shaped into a tissue strand (200 μm in diameter) by extruding tissue through a tapered glass cannula made by heating a commercially available blank (Kimble Kontes, Cat# 663500-0444). Hemiparkinsonian rats received transplants of ventral mesencephalic strands that were incubated for two h in a 95% air/5% CO_2 humidified atmosphere at 37°C in vehicle (Ca^{2+}/Mg^{2+}-free Hanks' balanced salt solution, n=11), in vehicle containing 10 μM PD169316 (n=14), or in vehicle containing 10 μM SB203580 (n=13). Each animal received a transplant of half of a ventral mesencephalon. Another 9 animals received infusion of only vehicle into the transplant site located in the denervated striatum (AP: 0.0 mm from bregma, LAT: 3.0 mm from the midline, VD: −3.5 to −7.5 mm below the dura) in 4.0 μl over 4 min. Animals were tested for response to intreperitoneal methamphetamine (5.0 mg/kg) three and six weeks after receiving transplants. Behavioral recovery was analyzed using mixed-effects analysis of variance appropriate for repeated measures ANOVA.

2.4. Morphological evaluation of grafts

All transplant recipients were sacrificed six weeks after transplantation. Graft-containing areas of each brain were sectioned on a cryotome in the coronal plane at 40 μm thickness and mounted on glass microscope slides. Every third section was stained for TH-immunoreactivity using a polyclonal antibody against rat TH and ABC staining kit (Vector). Endogenous peroxidase was inactivated by a 20 min treatment in methanol containing 20% hydrogen peroxide (v/v) at room temperature. Nonspecific binding was blocked with 10% goat serum in PBS containing 1% BSA and 0.3% Triton-X for 60 min at room temperature. The primary anti-TH antibody (1:100 dilution) was applied to each slide overnight at 37°C. Sections were then incubated with a biotinylated goat anti-rabbit IgG antibody and subsequently with avidin/biotinylated horseradish peroxidase complex, each for 2 h at room temperature. The peroxidase was visualized with diaminobenzidine dissolved in PBS and 0.03% hydrogen peroxide.

All TH-positive profiles were counted in each section. Abercrombie's correction [1] assumed cell diameter of 20 μm and was used to generate the final estimate of the number of surviving dopamine neurons in each animal. To assure that treatment with the inhibitors did not alter dopamine neuron cell size, which would render use of Abercrombie's correction inappropriate, one rat was selected from each transplant group for detailed neuron size analysis. The rat selected had closest to the median value of surviving dopamine neurons for each group. In each selected rat, images of all sections containing grafted cells were captured at ×400 magnification into SlideBook digital deconvolution software (Intelligent Imaging Innovations). The size of the soma for all dopamine neurons was determined using SlideBook's analysis tools. The total number of TH^+ somas measured was 353 for the animal receiving vehicle pre-treated tissue, 439 for the animal receiving PD169316 pre-treated tissue and 500 for the animal receiving SB203580 pre-treated tissue. For the measurement of the graft size and TH^+ fiber outgrowth, every third section was digitized using a Nikon slide scanner. Using the NIH Image program, area of the graft and area of the fiber outgrowth were manually outlined in each section. The areas were measured by the computer using a calibrated area analysis feature and volumes were calculated from the component areas.

3. Results

3.1. Effects of pyridinyl imidazole compounds on dopamine neuron survival and apoptosis

The survival of embryonic dopaminergic neurons in tissue culture is dependent on the presence of trophic factors contained in serum, and withdrawal of serum results in apoptosis. This model system has been used in the present studies to examine factors that rescue dopaminergic neurons from apoptotic cell death. In each experiment, primary neurons from ventral mesencephalon were grown in the presence of 5% human placental serum for 24 h. At that time, medium was replaced with identical medium or medium lacking serum in the presence or absence of increasing concentrations of the p38 MAP kinase inhibitors PD169316, SB203580, and SB202190. Twenty h after the media change, the cultures were fixed and stained with antibodies against tyrosine hydroxylase (TH) to identify surviving dopamine neurons. The structures of the pyridinyl imidazole compounds used in these experiments are shown in Fig. 1a. The inhibitors differ only by the para substitution in the phenyl ring that is in the 2-position of the imidazole ring. In control cultures fed with medium containing serum, there were 835±29 surviving TH^+ neurons/cm^2 (Fig. 1b). Serum withdrawal (20 h) reduced the number of surviving TH^+ neurons/cm^2 to 122±16 (P<0.001). All of the tested pyridinyl imidazole compounds, when added at the time of serum withdrawal, improved the survival of TH^+ neurons at concentrations shown to be effective in blocking p38 MAP kinase activity [7]. The survival effects of SB203580 and SB202190 reached their maximum at 100 and 200 μM, respectively. Application of SB203580 (100 μM) and SB202190 (200 μM) resulted in survival of 1321±283 and 1703±188 TH^+ neurons/cm^2, respectively. The highest dose (200 μM) of the SB203580 was toxic to dopamine neurons. The maximum effect of PD169316 was observed at 55 μM, when 1943±240 dopamine neurons survived. Because the inhibitors tested in this study have limited solubility above 10 μM, cultures supplemented with 55 μM imidazole inhibitors contained abundant undissolved inhibitor

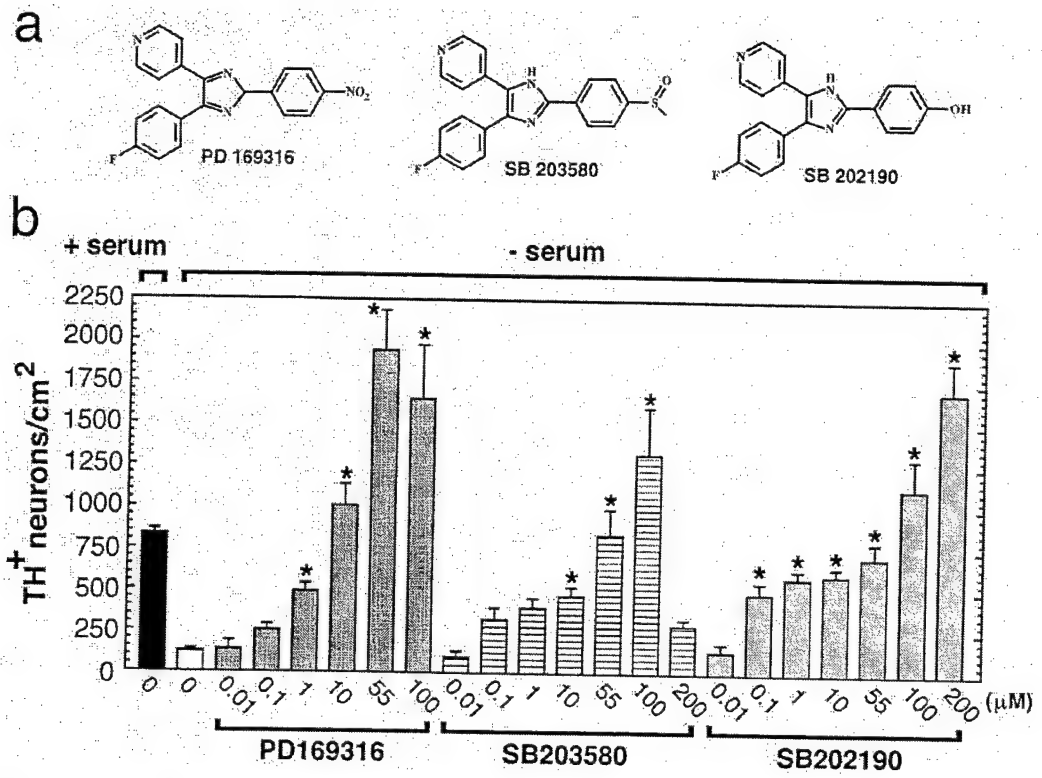

Fig. 1. The effects of pyridinyl imidazole compounds on the survival of embryonic dopamine neurons. (a) Structures of PD169316, SB203580, and SB202190. Note that the differences between the compounds exist in the para substitution in the phenyl ring that is in the 2-position of the imidazole ring. (b) Protection of dopamine neurons from serum withdrawal-induced death with pyridinyl imidazole compounds. Mesencephalic cultures were initially grown for 24 h in 5% human placental serum. At that time, medium was replaced with an identical medium (leftmost solid bar) or medium lacking serum in the presence (0.01–100/200 μM) or absence (open bar) of PD169316, SB203580 and SB202190 for 20 h. All inhibitors tested at 10 μM provided protection to dopamine neurons. At 10 μM, PD169316 was most potent inhibitor providing complete protection from death by serum withdrawal. Data are mean±S.E.M. (n=4–43) from up to 5 independent experiments. Statistical significance was determined using one-way ANOVA ($P<0.0001$; $F(21, 230)=22.7$). Means were considered different from −serum cultures when Newman–Keuls post-hoc test revealed $P<0.05$ (*).

crystals, which might have contributed to increased variability in cell survival observed in these cultures. Cultures supplemented with 10 μM of SB203580 or SB202190, at which concentration crystal formation was not a problem, had 470±56 and 601±48 surviving TH^+ neurons/cm^2, respectively. By contrast, 10 μM PD169316 protected all of the TH^+ neurons from serum withdrawal-induced death, supporting the survival of 1008±126 TH^+ neurons/cm^2. These experiments have revealed that all three inhibitors can fully protect dopamine cells from serum withdrawal. The order of potency for complete neuroprotection from serum withdrawal was PD169316>SB203580>SB202190. In some cases, high concentrations of the inhibitors augmented TH^+ cell survival above that observed in serum-containing cultures (PD169316 at 55 and 100 μM, SB203580 at 100 μM, and SB202190 at 200 μM, $P<0.01$).

The morphology of TH^+ neurons grown in the absence and presence of serum is shown in Fig. 2. Twenty h after the media change, dopamine neurons cultured in medium containing serum (with or without 10 μM PD169316) appeared healthy and contained long neurites and highly ramified growth cones (Fig. 2a, c). By contrast, dopamine neurons from which serum was withdrawn were fewer in number, had truncated neurites and lacked growth cones (Fig. 2b). Supplementation of the serum-withdrawn cultures with 10 μM PD169316 rescued the TH^+ neurons. Their morphology was indistinguishable from that of the serum-fed neurons (Fig. 2d).

To determine if PD169316 exerted its survival effects on dopamine neurons by reducing the rate of apoptosis, we co-stained rat ventral mesencephalic cultures with TH antibodies to identify surviving dopamine neurons and Hoechst 33258 dye to examine nuclear morphology. Apoptotic dopamine neurons were defined as TH^+ cells that contained one or more lobes of condensed nuclear chromatin. In the presence of serum, greater than 90% of TH^+ neurons showed normal nuclear morphology with the chromatin uniformly distributed throughout the nucleus (Fig. 3a). The apoptotic dopamine neurons showed marked nuclear condensation and had degenerating neurites (Fig. 3b). Maintenance of cell membrane integrity in the apoptotic dopamine neurons, another characteristic of apoptosis, was demonstrated by retention of TH enzyme within the apoptotic bodies (Fig. 3b). Removal of serum increased the number of adherent apoptotic cells by over 3-fold (Fig.

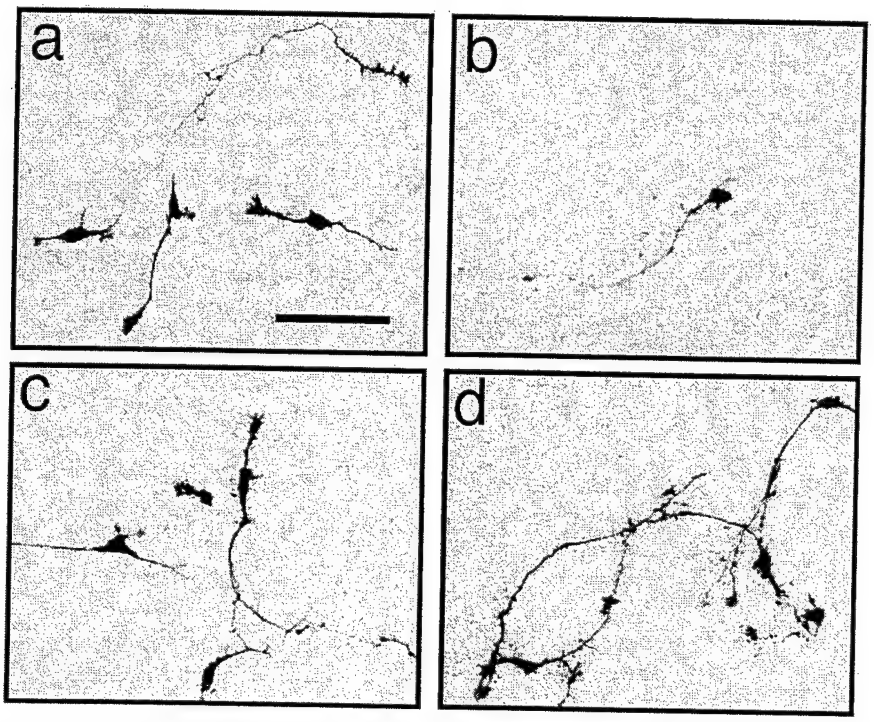

Fig. 2. PD169316 protects dopamine neurons from degeneration in vitro. (a–d) Micrographs of dopamine neurons 20 h following media change. Cells were immunostained using anti-TH antibody. (a) 5% serum only; (b) no serum; (c) 5% serum plus 10 μM PD169316; (d) no serum plus 10 μM PD169316. In these experiments, PD169316 acted as serum replacement. 10 μM PD169316 (d) restored both dopamine neuron survival and neurite outgrowth to that observed in serum-containing cultures (a). Note that addition of PD169316 to cultures supplemented with serum (c) did not further increase dopamine cell survival or neurite outgrowth. Scale bar=100 μm.

3c). PD169316 reduced the rate of apoptosis of dopamine neurons to control levels and SB203580 partially reduced the level of apoptosis seen after serum withdrawal.

3.2. Effects of pyridinyl imidazole compounds on dopamine neuron survival and function after transplantation

To determine whether inhibitors of p38 MAP kinase could increase the survival of dopamine neurons and accelerate motor recovery after transplantation, we transplanted rat ventral mesencephalic dopamine neurons obtained from embryonic day 15 rats into the brains of hemiparkinsonian rats. This rat model of Parkinson's disease is created by a unilateral injection of the neurotoxin 6-OHDA into the medial forebrain bundle leading to the death of dopamine neurons in substantia nigra and dopamine depletion in striatum [37,41]. Upon intraperitoneal injection of methamphetamine (5 mg/kg), lesioned animals run in circles in a direction ipsilateral to the lesion. This circling behavior can be abolished by transplantation of embryonic rat dopamine neurons into the denervated striatum [5]. Grafted dopamine neurons survive, project neurites, form synapses, and improve behavior [26].

Rats were lesioned and tested for rotational behavior two weeks later. Lesioned rats that showed motor asymmetry (greater than 3 rpm) in response to methamphetamine were transplanted with one of the following: (1) vehicle only; (2) mesencephalic tissue pretreated with vehicle; (3) mesencephalic tissue pretreated with 10 μM PD169316 or (4) mesencephalic tissue pretreated with 10 μM SB203580. For the pretreatment, all tissues were incubated for two h in a 95% air/5% CO_2 humidified atmosphere at 37°C. Inhibitor concentration of 10 μM was chosen for the transplantation experiments, because higher concentrations of the inhibitors result in an unacceptably high crystal formation upon contact with aqueous solutions. Inhibitors of p38 MAP kinase that have much better solubility in aqueous solutions are being developed [25].

Behavioral recovery was tested at three and six weeks following transplantation. Animals that received vehicle without tissue did not reduce their rotational rate over the six-week period. At three weeks, animals that received transplants of tissue pretreated with vehicle alone reduced their circling rate by 60% from the pretransplantation rate (Fig. 4). By contrast, recipients of transplants pretreated with the pyridinyl imidazole compounds had significantly accelerated reduction in their rotational rates when compared to the vehicle pretreated tissue recipients. The PD169316 pretreated group reduced their rotational rate by 90% ($P<0.01$), while the SB203580 pretreated group reduced their circling by 74% ($P<0.01$). At six weeks after transplantation, behavioral improvement continued (Fig. 4). The vehicle pretreated group showed a 77%

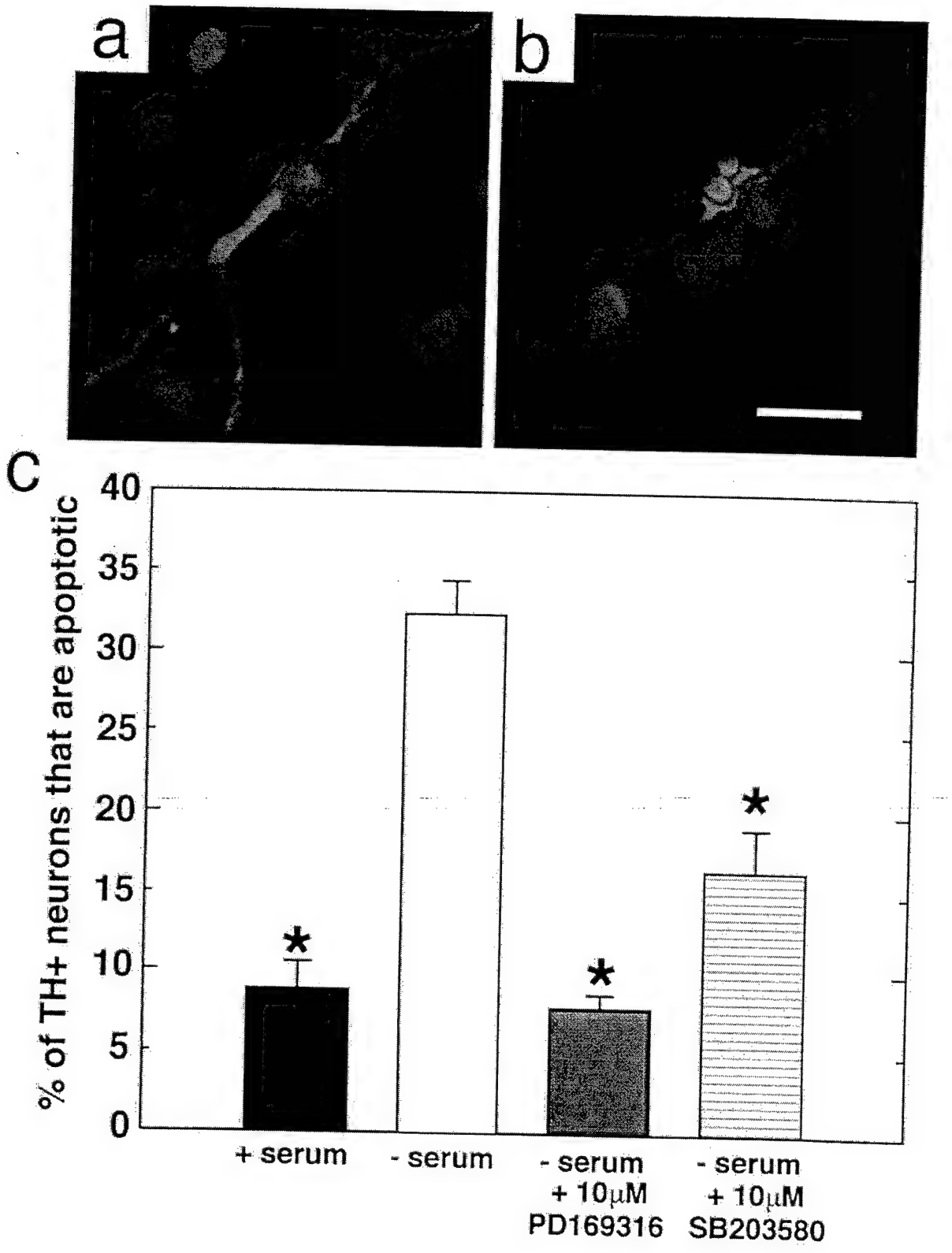

reduction in circling. The PD169316 pretreated group showed the greatest reduction in circling (99%) and was significantly different from the control group ($P<0.01$). The SB203580 pretreated group reduced their rotational rate by 82%, a value not statistically different from the vehicle pretreated group. Thus, animals receiving mesencephalic tissue that was pretreated with PD169316 completely stopped circling at six weeks after transplantation.

To determine if behavioral improvement coincided with increased survival of dopamine neurons in the grafts,

animals were sacrificed and their brains processed for tyrosine hydroxylase immunocytochemistry. Examples of coronal sections through grafts stained for TH are shown in Fig. 5a. Cell counting of TH^+ neurons in these coronal sections revealed that 1550±294 dopamine neurons survived in grafts pretreated with vehicle (Fig. 5b). The number of surviving TH^+ neurons doubled to 3023±518 when the tissue was pretreated with PD169316 ($P<0.05$). Although pretreatment of tissue with SB203580 increased the number of surviving dopamine neurons to 2321±394, the increase was not statistically significant. Analysis of the graft size (Fig. 5c) and TH^+ fiber outgrowth (Fig. 5d) using the NIH Image program revealed that pretreatment of mesencephalic tissue with PD169316 prior to transplantation increased the graft size by 140% ($P<0.01$), while pretreatment of the tissue with SB203580 increased the graft size by 100% ($P<0.05$). Preincubation with either PD169316 or SB203580 also augmented the TH^+ fiber outgrowth by 130% ($P<0.01$).

To assure that treatment with the inhibitors did not alter dopamine neuron cell size, which would render use of Abercrombie's correction inappropriate, one rat was selected from each transplant group for detailed neuron size analysis. The rat selected had closest to the median value of surviving dopamine neurons for each group. Measurement of soma size of TH^+ neurons from images captured at ×400 magnification into SlideBook digital deconvolution software revealed that average area of TH^+ cell soma was not changed by the ex vivo inhibitor treatment (Fig. 6). Specifically, average area of TH^+ cell soma of cells in tissue treated with the vehicle was 177±4 μm^2, 180±3 μm^2 in tissue treated with PD169316, and 172±3 μm^2 in tissue treated with SB203580.

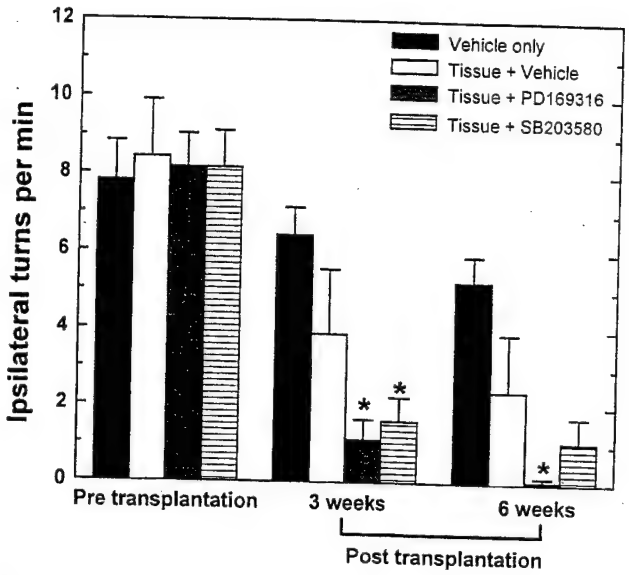

Fig. 4. Reduction in circling behavior following neurotransplantation. All animals were injected with methamphetamine (5 mg/kg; i.p.) to test motor asymmetry after a unilateral 6-OHDA lesion. High rotations indicate dopamine imbalance (lesion severe), while low rotations indicate dopamine level normalization (lesion corrected). Net ipsilateral rotation scores are shown for four experimental groups that received intrastriatal transplants: (1) vehicle only, ($n=9$); (2) tissue+vehicle ($n=11$); (3) tissue+10 μM PD169316 ($n=14$) and (4) tissue+10 μM SB203580 ($n=13$). Rats were tested prior to transplantation (two weeks after lesioning) and three and six weeks after transplantation. At three weeks, groups transplanted with tissues treated with both PD and SB compounds had significantly lower rotational scores than controls receiving vehicle-pretreated tissue ($P<0.01$). PD169316 treated group was the only group to stop rotating at six weeks after transplantation ($P<0.01$ vs. tissue+vehicle). Data are mean±S.E.M. Significance was determined using two-way ANOVA ($P<0.001$; $F_{(6, 86)}=4.7$) followed by a Fisher LSD post-hoc test.

4. Discussion

Results from these studies indicate that pyridinyl imidazole inhibitors of p38 MAP kinase improve survival of dopamine neurons both in tissue culture and after neurotransplantation in hemiparkinsonian rats. The improved survival of grafts treated with the p38 MAP kinase inhibitors correlated with more rapid improvement in motor behavior. These data suggest that apoptotic programmed cell death occurring in vivo after transplantation results, at least in part, from activation of p38 MAP kinase. This outcome is consistent with in vitro experiments showing that inhibitors of p38 MAP kinase block apoptosis of neurons [15,16,23]. In differentiated PC12 cells that were deprived of nerve growth factor (NGF) for 16 h, activity of p38 MAP kinase was dramatically elevated and correlated with increase in apoptosis [23]. A selective p38 MAP kinase inhibitor, PD169316, and insulin abolished this increase in kinase activity and blocked apoptosis in PC12 cells under conditions of NGF withdrawal.

Fig. 3. Pyridinyl imidazole inhibitors rescue dopamine neurons from apoptosis. (a and b), Micrographs showing dopamine neurons (green) identified using anti-TH primary antibody followed by FITC-conjugated secondary antibody and nuclei (blue) stained with Hoechst 33258. All cells were cultured in 5% human placental serum for 24 h. At that time, medium was replaced with an identical medium or medium lacking serum in the presence or absence of 10 μM PD169316 or 10 μM SB203580. All cultures were fixed 18 h following media change. (a) Micrograph showing a healthy dopamine neuron among several healthy non-dopaminergic nuclei in serum supplemented culture. (b) An apoptotic dopamine neuron containing two lobes of condensed chromatin. Note degeneration of the neurites and retention of TH within the apoptotic body. Scale bar=25 μm. (c) Quantitation of the percent of adhering TH^+ neurons that are apoptotic. In the presence of serum, 8.8% of dopamine neurons were apoptotic. Serum withdrawal for 18 h raised apoptosis in dopamine neurons to 32.3%. Addition of 10 μM PD169316 completely prevented the increase in apoptosis induced by serum withdrawal (7.8% dopamine neurons were apoptotic). SB203580 reduced apoptosis to 16.5%. Data are mean±S.E.M. In this experiment, a total of 5066 TH^+ neurons were examined for apoptotic morphology. Statistical significance was determined using one-way ANOVA ($P<0.001$; $F_{(3, 23)}=34.5$). Asterisks signify $P<0.001$ (compared to −serum) based on Newman–Keuls post-hoc test.

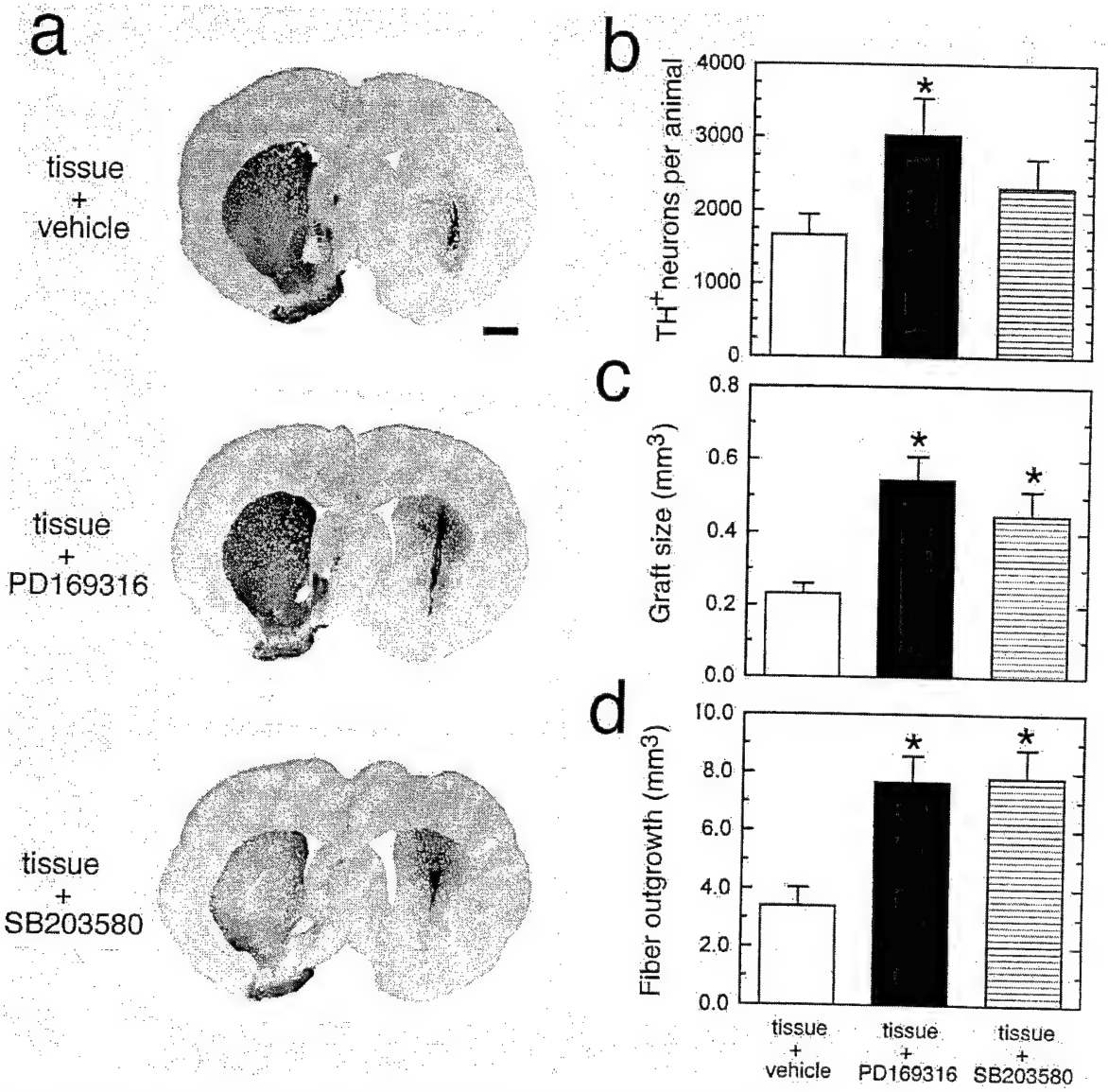

Fig. 5. Morphological and histological graft assessment. (a) Coronal sections showing tyrosine hydoxylase (TH) immunostaining of the representative grafts transplanted into denervated adult rat striatum. Note that even under gross examination, both graft size and TH^+ fiber outgrowth are greatest in the graft pretreated with PD169316 (middle section). Scale bar=1 mm. (b) Number of surviving transplanted TH^+ neurons per animal. PD169316 doubled TH^+ neuron survival ($P<0.01$; t-test. (c) Graft size was also significantly increased ($P<0.01$; $F_{(2,37)}=7.0$) by PD199316 ($P<0.01$) and SB203580 ($P<0.05$). (d) The imidazole inhibitors significantly extended fiber outgrowth ($P<0.01$; $F_{(2,37)}=7.4$). Data are mean±S.E.M. ($n=9-14$). Statistical analysis was done using one-way ANOVA followed by a Newman–Keuls post-hoc test.

Pyridinyl inhibitors of p38 MAP kinase, SB203580 and SB202190, have been also shown to protect different populations of chick embryonic neurons from apoptosis induced by trophic factor withdrawal in vitro [16]. Although SB203580 and SB202190 partly protected sensory, sympathetic, ciliary and motor neurons from trophic factor withdrawal, using an optimal concentration of the inhibitors (100 μM), ciliary neuron survival was increased to no more than 80% of controls. Effects on the other types of embryonic chick neurons were lesser. By contrast, in our study, concentrations of PD169316 as low as 10 μM protected 100% of dopamine neurons from serum withdrawal-induced apoptosis. Our experiments also revealed that all p38 MAP kinase inhibitors, when tested at 100 μM in mesencephalic cultures from which serum was withdrawn, significantly increased dopamine neuron survival above that observed in serum-fed cultures. Activation of p38 MAP kinase by trophic factor withdrawal is not unique to neurons, as Rat-1 fibroblasts deprived of serum exhibit similar increases in apoptosis and p38 MAP kinase activity, both of which can be blocked by PD169316 [23].

While in our mesencephalic cultures morphology of the dopamine neurons protected by PD169316 was identical to that observed in serum-fed cultures, in chick embryonic neurons, under trophic factor withdrawal, the SB compounds were unable to fully restore normal neurite mor-

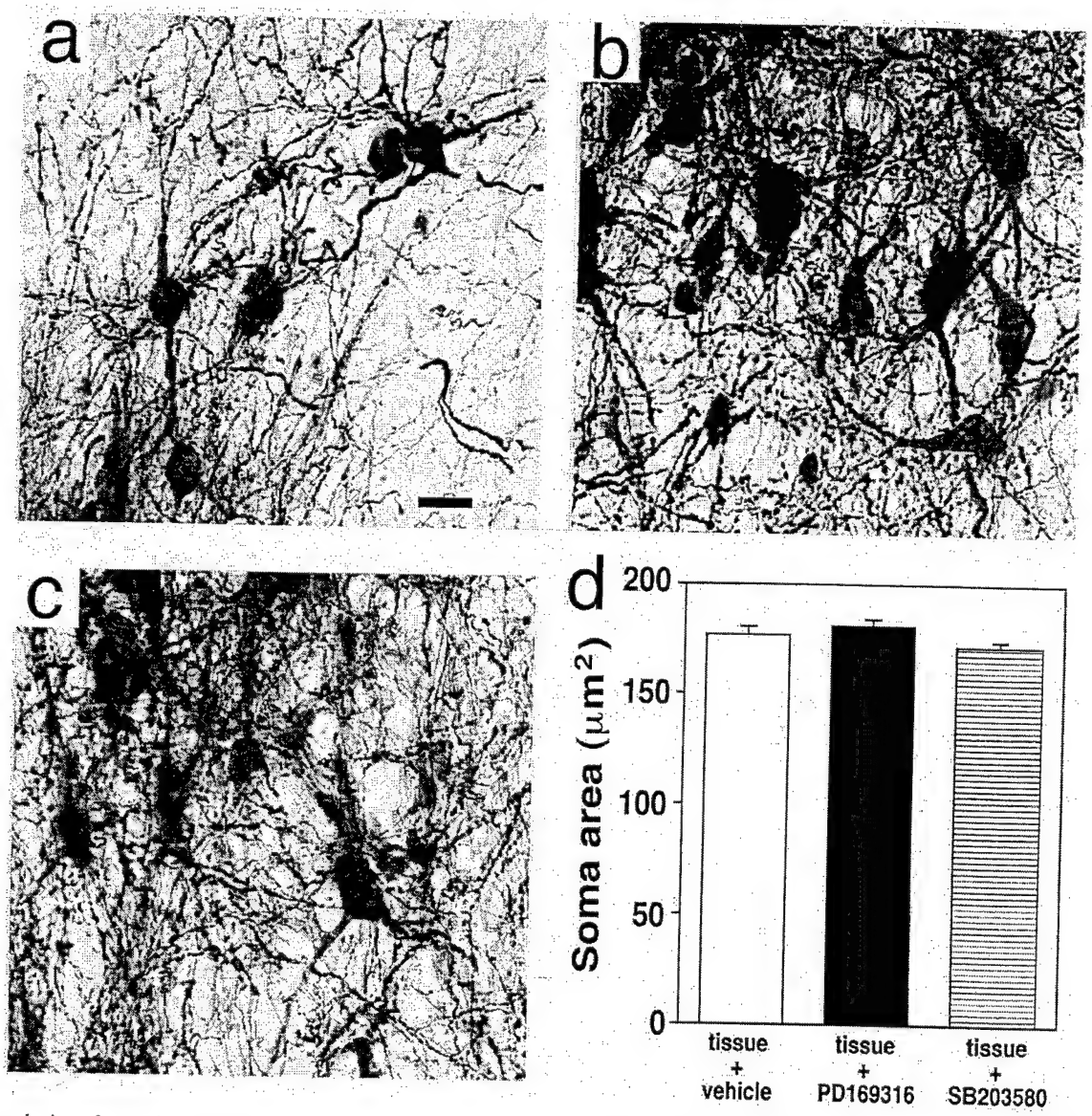

Fig. 6. Preincubation of ventral mesencephalic tissue strands with pyridinyl inhibitors of p38 MAP kinase does not alter the size of transplanted dopamine neurons. TH-immunoreactive cells from (a) transplant of ventral mesencephalic tissue pretreated with vehicle, (b) transplant pretreated with 10 μM PD169316, and (c) transplant pretreated with 10 μM SB203580. Scale bar=20 μm. (d) Mean soma area of TH^+ neurons found in three different experimental groups six weeks after grafting.

phology [16]. Because one of the initial morphological changes characteristic of apoptosis is neurite degeneration, it is possible that inhibitors of p38 MAP kinase maintain normal neuronal morphology in cultures deprived of trophic factors by inhibiting the pro-apoptotic cascades in the neurites and synaptic terminals. Evidence of synaptic apoptosis is growing, for reviews see [29,30]. Exposure of isolated synaptosomes to staurosporine and Fe^{2+}, at concentrations that induce apoptosis in cultured primary neurons, produced changes characteristic of apoptosis including flipping of phosphatidylserines to the outer leaflet of the membrane, activation of caspase-3, mitochondrial calcium uptake, mitochondrial membrane depolarization and accumulation of oxygen radicals [31]. Caspase activation and mitochondrial membrane depolarization precede and are required for nuclear apoptotic events. In glutamate-induced apoptosis, signals for caspase activation are propagated from dendrites toward the soma [31].

The other member of stress-activated protein kinase family, c-Jun N-terminal kinase (JNK), is activated by many of the same apoptotic stimuli that activate p38 MAP kinase. In three models of survival factor withdrawal-induced apoptosis, JNK was determined to be necessary using dominant negative mutants of JNK, its downstream target c-jun, and its upstream activator [13,14,47]. Recent evidence using novel inhibitor of the JNK signaling pathway, CEP-1347, points to JNK1 as a mediator of trophic factor withdrawal-induced apoptosis in motoneurons [28]. Potential importance of the stress-activated

protein kinase pathways in apoptosis is further underscored by findings showing rapid activation of both JNK and p38 MAP kinase in primary cerebellar granule neurons following exposure to glutamate [20]. The p38 MAP kinase activation in cerebellar granule neurons occurred via *N*-methyl-D-aspartate receptors and involved calcium. Similarly to the antiapoptotic effects of SB203580 on the PC12 cells and fibroblasts exposed to serum withdrawal, inhibition of p38 MAP kinase using SB203580 reduced glutamate-induced apoptosis in cerebellar granule cells [20].

It is conceivable that inhibition of apoptosis by SB203580 and PD169316 observed in our study resulted from a combined blockade of activities of both p38 MAP kinase and JNK. This conjecture is supported by a recent report showing that SB203580 can inhibit JNK activity in CHO cells [44]. While 0.1 μM SB203580 inhibited more than 50% of p38 MAP kinase activity with no effect on JNK1 and 2 activity, incubation of the cells with 10 μM inhibitor reduced the activities of JNK2β1 and JNK2β2 to basal levels [44].

To our knowledge, our report is first to describe neuroprotective actions of p38 inhibitors in vivo. Despite the rescue of many of the transplanted dopamine neurons by p38 MAP kinase inhibitors, the majority of dopamine neurons did not survive transplantation. Further improvement in grafting may come from short-term systemic administration of the inhibitors to sustain higher inhibitor concentration during the first week after grafting when neuronal apoptosis is greatest [46]. This short treatment paradigm may reduce potential for toxicity of long-term treatment, thereby enhancing the potential for use of these inhibitors in humans. More potent and more soluble p38 MAP kinase inhibitors are being developed [25].

Several other approaches to improve survival and function of dopamine neurons in transplants have shown some promise, for review see [4]. Preincubation of ventral mesencephalic tissue prior to transplantation with a combination of basic fibroblast growth factor (bFGF), insulin-like growth factor-I (IGF-I), and glial-cell line derived neurotrophic factor (GDNF) results in improved survival of transplanted dopamine neurons one and seven days following transplantation [46]. These survival-promoting effects of the growth factors are attributed to the reduction in the number of apoptotic cells following grafting. Alternatively, co-transplantation of naturally occurring or genetically-modified cells together with ventral mesencephalic cells has been shown to enhance graft survival and function. Testis-derived Sertoli cells, known for their ability to produce a variety of growth factors and Fas ligand, when co-transplanted with the rat ventral mesencephalic cells enhance survival of dopamine neurons in the grafts [45]. Co-transplantation of rat fibroblasts genetically modified to express bFGF also improved graft survival and function [40].

In yet another strategy, transgenic neural tissue was used in attempts to reduce oxidative stress and apoptosis following transplantation. Grafting of transgenic mouse ventral mesencephalon overexpressing Cu/Zn superoxide dismutase enhanced survival of transplanted dopamine neurons in a rat model of Parkinson's disease [34]. Comparable improvements in dopamine neuron survival have been observed in grafts receiving cells treated with inhibitors of free radical generation, lazaroids U-743889G and U-83836E [33]. By contrast, efforts to inhibit apoptosis in transplanted neurons by grafting mouse mesencephalic tissue overexpressing an anti-apoptotic protein, Bcl-2, failed to improve survival and function of the grafts, but resulted in a significant enhancement of dopaminergic fiber outgrowth [39]. A more efficatious method for reducing apoptosis in the grafts employed a pretreatment of the mesencephalic cell suspensions with a caspase inhibitor, Ac-YVAD-cmk, prior to transplantation [38]. Grafts receiving cells exposed to the caspase inhibitor contained nearly 400% more surviving dopamine neurons than control grafts.

Further potential for augmenting graft survival and overall transplant outcome may lie in the use of the p38 MAP kinase inhibitors in combination with growth factors [40,46], antioxidants [33,34], or other antiapoptotic agents such as caspase inhibitors [38], which when used as monotherapy have already been shown to be beneficial. The advantages that the pyridinyl compounds have over growth factors and caspase inhibitors for preventing apoptosis in vivo include their low molecular weight, acceptable systemic toxicity [2,25] and ability to cross the blood–brain barrier. These characteristics make the pyridinyl imidazole compounds promising candidate drugs for improving survival of dopamine neurons following transplantation into humans.

Acknowledgements

We thank Cindy Hutt and Pat Bell for their technical work, Dr. Kim Bjugstad for help with statistical analysis, Dr. Jenifer Monks for help with computer imaging, Dr. Joe Gal for constructive comments, and Dr. Alan Saltiel of Parke-Davis Pharmaceuticals for providing PD169316. This research was supported by U.S. Public Health Grants NS18639, NIGMS GM07063, M01 RR00069 (C.R.F), NS38619 (K.A.H. and W.M.Z.) and VA Merit, VA Research Enhancement Award and DOD-DAMD17-99-1-9481 (K.A.H.).

References

[1] M. Abercrombie, Estimation of nuclear population from microtome sections, The Anatomical Record 94 (1946) 239–247.

[2] A.M. Badger, J.N. Bradbeer, B. Votta, J.C. Lee, J.L. Adams, D.E. Griswold, Pharmacological profile of SB 203580, a selective inhibitor of cytokine suppressive binding protein/p38 kinase, in animal

models of arthritis, bone resorption, endotoxin shock and immune function, J. Pharmacol. Exp. Therap. 279 (1996) 1453–1461.
[3] K.D. Beck, B. Knüsel, F. Hefti, The nature of the trophic action of brain-derived neurotrophic factor, des (1-3)-insulin-like growth factor-1, and basic fibroblast growth factor on mesencephalic dopaminergic neurons developing in culture, Neuroscience 52 (1992) 855–866.
[4] P. Brundin, J. Karlsson, M. Emgard, G.S. Schierle, O. Hansson, A. Petersen, R.F. Castilho, Improving the survival of grafted dopaminergic neurons: a review over current approaches, Cell Transplant. 9 (2000) 179–195.
[5] E.D. Clarkson, W.M. Zawada, F.S. Adams, K.P. Bell, C.R. Freed, Strands of mesencephalic tissue show greater dopamine neuron survival and better behavioral improvement than cell suspensions after transplantation in parkinsonian rats, Brain Res. 806 (1998) 60–68.
[6] G.C. Cotzias, M.H. Van Woert, L.M. Schiffer, Aromatic amino acids and modification of parkinsonism, New Engl. J. Med. 276 (1967) 374–379.
[7] A. Cuenda, J. Rouse, Y.N. Doza, R. Meier, P. Cohen, T.F. Gallagher, P.R. Young, J.C. Lee, SB203580 is a specific inhibitor of a MAP kinase homologue which is stimulated by cellular stresses and interleukin 1, FEBS Lett. 364 (1995) 229–233.
[8] S.B. Dunnett, A. Björklund, Staging and dissection of rat embryos, in: S.B. Dunnett, A. Björklund (Eds.), Neural Transplantation: A Practical Approach, Oxford University Press, New York, 1992, pp. 1–19.
[9] H. Ehringer, O. Hornykiewicz, Verteilung von noradrenalin and dopamin (3-hydroxytyramin) i.m. gehirn des menschen und ihr verhalten bei erkrankungen des extrapyramidalen systems, Klin. Wochenschr. 38 (1960) 1236–1239.
[10] C.R. Freed, R.E. Breeze, N.L. Rosenberg, S.A. Schneck, T.H. Wells, J.N. Barrett, S.T. Grafton, S.C. Huang, D. Eidelberg, D.A. Rottenberg, Transplantation of human fetal dopamine cells for Parkinson's disease, Arch. Neurol. 47 (1990) 505–512.
[11] C.R. Freed, R.E. Breeze, N.L. Rosenberg, S.A. Schneck, E. Kriek, J.X. Qi, T. Lone, Y.B. Zhang, J.A. Synder, T.H. Wells, L.O. Ramig, L. Thompson, J.C. Mazziotta, S.C. Huang, S.T. Grafton, D. Brooks, G. Sawle, G. Schroter, A.A. Ansari, Survival of implanted fetal dopamine cells and neurologic improvement 12 to 46 months after transplantation for Parkinson's disease, New Engl. J. Med. 327 (1992) 1549–1555.
[12] T.B. Freeman, C.W. Olanow, R.A. Hauser, G.M. Nauert, D.A. Smith, C.V. Borlongan, P.R. Sanberg, D.A. Holt, J.H. Kordower, F.J. Vingerhoets, B.J. Snow, D. Calne, L.L. Gauger, Bilateral fetal nigral transplantation into the postcommissural putamen in Parkinson's disease, Ann. Neurol. 38 (1995) 379–388.
[13] S.M. Frisch, K. Vuori, D. Kelaita, S. Sicks, A role for jun-N-terminal kinase in anoikis; suppression by bcl-2 and crmA, J. Cell. Biol. 135 (1996) 1377–1382.
[14] J. Ham, C. Babij, J. Whitfield, C.M. Pfarr, D. Lallemand, D.M. Yaniv, L.L. Rubin, A c-jun dominant negative mutant protects sympathetic neurons against programmed cell death, Neuron 14 (1995) 927–939.
[15] K.A. Heidenreich, J.L. Kummer, Inhibition of p38 mitogen-activated protein kinase by insulin in cultured fetal neurons, J. Biol. Chem. 271 (1996) 9891–9894.
[16] S. Horstmann, P.J. Kahle, G.D. Borasio, Inhibitors of p38 mitogen-activated protein kinase promote neuronal survival in vitro, J. Neurosci. Res. 52 (1998) 483–490.
[17] S. Huang, Y. Jiang, Z. Li, E. Nishida, P. Mathias, S. Lin, R.J. Ulevitch, G.R. Nemerow, J. Han, Apoptosis signaling pathway in T cells is composed of ICE/Ced-3 family proteases and MAP kinase kinase 6b, Immunity 6 (1997) 739–749.
[18] H. Ichijo, E. Nishida, K. Irie, P. ten Dijke, M. Saitoh, T. Moriguchi, M. Takagi, K. Matsumoto, K. Miyazono, Y. Gotoh, Induction of apoptosis by ASK1, a mammalian MAPKKK that activates SAPK/JNK and p38 signaling pathways, Science 275 (1997) 90–94.
[19] P. Juo, C.J. Kuo, S.E. Reynolds, R.F. Konz, J. Raingeaud, R.J. Davis, H.P. Biemann, J. Blenis, Fas activation of the p38 mitogen-activated protein kinase signalling pathway requires ICE/CED-3 family proteases, Mol. Cell Biol. 17 (1997) 24–35.
[20] H. Kawasaki, T. Morooka, S. Shimohama, J. Kimura, T. Hirano, Y. Gotoh, E. Nishida, Activation and involvement of p38 mitogen-activated protein kinase in glutamate-induced apoptosis in rat cerebellar granule cells, J. Biol. Chem. 272 (1997) 18518–18522.
[21] O.V. Kopyov, D. Jacques, A. Lieberman, C.M. Duma, R.L. Rogers, Clinical study of fetal mesencephalic intracerebral transplants for the treatment of Parkinson's disease, Cell Transplantation 5 (1996) 327–337.
[22] J.H. Kordower, T.B. Freeman, B.J. Snow, F.J. Vingerhoets, E.J. Mufson, P.R. Sanberg, R.A. Hauser, D.A. Smith, G.M. Nauert, D.P. Perl, C.W. Olanow, Neuropathological evidence of graft survival and striatal reinnervation after the transplantation of fetal mesencephalic tissue in a patient with Parkinson's disease, New Engl. J. Med. 332 (1995) 1118–1124.
[23] J.L. Kummer, P.K. Rao, K.A. Heidenreich, p38 MAP kinase mediates apoptosis induced by withdrawal of trophic factors, J. Biol. Chem. 272 (1997) 20490–20494.
[24] O. Lindvall, P. Brundin, H. Widner, S. Rehncrona, B. Gustavii, R. Frackowiak, K.L. Leenders, G. Sawle, J.C. Rothwell, C.D. Marsden, A. Björklund, Grafts of fetal dopamine neurons survive and improve motor function in Parkinson's disease, Science 247 (1990) 574–577.
[25] J.N. Liverton, J.W. Butcher, C.F. Claiborne, D.A. Claremon, B.E. Libby, K.T. Nguyen, S.M. Pitzenberger, H.G. Selnick, G.R. Smith, A. Tebben, J.P. Vacca, S.L. Varga, L. Agarwal, K. Dancheck, A.J. Forsyth, D.S. Fletcher, B. Frantz, W.A. Hanlon, C.F. Harper, S.J. Hofsess, M. Kostura, J. Lin, S. Luell, E.A. O'Neill, C.J. Orevillo, M. Pang, J. Parsons, A. Rolando, Y. Sahly, D.M. Visco, S.J. O'Keefe, Design and synthesis of potent, selective, and orally bioavailable tetrasubstituted imidazole inhibitors of p38 mitogen-activated protein kinase, J. Med. Chem. 42 (1999) 2180–2190.
[26] T.J. Mahalik, T.E. Finger, I. Strömberg, L. Olson, Substantia nigra transplants into denervated striatum of the rat: ultrastructure of graft and host interconnections, J. Comp. Neurol. 240 (1985) 60–70.
[27] T.J. Mahalik, W.E. Hahn, G.H. Clayton, G.P. Owens, Programmed cell death in developing grafts of fetal substantia nigra, Exp. Neurol. 129 (1994) 27–36.
[28] A.C. Maroney, M.A. Glicksman, A.N. Basma, K.M. Walton, E. Knight Jr., C.A. Murphy, B.A. Bartlett, J.P. Finn, T. Angeles, Y. Matsuda, N.T. Neff, C.A. Dionne, Motoneuron apoptosis is blocked by CEP-1347 (KT 7515), a novel inhibitor of the JNK signaling pathway, J. Neurosci. 18 (1998) 104–111.
[29] M.P. Mattson, Apoptotic and anti-apoptotic synaptic signaling mechanisms, Brain Pathol. 10 (2000) 300–312.
[30] M.P. Mattson, W. Duan, 'Apoptotic' biochemical cascades in synaptic compartments: Roles in adaptive plasticity and neurodegenerative disorders, J. Neurosci. Res. 58 (1999) 152–166.
[31] M.P. Mattson, J.N. Keller, J.G. Begley, Evidence for synaptic apoptosis, Exp. Neurol. 153 (1998) 35–48.
[32] T. Morooka, E. Nishida, Requirement of p38 mitogen-activated protein kinase for neuronal differentiation in PC12 cells, J. Biol. Chem. 273 (1998) 24285–24288.
[33] N. Nakao, E.M. Frodl, W.-M. Duan, H. Widner, P. Brundin, Lazaroids improve the survival of grafted rat embryonic dopamine neurons, Proc. Natl. Acad. Sci. USA 91 (1994) 12408–12412.
[34] N. Nakao, E.M. Frodl, H. Widner, E. Carlson, F.A. Eggerding, C.J. Epstein, P. Brundin, Overexpressing Cu/Zu superoxide dismutase enhances survival of transplanted neurons in a rat model of Parkinson's disease, Nature Med. 1 (1995) 226–231.
[35] K. Ono, J. Han, The p38 signal transduction pathway: Activation and function, Cell. Signalling 12 (2000) 1–13.
[36] M. Peschanski, G. Defer, J.P. N'Guyen, F. Ricolfi, J.C. Monfort, P. Remy, C. Geny, Y. Samson, P. Hantraye, R. Jeny, A. Gaston, Y. Kéravel, J.D. Degos, P. Cesaro, Bilateral motor improvement and

alteration of L-dopa effect in two patients with Parkinson's disease following intrastriatal transplantation of foetal ventral mesencephalon, Brain 117 (1994) 487–499.

[37] J.B. Richards, K.E. Sabol, C.R. Freed, Unilateral dopamine depletion causes bilateral deficits in conditioned rotation in rats, Pharmacol. Biochem. Behav. 36 (1990) 217–223.

[38] G.S. Schierle, O. Hansson, M. Leist, P. Nicotera, H. Widner, P. Brundin, Caspase inhibition reduces apoptosis and increases survival of nigral transplants, Nature Med. 5 (1999) 97–100.

[39] G.S. Schierle, M. Leist, J.C. Martinou, H. Widner, P. Nicotera, P. Brundin, Differential effects of Bcl-2 overexpression on fibre outgrowth and survival of embryonic dopaminergic neurons in intracerebral grafts, Eur. J. Neurosci. 11 (1999) 3073–3081.

[40] H. Takayama, J. Ray, H.K. Raymon, A. Baird, J. Hogg, L.J. Fisher, F.H. Gage, Basic fibroblast growth factor increases dopaminergic graft survival and function in a rat model of Parkinson's disease, Nature Med. 1 (1995) 53–58.

[41] U. Ungerdstedt, G.W. Aurbuthnott, Quantative recording of rotational behavior in rats after 6-hydroxydopamine lesions of the nigrostriatal dopamine system, Brain Res. 24 (1970) 485–493.

[42] Y. Wang, S. Huang, V.P. Sah, J. Ross, J.H. Brown, J. Han, K.R. Chen, Cardiac muscle cell hypertrophy and apoptosis induced by distinct members of the p38 mitogen activated protein kinase family, J. Biol. Chem. 273 (1998) 2161–2168.

[43] G.K. Wenning, P. Odin, P. Morrish, S. Rehcrona, H. Widner, P. Brundin, J.C. Rothwell, R. Brown, B. Gustavii, P. Hagell, M. Jahanshahi, G. Sawle, A. Björklund, D.J. Brooks, C.D. Marsden, N.P. Quinn, O. Lindvall, Short- and long-term survival and function of unilateral intrastriatal dopaminergic grafts in Parkinson's disease, Ann. Neurol. 42 (1997) 95–107.

[44] A.J. Whitmarsh, S.-H. Yang, M.S.-S. Su, A.D. Sharrocks, R.J. Davis, Role of p38 and JNK mitogen-activated protein kinases in the activation of ternary complex factors, Mol. Cell. Biol. 17 (1997) 2360–2371.

[45] A.E. Willing, A.I. Othberg, S. Saporta, A. Anton, S. Sinibaldi, S.G. Poulos, D.F. Cameron, T.B. Freeman, P.R. Sanberg, Sertoli cells enhance the survival of co-transplanted dopamine neurons, Brain Res. 822 (1999) 246–250.

[46] W.M. Zawada, D.J. Zastrow, E.D. Clarkson, F.S. Adams, K.P. Bell, C.R. Freed, Growth factors improve immediate survival of embryonic dopamine neurons after transplantation into rats, Brain Res. 786 (1998) 96–103.

[47] Z. Xia, M. Dickens, J. Raingeaud, R.J. Davis, M.E. Greenberg, Opposing effects of ERK and JNK-p38 MAP kinases on apoptosis, Science 270 (1995) 1326–1331.

Experimental Neurology **168,** 183–191 (2001)
doi:10.1006/exnr.2000.7593, available online at http://www.idealibrary.com on IDEAL®

Appendix 4

IGF-I and bFGF Improve Dopamine Neuron Survival and Behavioral Outcome in Parkinsonian Rats Receiving Cultured Human Fetal Tissue Strands

Edward D. Clarkson,* W. Michael Zawada,†,‡,§ K. Pat Bell,‡ James E. Esplen,‡ Paul K. Choi,‡ Kim A. Heidenreich,§,¶,‖ and Curt R. Freed†,¶,‡,§,‖

*U.S. Army Medical Research Institute of Chemical Defense, 3100 Ricketts Point Road, MCMR-UV-DB, Aberdeen Proving Grounds, Maryland 21010-5400; †Department of Medicine, ¶Department of Pharmacology, ‡Division of Clinical Pharmacology, and §Neuroscience Program, University of Colorado School of Medicine, 4200 East Ninth Avenue, Denver, Colorado 80262; and ‖Denver Veterans Administration Medical Center, Denver, Colorado 80220

Received June 21, 1999; accepted October 13, 2000

To promote dopamine cell survival in human fetal tissue strands transplanted into immunosuppressed 6-OHDA-lesioned rats, we have preincubated tissue in insulin-like growth factor-I (IGF-I, 150 ng/ml) and basic fibroblast growth factor (bFGF, 15 ng/ml) *in vitro* for 2 weeks. Growth factor treatment did not affect the rate of homovanillic acid production *in vitro* but increased overall dopamine neuron survival in animals after transplant from 1240 ± 250 to 2380 ± 440 neurons ($P < 0.05$). Animals in the growth factor-treated group had a significantly greater reduction in methamphetamine-induced rotation (66%) compared to control transplants (30%, $P < 0.05$). We conclude that *in vitro* preincubation of human fetal tissue strands with IGF-I and bFGF improves dopamine cell survival and the behavioral outcome of transplants.

Key Words: **Parkinson's disease; human fetal tissue; 6-OHDA; transplantation; IGF-I; bFGF.**

INTRODUCTION

In Parkinson's disease, progressive deterioration of motor function results from the loss of nigrostriatal dopamine neurons and consequent dopamine depletion in the caudate and putamen (17). Among neurological disorders, Parkinson's disease is a prime candidate for a new strategy for treatment because drug therapy loses its effectiveness after 5 to 10 years. In 1979, Björklund and Stenevi (5) and Perlow *et al.* (43) demonstrated the potential benefits of mesencephalic grafts in parkinsonian rats. Since then, fetal tissue transplantation has been developed as a treatment for Parkinson's disease in humans (19–26, 32, 35, 59). Decisions about the appropriate age of human fetal donor tissue and its preparation have been based on extrapolation from the embryonic development of rodents as well as direct transplantation of human fetal tissue into parkinsonian rats (11, 26, 31, 49–52, 55–58).

A major problem with neurotransplantation is that up to 95% of embryonic dopamine neurons die after transplantation (7, 33). Since cells in transplants of embryonic mesencephalon have been shown to undergo apoptotic cell death *in vivo* (36, 62), we and others are examining possible uses of neurotrophic factors to reduce apoptosis (12, 13, 28, 37, 38, 47, 48, 61, 62). Two of the growth factors being examined are insulin-like growth factor-I (IGF-I) and basic fibroblast growth factor (bFGF) which improve dopamine neuron survival *in vitro* (30) and *in vivo* (53). We have recently shown that dopamine neuron survival can be improved by a 2-h preincubation of transplanted tissue with the growth factor combination of glial cell line-derived neurotrophic factor (GDNF), IGF-I and bFGF (62). We have also shown that a combination of IGF-I and bFGF reduces the rate at which dopamine neurons undergo apoptosis *in vitro* (61). The growth factors may be acting indirectly through stimulation of trophic factor production by astrocytes (18), since the neuroprotective effect can be blocked by inhibition of astrocyte proliferation with cytosine arabinoside (61). We have found that most dopamine cell death occurs in the first day to the first week after transplant (62). This result indicates that short-term induction of astrocytes by IGF-I and bFGF *in vivo* may be sufficient to protect transplanted dopamine neurons from programmed cell death.

To provide time for quality control of tissue prior to transplantation, we have developed methods for maintaining human embryonic cells in culture for extended periods of 1 to 4 weeks prior to transplant (20, 21). In a further effort to improve survival of cells after transplant, we have now tested whether long-term (14 day)

0014-4886/01 $35.00

in vitro incubation of human fetal tissue with the combination of IGF-I and bFGF will promote the subsequent survival of these cells after transplantation into hemiparkinsonian rats.

Currently in our laboratory, strands of human fetal tissue placed in tissue culture are tested for dopamine production by measuring the concentration of the dopamine metabolite homovanillic acid (HVA) in tissue culture supernatant. The *in vitro* storage method is also critical for accumulating a sufficient quantity of tissue for transplantation and for demonstrating that the tissue is not infected with bacteria, viruses, or fungi. The *in vitro* environment provides an opportunity to treat tissue with trophic factors in an effort to improve survival of cells following transplantation.

MATERIALS AND METHODS

Preparation of Fetal Tissue

Postmitotic embryonic dopamine cells from early in development, 13 to 15 days after conception in the rat and 45 to 55 days after conception in the human (40), are able to survive and develop when implanted in the adult Parkinsonian brain (9, 10, 33, 50). Only tissue from human embryos in this developmental range was used in this study.

Fetal tissue was obtained after elective abortion by standard clinical methods and with the use of sterile collection apparatus. Women donating tissue signed specific informed consent for experimental use of tissue. The consent and all collection methods complied with state and federal laws and were approved by the Colorado Combined Institutional Review Board. The rostral half of ventral mesencephalon containing dopamine cells was dissected as a block about 2 by 4 by 1 mm. This block was then cut in half down the midline to generate two identical pieces of mesencephalon. These pieces are referred to subsequently as a "matched pair." The tissue was washed in three petri dishes each containing ~20 ml of cold calcium- and magnesium-free Hanks' balanced salt solution (HBSS).

Tissues strands were created by extruding one half of a mesencephalon through a glass cannula with a luer adaptor at one end and a taper to a 0.2-mm bore at the other (14, 20, 21). These extruders were made by heating and drawing a commercially available blank (Kimble Kontes, Cat. No. 663500-0444, Vineland, NJ). Mesencephalic tissue was aspirated into the hub of a 1 ml tuberculin syringe in HBSS and then slowly ejected through the buffer-filled glass extruder. Care was taken to avoid excess pressure during extrusion, which could cause compression/decompression damage to the tissue. Strands were extruded into 4 ml culture medium in one well of a six-well plastic tissue culture plate (Corning Inc., Corning, NY). Medium was F12 containing 5% dialyzed human placental serum (heat inactivated at 55°C for 30 min), heparin (1 μg ml^{-1}) to bind bFGF (63), 2.2 μg ml^{-1} ascorbic acid, 10 μg ml^{-1} vancomycin (Eli Lilly & Co., Indianapolis, IN), 2 μg ml^{-1} gentamicin (Elkins-Sinn Inc., Cherry Hill, NJ), and 2 mM L-glutamine (Sigma, St. Louis, MO).

Human recombinant IGF-I (150 ng/ml; Cephalon Inc., Philadelphia, PA) and human recombinant bFGF (15 ng/ml; Scios Inc., Mountain View, CA) were added to the medium immediately after strands were placed in culture. Medium was changed at 3, 6, 9, 12, and 14 days after strands were placed in culture. This was done by removing and freezing 2 ml of medium for later HVA analysis and then adding 2 ml of fresh medium together with fresh IGF-I and bFGF.

High-Performance Liquid Chromatography (HPLC) Analysis

Testing for the content of HVA in tissue culture extracts used HPLC with electrochemical detection (Bioanalytical Systems) as previously described (3, 29). Separation was achieved on a Spherisorb ODSA microbore column (1 × 100 mm, Keystone Scientific) using a mobile phase containing, per liter, 13.7 ml phosphoric acid, 4.1 g trichloroacetic acid, 0.5 g sodium EDTA, 0.4 g octyl sodium sulfate, and 8% methanol (pH 3.0). Any detectable HVA in the medium blank was subtracted from each sample.

Unilateral 6-OHDA Injections

Male Sprague–Dawley rats (250–350 g) were anesthetized with equithesin (4 ml/kg) and placed in a stereotaxic frame. A 30-gauge cannula was then lowered into the medial forebrain bundle at the following coordinates: AP, −4.3 mm posterior to bregma; L, 1.5 mm from the midline; VD, −7.5 mm from the dura (42). Ten micrograms of 6-OHDA HBr (RBI, Natick, MA), dissolved in 5 μl sterile saline containing 0.2% ascorbate, was infused at 1 μl/min over 5 min (55). The cannula was left in place an additional 2 min with no infusion. Then the pump was started and the cannula was withdrawn while infusing saline. Lesions were tested behaviorally as noted below and confirmed histologically postmortem by the unilateral loss of TH-immunoreactive dopamine neurons in the substantia nigra.

Methamphetamine and Apomorphine-Induced Rotation

Two weeks after surgery, the completeness of the lesion was assessed by measuring turning behavior in response to methamphetamine HCl (5.0 mg/kg, ip, Sigma) and apomorphine (0.05 mg/kg, sc, Sigma) in a flat-bottomed rotometer. Methamphetamine circling was selected as the primary behavioral variable. Briefly, the rotometer consisted of a plexiglass cylinder

20 cm in diameter. The rat was tethered to a counter with a harness fastened around its chest. Rats that circled ipsilateral to the lesion more than 3.0 rpm during the period of 30 to 120 min after methamphetamine injection were used for transplantation and further rotational testing. Average ipsilateral rotation of animals chosen for the experiments was 8.3 rpm for controls and 7.2 rpm for IGF-I/bFGF-treated group. We have previously demonstrated (45) that in our methamphetamine-induced circling test performed in flat-bottomed Plexiglas cylinders, circling above 2 rpm correlates with >95% dopamine depletion. In contrast, Ungerstedt and Arbuthnott demonstrated that when methamphetamine-induced circling test is performed in hemispherical bowls instead of cylinders, higher circling rates (4–6 rpm) predict >95% dopamine depletion (55).

Circling after apomorphine was also addressed. Rats that showed apomorphine-induced turning contralateral to the lesion of greater than 3.0 rpm during the period of 0 to 30 min after injection were considered to be positive for an apomorphine effect and had apomorphine data collected. Average apomorphine-induced rotation of animals chosen for the experiments was 8.1 rpm for controls and 6.1 rpm for IGF-I/bFGF-treated group. Of the six pairs of rats that were positive for methamphetamine-induced rotation, only five pairs were positive for apomorphine-induced rotation. Methamphetamine- and apomorphine-induced turning was measured 4, 8, and 10.5 weeks after transplantation to test the behavioral effect of developing neural grafts. To prevent possible confounding of drug test effects, methamphetamine-induced turning was measured 48 h after apomorphine testing.

Transplantation of Embryonic Tissue

Recipient animals were anesthetized with equithesin (4 ml/kg). Three burr holes were made through the skull and a 20-gauge guide cannula supported by a motorized stereotaxic arm (Narishige, Tokyo) was used for transplantation. The cannula was lowered into the brain to 3.0 or 3.5 mm below the dura. Three transplant sites were required to accommodate all of the tissue present in one-half of a human mesencephalon. Transplant coordinates were: (i) AP 0.0 mm from bregma, L 2.0 mm from midline, VD −7.0 to −3.0 mm below dura; (ii) AP 0.0 mm from bregma, L 3.5 mm from midline, VD −7.5 to −3.5 mm below dura; and (iii) AP 1.0 mm anterior to bregma, L 3.5 mm from midline, VD −7.0 to −3.0 mm below dura. Animals were paired based on whether they received growth-factor-treated or nontreated tissue from the same human mesencephalon.

Matched pair tissue strands representing half-mesencephalons were removed from tissue culture, reextruded as described above, and then drawn up into a 24-gauge Stainless-steel transplantation cannula in a volume between 4 and 8 μl. The transplantation cannula (which protruded 4 mm beyond the guide) was then inserted through the guide cannula to a final depth of 7 or 7.5 mm below the dura. The tissue was ejected with the aid of a syringe pump over 4 min. For each transplant, the pump was switched on and allowed to run for 15 s and then the cannula was withdrawn at a rate of 1 mm/min with the pump running. At the top of the tract (after 4 min) the pump and guide cannula were stopped for 2 min to allow the pressure to equilibrate. Afterward, withdrawal was continued while about 4 μl of HBSS was pumped through the cannula. No sham transplants were done since in our previous work we found that shams had no improvement in amphetamine- (44) and methamphetamine-induced rotation (15, 60). All transplanted rats were immunosuppressed 24 h prior to transplantation with cyclosporine A (Sandimmune; 10 mg/kg; sc; Sandoz) and daily thereafter for the duration of the experiment.

Tyrosine Hydroxylase Immunohistochemistry

At 10.5 weeks after transplant, following behavioral testing, animals were killed by chloral hydrate overdose (2 g/kg, ip) and intracardially perfused with heparinized saline (30 units/ml) followed by 4% phosphate-buffered paraformaldehyde. The brains were postfixed for 2 days in the same fixative and cryoprotected in 30% sucrose. Forty-micrometer sections were cut on a freezing microtome, and each section was processed for TH immunohistochemistry.

The staining procedure supplied by the manufacturer was used. After blocking for 1 h with 10% goat serum, 1% BSA, and 0.3% Triton-X at 37°C, the slices were incubated in polyclonal, affinity-purified rabbit anti-rat TH antibody 1:200 (Pel-Freez, Rogers, AR) for 16 h at 37°C. Sections were then incubated with a secondary biotinylated, affinity-purified, goat anti-rabbit IgG antibody and subsequently with avidin/biotinylated horseradish peroxidase complex, each for 4 h at room temperature (Vector Lab, Burlingame, CA). The peroxidase was visualized with diaminobenzidine dissolved in PBS and 0.03% hydrogen peroxide.

Anatomical Analysis

The total number of dopamine neurons within the transplant tracts was estimated by counting all TH-positive cells in every third section from the area of the striatum-containing transplant. Sequential section stereological counting (16) was not possible since the 40-μm sections were collected six sections per single well of a 24-well plate and were thus randomized per well. For each animal, sections were collected in multiple wells and at least 16 sections from each transplant were examined for the presence of dopamine neurons. Abercrombie's correction (1) with an assumed

cell diameter of 20 μm was used to generate the final estimate of the number of surviving dopamine neurons in each animal. Work previously done in our laboratory has shown that treatment with a combination of IGF-I and bFGF does not affect transplanted dopamine neuron size (14). To assure that treatment with IGF-I and bFGF did not alter dopamine neuron cell size, which would render use of Abercrombie's correction inappropriate, one rat was selected from each transplant group for detailed neuron size analysis. The rat selected had closest to the median value of surviving dopamine neurons for each group. In each selected rat, images of all sections containing grafted cells were captured at ×400 magnification into SlideBook digital deconvolution software (Intelligent Imaging Innovations). The size of the soma for all dopamine neurons was determined using SlideBook's analysis tools. The total number of TH^+ somas measured was 197 for the control and 408 for the animal receiving IGF-I/bFGF treatment.

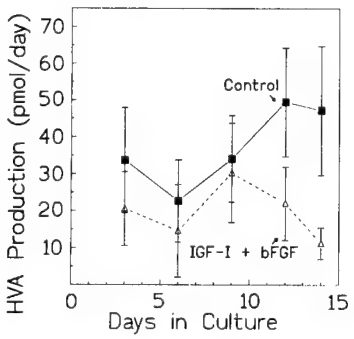

FIG. 1. Effects of growth factor treatment on HVA production in human fetal tissue. Matched pairs of mesencephalon strands were made by bisecting fragments of human fetal ventral mesencephalon, extruding through a 0.2-mm-diameter cannula, and treating for 2 weeks either with IGF-I (150 ng/ml) + bFGF (15 ng/ml) in F12 medium supplemented with 5% human placental serum (open triangles) or with F12 supplemented with serum alone (solid squares). Testing for the content of HVA in tissue culture extracts was done by HPLC with electrochemical detection (2, 32). All data represent the mean ± SEM (n = 6 pairs).

Statistical Analysis

The behavioral data were analyzed via SAS Procedures GLM and Mixed (SAS Institute, Cary, NC) using a mixed effects model appropriate for repeated measures data (34). This method accounts for variability between rats as well as between multiple measurements on the same rat. The TH^+ neuron survival and TH^+ neuron soma size data were analyzed using Student's t test and InStat statistical software (GraphPad, San Diego, CA).

RESULTS

Measurement of the stable dopamine metabolite HVA in the medium of cultured fetal strands provides evidence for ongoing production of dopamine in the tissue culture (Fig. 1). Levels of HVA production per day appeared to be lower in fetal strands treated with the combination of IGF-I and bFGF, though these differences did not reach statistical significance (n = 6, $P > 0.2$). The same trend was seen in cumulative HVA levels, with IGF-I/bFGF-treated strands producing a total of 320 ± 130 pmol after 14 days *in vitro* and untreated control strands producing 490 ± 130 pmol after 14 days *in vitro* (data not shown). This difference was not statistically significant.

Figure 2 shows that animals receiving growth-factor-treated human fetal mesencephalon had a significantly greater behavioral improvement than animals transplanted with human mesencephalon not treated with growth factors. Transplants of growth-factor-treated strands led to a significant reduction in methamphetamine-induced rotation at 10.5 weeks post-transplant when compared to control strands ($P < 0.05$; Fig. 2A). Growth-factor-treated strands appeared to cause a more rapid improvement in apomorphine circling when compared to control strands (Fig. 2B). However, these apparent differences did not reach statistical significance ($P > 0.05$). By 10.5 weeks, both groups had nearly stopped circling to apomorphine, indicating that enough human dopamine cells survived to eliminate apomorphine circling.

The number of surviving dopamine neurons in grafts of animals sacrificed 10.5 weeks after transplant is shown in Fig. 3A. Transplants of fetal tissue strands treated with the combination of IGF-I/bFGF had better dopamine neuron survival than untreated control grafts. In animals receiving one-half a human mesencephalon treated with growth factors, a total of 2380 ± 440 dopamine neurons survived (Fig. 3A). By contrast, animals receiving the non-growth-factor-treated half mesencephalon had only 1240 ± 250 surviving dopamine neurons ($P < 0.05$; Fig. 3A). Photomicrographs of representative sections from untreated and growth-factor-treated grafts are shown in Figs. 3B and 3C.

To assure that growth factor treatment did not alter dopamine neuron cell size, which would render use of Abercrombie's correction inappropriate, one rat was selected from each transplant group for detailed neuron size analysis. The rat selected had closest to the median value of surviving dopamine neurons for each group. Measurement of soma size of TH^+ neurons from images captured at ×400 magnification into SlideBook digital deconvolution software revealed that average area of TH^+ cell soma was not changed by the *ex vivo* growth factor treatment (Fig. 4A). Specifically, average area of TH^+ cell soma of control cells was 193 ± 3 μm^2 and 187 ± 2 μm^2 in tissue treated with IGF-I and bFGF. Photomicrographs of representative TH^+ cells in untreated and growth-factor-treated grafts are shown in Figs. 4B and 4C.

DISCUSSION

Our study demonstrates that treating individual fragments of human fetal ventral mesencephalon with a combination of IGF-I/bFGF for 2 weeks in tissue culture leads to better survival of dopamine neurons after transplant into immunosuppressed hemiparkinsonian rats. Previous work in our laboratory has shown that combinations of IGF-I and bFGF reduce the rate of apoptotic death in rat dopamine neurons *in vitro* (61), and pretreatment with a combination of GDNF, IGF-I, and bFGF improves cell survival after transplant (62). Cotransplantation of bFGF-expressing fibroblasts with rat mesencephalic dopamine neurons greatly enhanced survival of transplanted cells and accelerated behavioral recovery (53). We hypothesize that treatment of human fetal tissue with IGF-I/bFGF reduces the rate of apoptotic death that occurs while the strands are in culture. Because these growth factors appear to work indirectly by stimulating astrocyte proliferation and neurotrophic factor production (18, 53, 61), the ben-

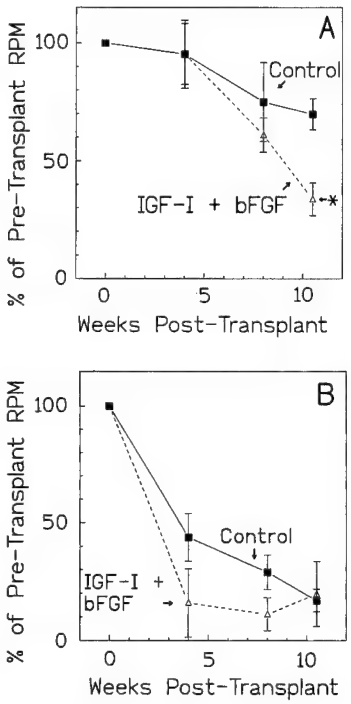

FIG. 2. Effects of transplanted human fetal tissue on behavioral deficits in 6-OHDA-lesioned rats. Matched pairs of mesencephalon strands were treated either with IGF-I + bFGF (open triangles) or with no growth factors (control, solid squares). Tissue was transplanted into striatum of 6-OHDA-lesioned rats. (A) rotational rate induced by methamphetamine (5 mg/kg, ip). Animals receiving growth-factor-treated strands had an improvement at 10.5 weeks posttransplant compared to controls. Asterisk represents statistical significance at $P < 0.05$ compared to controls using a mixed effects analyses of variance (29) ($n = 6$ pairs) and (B) rotational rate induced by apomorphine (0.05 mg/kg, sc). Animals receiving growth-factor-treated strands had their rotational rate induced by apomorphine measured at 4, 8, and 10.5 weeks after transplantation. Although the growth-factor-treated animals had a greater reduction in apomorphine-induced circling, this rate of reduction was not significantly greater when compared to controls.

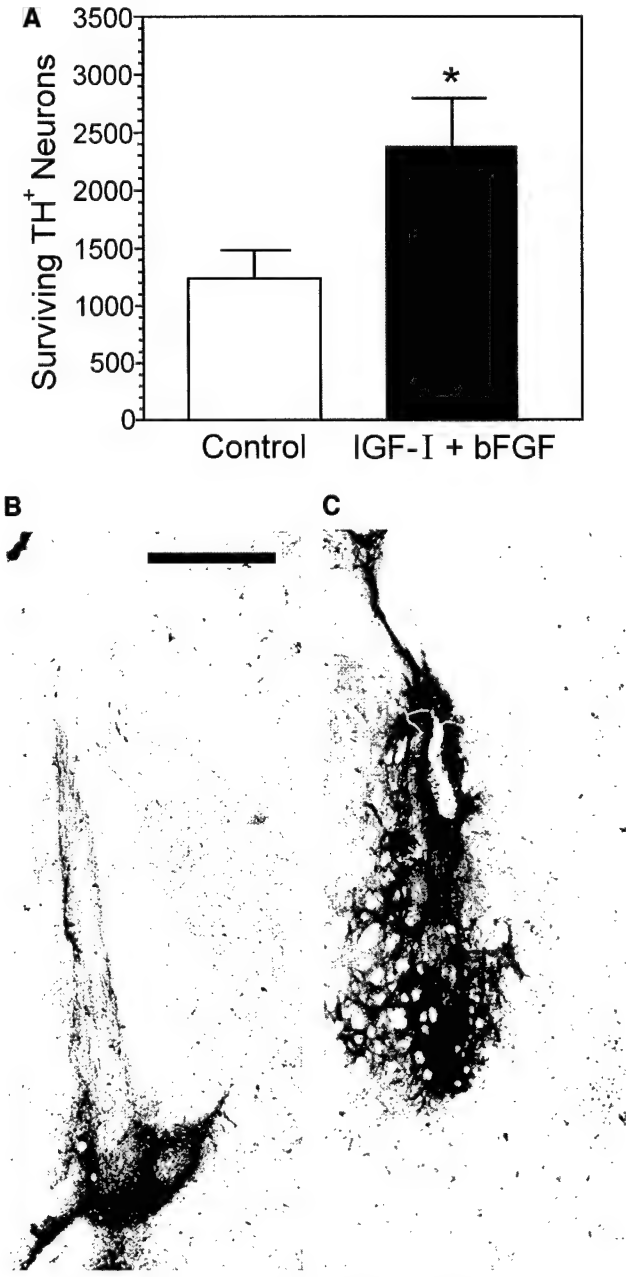

FIG. 3. Effects of treatment with IGF-I + bFGF on human dopamine neurons transplanted into 6-OHDA-lesioned rats. (A) Matched pairs of mesencephalon strands treated with IGF-I + bFGF (solid bar) and control tissue (open bar) were transplanted into 6-OHDA-lesioned rats. At 10.5 weeks posttransplant the rats were sacrificed, brain sections made at 40 μm, sections were stained for TH immunoreactivity, and all TH^+ neurons were counted. Estimates are for the whole brain using Abercrombie's correction (1). Data are presented as the mean ± SEM. Significance was shown by the Student's t test. Dopamine neuron survival was significantly enhanced by IGF-I and bFGF ($^*P < 0.05$, $n = 6$). (B) Micrograph showing TH^+ neurons in a representative control graft. (C) Micrograph showing TH^+ neurons in a representative graft treated with a combination of IGF-I and bFGF. Bar in B and C, 500 μm.

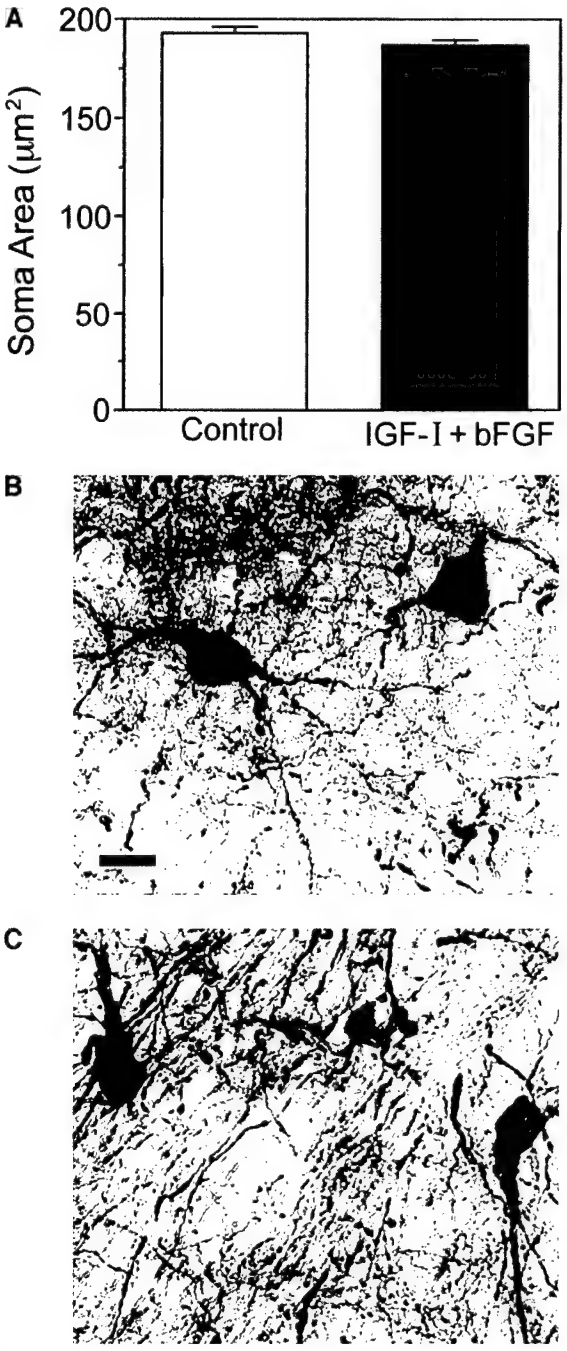

FIG. 4. Dopamine neuron cell size analysis. (A) Mean soma area of TH^+ neurons found in two different experimental groups 10.5 weeks after grafting. Student's *t* test confirmed that the IGF-I and bFGF treatment had no significant effect on the mean soma area of transplanted dopamine neurons. (B) Transplant of control ventral mesencephalic tissue showing TH^+ neurons. (C) Transplant of growth factor combination-treated tissue. Bar for B and C, 20 μm.

eficial effect of growth factor treatment may also carry over for a few days after transplantation.

In addition to antiapoptotic properties of some growth factors, treatment with inhibitors of specific proapoptotic pathways has proven to be neuroprotective (8). Specifically, 2-h preincubation of rat ventral mesencephalic cell suspension with a caspase inhibitor, Ac-YVAD-cmk, tripled survival of transplanted dopamine neurons (47). By contrast, transplantation of mouse ventral mesencephalon overexpressing the antiapoptotic protein Bcl-2 did not affect dopamine neuron survival, although fiber outgrowth was improved in such grafts (48). Other neuroprotective treatments attempt to reduce free radical damage to transplanted cells. An approach that has shown promise in protecting transplanted dopamine neurons has treated cell suspensions with antioxidants such as lazaroids (37, 41). The lazaroid trilazad mesylate improves survival of cultured human embryonic dopamine neurons (41). Another effective strategy is transplantation of mesencephalic tissue overexpressing Cu/Zn superoxide dismutase (38).

Storing dopamine neurons prior to transplantation is critically important for accumulation of enough specimens for a transplant operation and to test tissue for infection. To store dopamine neurons prior to transplantation, freshly dissected ventral mesencephalon can be placed in hibernation medium at 10°C for up to several days (46, 54). In our study, human embryonic brain tissue was stored at 10°C for up to several hours prior to dissection and was then placed in tissue culture for 2 weeks. We have found that dopamine cells in culture medium containing 5% human placental serum and a combination of IGF-I and bFGF have nearly 100% increased survival in transplants compared to cells cultured without growth factors. Others have shown that supplementation of hibernating cells with a combination of 8% human placental cord serum, GDNF and brain-derived neurotrophic factor improved TH-immunoreactive cell survival by 40% (54). Rat ventral mesencephalic tissue hibernated for 6 days in GDNF-containing medium enhanced 6-week survival of transplanted dopamine neurons by 30% (2). Cryopreservation would be desirable for long-term storage of cells. Unfortunately, cryopreservation methods lead to unacceptable losses of rat and human mesencephalic cells, regardless if the cells are cryopreserved as tissue fragments or cell suspension (46). Transplantation of cryopreserved human embryonic dopamine neurons reduced survival of dopamine neurons to only 9% of fresh tissue control grafts (27).

Since bFGF can expand the progenitor population for dopamine neurons in embryonic rat cultures (6), it is possible that the IGF-I/bFGF combination may lead to more surviving dopamine neurons by promoting progenitor cell division in human fetal tissue strands. The observed increase in dopamine neuron survival in animals receiving IGF-I/bFGF-treated fetal tissue correlates with the greater improvement in behavioral deficits seen in animals receiving growth-factor-treated fetal tissue compared to control tissue. Although treatment with the IGF-I/bFGF combination led to faster

recovery of methamphetamine-induced circling, complete behavioral recovery was not achieved due to the slow maturation of human dopamine grafts in the rat host (4, 50).

For the past 10 years, we have prepared embryonic tissue as strands for transplantation into patients with Parkinson's disease (20, 21). Since we have shown that treatment of these strands with the combination of IGF-I and bFGF can nearly double the survival of dopamine neurons in transplants as well as significantly improve behavioral effects of transplants, growth factor pretreatment may prove useful for improving dopamine neuron survival after transplantation in Parkinson's disease patients.

ACKNOWLEDGMENTS

The authors thank Dr. J. A. Abraham from Scios Inc., Mountain View, California, for providing bFGF and Dr. J. M. Farah from Cephalon Inc., West Chester, Pennsylvania, for providing IGF-I for these studies. This work was supported by USPHS R01 NS29982 and R01 NS18639; the General Clinical Research Centers Program National Centers for Research Resources, NIH (M01 RR00069); and The Program to End Parkinson's Disease (C.R.F.) and R01 NS38619 (K.A.H. and W.M.Z.).

REFERENCES

1. Abercrombie, M. 1946. Estimation of nuclear population from microtome sections. *Anat. Rec.* **94:** 239–247.
2. Apostolides, C., E. Sanford, M. Hong, and I. Mendez. 1998. Glial cell line-derived neurotrophic factor improves intrastriatal graft survival of stored dopaminergic cells. *Neuroscience* **83:** 363–372.
3. Amus, P. A., and C. R. Freed. 1979. Reversed-phase high-performance liquid chromatography of catecholamines and their congeners with simple acids as ion-pairing reagents. *J. Chromatogr.* **169:** 303–311.
4. Belkadi, A. M., C. Gény, S. Naimi, R. Jeny, M. Peschanki, and D. Riche. 1997. Maturation of fetal human neural xenografts in the adult rat brain. *Exp. Neurol.* **144:** 369–380.
5. Björklund, A., and U. Stenevi. 1979. Reconstruction of the nigrostriatal dopamine pathway by intracerebral nigral transplants. *Brain Res.* **177:** 555–560.
6. Bouvier, M. M., and C. Mytilineou. 1995. Basic fibroblast growth factor increases division and delays differentiation of dopamine precursors in vitro. *J. Neurosci.* **15:** 7141–7149.
7. Brundin, P., O. Isacson, and A. Björklund. 1985. Monitoring of cell viability in suspensions of embryonic CNS tissue and its use as a criterion for intracerebral graft survival. *Brain Res.* **331:** 251–259.
8. Brundin, P., J. Karlsson, M. Emgrad, G. S. Schierle, O. Hansson, A. Petersen, and R. F. Castilho. 2000. Improving the survival of grafted dopaminergic neurons: A review over current approaches. *Cell Transplant.* **9:** 179–195.
9. Brundin, P., O. G. Nilsson, R. E. Strecker, O. Lindvall, B. Asted, and A. Björklund. 1986. Behavioral effects of human fetal dopamine neurons grafted in a rat model of Parkinson's disease. *Exp. Brain Res.* **65:** 235–240.
10. Brundin, P., R. E. Strecker, H. Widner, D. J. Clarke, O. G. Nilsson, B. Astedt, O. Lindvall, and A. Björklund. 1988. Human fetal dopamine neurons grafted in a rat model of Parkinson's disease: Immunological aspects, spontaneous and drug-induced behavior, and dopamine release. *Exp. Brain Res.* **70:** 192–208.
11. Clarke, D. J., P. Brundin, R. E. Strecker, O. G. Nilsson, A. Björklund, and O. Lindvall. 1998. Human fetal dopamine neurons grafted in a rat model of Parkinson's disease: Ultrastructural evidence for synapse formation using tyrosine hydroxylase immunocytochemistry. *Exp. Brain Res.* **73:** 115–126.
12. Clarkson, E. D., W. M. Zawada, and C. R. Freed. 1995. GDNF reduces apoptosis in dopaminergic neurons *in vitro*. *NeuroReport* **7:** 145–149.
13. Clarkson, E. D., W. M. Zawada, and C. R. Freed. 1997. GDNF improves survival and reduces apoptotic cell death in human embryonic dopaminergic neurons *in vitro*. *Cell Tissue Res.* **289:** 207–210.
14. Clarkson, E. D., W. M. Zawada, F. S. Adams, P. K. Bell, and C. R. Freed. 1998. Embryonic mesencephalic tissue strands show greater dopamine neuron survival and better behavioral outcome than cell suspensions after transplantation in parkinsonian rats. *Brain Res.* **806:** 60–68.
15. Clarkson, E. D., F. G. La Rosa, J. Edwards-Prasad, D. A. Weiland, S. W. Witta, C. R. Freed, and K. N. Prasad. 1998. Improvement of neurological deficits in 6-hydroxydopamine-lesioned rats after transplantation with allogeneic simian virus 40 large tumor antigen gene-induced immortalized dopamine cells. *Proc. Natl. Acad. Sci. USA* **95:** 1265–1270.
16. Coggeshall, R. E., and H. A. Lekan. 1996. Methods for determining numbers of cells and synapses: A case for more uniform standards of review. *J. Comp. Neurol.* **364:** 6–15.
17. Ehringer, H., and O. Hornykiewicz. 1960. Verteilung von noradrenalin and dopamin (3-hydroxytyramin) im gehirn des menschen und ihr verhalten bei erkrankungen des extrapyramidalen systems. *Klin. Wochenschr.* **38:** 1236–1239.
18. Engele, J., and M. C. Bohn. 1991. The neurotrophic effects of fibroblast growth factors on dopaminergic neurons *in vitro* are mediated by mesencephalic glia. *J. Neurosci.* **11:** 3070–3078.
19. Freed, C. R., R. E. Breeze, N. L. Rosenberg, S. A. Schneck, T. H. Wells, J. N. Barrett, S. T. Grafton, S. C. Huang, D. Eidelberg, and D. A. Rotenberg. 1990. Transplantation of human fetal dopamine cells for Parkinson's disease: Results at 1 year. *Arch. Neurol.* **47:** 505–512.
20. Freed, C. R., R. E. Breeze, N. L. Rosenberg, S. A. Schneck, *et al.* 1991. Fetal neural implants for Parkinson's disease: Results at 15 months. In *Restorative Neurology, Intracerebral Transplantation in Movement Disorders,* Vol. 4, pp. 69–77. Elsevier, Amsterdam.
21. Freed, C. R., R. E. Breeze, N. L. Rosenberg, S. A. Schneck, E. Kriek, J. X. Qi, T. Lone, Y. B. Zhang, J. A. Snyder, T. H. Wells, L. O. Ramig, L. Thompson, J. C. Mazziotta, S. C. Huang, S. T. Grafton, D. Brooks, G. Sawle, G. Schroter, and A. A. Ansari. 1992. Survival of implanted fetal dopamine cells and neurologic improvement 12 to 46 months after transplant for Parkinson's disease. *N. Engl. J. Med.* **327:** 1549–1555.
22. Freed, C. R., R. E. Breeze, N. L. Rosenberg, and S. A. Schneck. 1992. Embryonic dopamine cell implants as a treatment for the second phase of Parkinson's disease: Replacing failed nerve terminals. In *Advances in Neurology* (H. Narabayashi, T. Nagatsu, N. Yanagisawa, and Y. Mizuno, Eds.), Vol. 60, pp. 721–728. Raven Press, New York.
23. Freed, C. R., R. E. Breeze, S. A. Schneck, R. A. E. Bakay, and A. A. Ansari. 1995. Fetal neural transplantation for Parkinson disease. In *Clinical Immunology: Principles and Practice* (R. R. Rich, Eds.), pp. 1677–1687. Mosby–Year Book, St. Louis, MO.
24. Freeman, T. B., M. S. Spence, B. D. Boss, D. H. Spector, R. E. Strecker, C. W. Olanow, and J. H. Kordower. 1991. Development of dopaminergic neurons in the human substantia nigra. *Exp. Neurol.* **113:** 344–353.

25. Freeman, T. B., C. W. Olanow, R. A. Hauser, G. M. Nauert, D. A. Smith, C. V. Borlongan, P. R. Sanberg, D. A. Holt, J. H. Kordower, F. J. G. Vingerhoets, B. J. Snow, D. Calne, and L. Gauger. 1995. Bilateral fetal nigral transplantation into the postcommissural putamen in Parkinson's disease. *Ann. Neurol.* **38:** 379–388.

26. Freeman, T. B., P. R. Sanberg, G. M. Nauert, C. V. Borlongan, E.-Z. Liu, B. D. Boss, D. Spector, C. W. Olanow, and J. H. Kordower. 1995. The influence of donor age on the survival of solid and suspension intraparenchymal human embryonic nigral grafts. *Cell Transplant.* **4:** 141–154.

27. Frodl, E. M., W. M. Duan, H. Sauer, A. Kupsch, and P. Brundin. 1994. Human embryonic neurons xenografted to the rat: Effects of cryopreservation and varying regional source of donor cells on transplant survival, morphology and function. *Brain Res.* **647:** 286–298.

28. Hefti, F. 1997. Neurotrophic factor therapy—Keeping score. *Nature Med.* **3:** 497–498.

29. Herregodts, P., and Y. Michotte. 1987. Combined ion-pair extraction and high-performance liquid chromatography for the determination of the biogenic amines and their major metabolites in single brain tissue samples. *J. Chromatogr.* **421:** 51–60.

30. Knusel, B., P. P. Michel, J. S. Schwaber, and F. Hefti. 1990. Selective and nonselective stimulation of central cholinergic and dopaminergic development *in vitro* by nerve growth factor, basic fibroblast growth factor, epidermal growth factor, insulin and insulin-like growth factors I and II. *J. Neurosci.* **10:** 558–570.

31. Kondoh, T., L. L. Pundt, and W. C. Low. 1995. Development of human fetal ventral mesencephalic grafts in rats with 6-OHDA lesions of the nigrostriatal pathway. *Neurosci. Res.* **21:** 223–233.

32. Kopyov, O. V., D. Jacques, A. Lieberman, C. M. Duma, and R. L. Rogers. 1996. Clinical study of fetal mesencephalic intracerebral transplants for the treatment of Parkinson's disease. *Cell Transplant.* **5:** 327–337.

33. Kordower, J. H., T. B. Freeman, B. J. Snow, F. J. G. Vingerhoets, E. J. Mufson, P. R. Sanberg, R. A. Hauser, D. A. Smith, M. Nauert, D. P. Perl, and C. W. Olanow. 1995. Neuropathological evidence of graft survival and striatal reinnervation after the transplantation of fetal mesencephalic tissue in a patient with Parkinson's disease. *N. Engl. J. Med.* **322:** 1118–1124.

34. Laird, N. M., and J. H. Ware. 1982. Random effects for longitudinal data. *Biometrics* **38:** 963–974.

35. Lindvall, O., P. Brundin, H. Widner, S. Rehncrona, B. Gustavii, R. Frackowiak, K. L. Leenders, G. Sawle, J. C. Rothwell, C. D. Marsden, and A. Björklund. 1990. Grafts of fetal dopamine neurons survive and improve motor function in Parkinson's disease. *Science* **247:** 574–577.

36. Mahalik, T. J., W. E. Hahn, G. H. Clayton, and G. P. Owens. 1994. Programmed cell death in developing grafts of fetal substantia nigra. *Exp. Neurol.* **129:** 27–36.

37. Nakao, N., E. M. Frodl, W.-M. Duan, H. Widner, and P. Brundin. 1994. Lazaroids improve the survival of grafted rat embryonic dopamine neurons. *Proc. Natl. Acad. Sci. USA* **91:** 12408–12412.

38. Nakao, N., E. M. Frodl, H. Widner, E. Carlson, F. A. Eggerding, C. J. Epstein, and P. Brundin. 1995. Overexpressing Cu/Zu superoxide dismutase enhances survival of transplanted neurons in a rat model of Parkinson's disease. *Nature Med.* **1:** 226–231.

39. Olanow, C. W., J. H. Kordower, and T. B. Freeman. 1996. Fetal nigral transplantation as a therapy for Parkinson's disease. *Trends Neurosci.* **19:** 102–109.

40. O'Rahilly, R., and F. Muller. 1987. *Developmental Stages in Human Embryos,* Carnegie Institution of Washington publication 637. Meriden-Stinehour Press, Meriden, CT.

41. Othberg, A., M. Keep, P. Brundin, and O. Lindvall. 1997. Trilazad mesylate improves survival of rat and human embryonic mesencephalic neurons *in vitro. Exp. Neurol.* **147:** 498–502.

42. Paxinos, G., and C. Watson. 1986. *The Rat Brain in Stereotaxic Coordinates.* Academic Press, New York.

43. Perlow, M. J., W. J. Freed, B. J. Hoffer, A. Seiger, L. Olson, and R. J. Wyatt. 1979. Brain grafts reduce motor abnormalities produced by destruction of nigrostriatal dopamine system. *Science* **204:** 643–647.

44. Richards, J. B., K. E. Sabol, and C. R. Freed. 1990 Unilateral dopamine depletion causes bilateral deficits in conditioned rotation in rats. *Pharmacol. Biochem. Behav.* **36:** 217–223.

45. Richards, J. B., K. E. Sabol, E. H. Kriek, and C. R. Freed. 1993. Trained and amphetamine-induced circling behavior in lesioned, transplanted rats. *J. Neural Transm. Plast.* **4:** 157–166.

46. Sauer, H. 2000. Pregraft tissue storage methods for intracerebral transplantation. In *Neuromethods: Neural Transplantation Methods* (S. B. Dunnet, A. A. Boulton, and G. B. Baker, Eds.), Vol. 36, pp. 27–40. Humana Press, Totowa, NJ.

47. Schierle, G. S., O. Hansson, M. Leist, P. Nicotera, H. Widner, and P. Brundin. 1999. Caspase inhibition reduces apoptosis and increases survival of nigral transplants. *Nature Med.* **5:** 97–100.

48. Schierle, G. S., M. Leist, J. C. Martinou, H. Widner, P. Nicotera, and P. Brundin. 1999. Differential effects of Bcl-2 overexpression on fibre outgrowth and survival of embryonic dopaminergic neurons in intracerebral transplants. *Eur. J. Neurosci.* **11:** 3073–3081.

49. Spenger, C., N. S. Haque, L. Studer, L. Evtouchenko, B. Wagner, B. Buhler, U. Lendahl, and R. W. Seiler. 1996. Fetal ventral mesencephalon of human and rat origin maintained in vitro and transplanted to 6-hydroxydopamine-lesioned rats gives raise to grafts rich in dopaminergic neurons. *Exp. Brain Res.* **112:** 47–57.

50. Strömberg, I., M. Bygdeman, M. Goldstein, A. Seiger, and L. Olson. 1986. Human fetal substantia nigra grafted to the dopamine-denervated striatum of immunosuppressed rats: Evidence for functional reinnervation. *Neurosci. Lett.* **71:** 271–276.

51. Strömberg, I., P. Almqvist, M. Bygdeman, T. E. Finger, G. Gerhardt, A. C. Granholm, T. J. Mahalik, A. Seiger, B. Hoffer, and L. Olson. 1988. Intracerebral xenografts of human mesencephalic tissue into athymic rats: Immunochemical and *in vivo* electrochemical studies. *Proc. Natl. Acad. Sci. USA* **85:** 8331–8334.

52. Strömberg, I., M. Bygdeman, M. Goldstein, A. Seiger, and L. Olson. 1988. Human fetal substantia nigra grafted to the dopamine-denervated striatum of immunosuppressed rats: Evidence for functional reinnervation. *Neurosci. Lett.* **71:** 271–276.

53. Takayama, H., J. Ray, H. K. Raymon, A. Baird, L. J. Fisher, and F. H. Gage. 1995. Basic fibroblast growth factor increases dopaminergic graft survival and function in a rat model of Parkinson's disease. *Nature Med.* **1:** 53–58.

54. Thajeb, P., Z. D. Ling, E. D. Potter, and P. M. Carvey. 1997. The effects of storage conditions and trophic supplementation on the survival of fetal mesencephalic cells. *Cell Transplant.* **6:** 297–307.

55. Ungerstedt, U., and G. W. Arbuthnott. 1970 Quantitative recording of rotational behavior in rats after 6-hydroxydopamine lesions of the nigrostriatal dopamine system. *Brain Res.* **24:** 485–490.

56. Van Horne, C. G., T. Mahalik, B. Hoffer, M. Bygdeman, P. Almqvist, P. Stieg, A. Seiger, L. Olson, and I. Strömberg. 1990 Behavioral and electrophysiological correlates of human mesencephalic dopaminergic xenograft function in the rat striatum. *Brain Res. Bull.* **25:** 325–334.

57. Walters, A. M., D. J. Clarke, H. F. Bradford, and G. H. Stern. 1992. The properties of cultured fetal human and rat brain tissue and its use as grafts for the relief of the parkinsonian syndrome. *Neurochem. Res.* **17:** 893–900.

58. Wang, Y., J. C. Lin, A. L. Chiou, J. Y. Liu, and F. C. Zhou. 1995. Human ventromesencephalic grafts restore dopamine release and clearance in hemiparkinsonian rats. *Exp. Neurol.* **136:** 98–106.

59. Widner, H., J. Tetrud, S. Rehncrona, B. Snow, P. Brundin, B. Gustavii, and J. W. Langston. 1992. Bilateral fetal mesencephalic grafting in two patients with Parkinsonism induced by 1-methyl-4-phenyl-1,2,3,6-tetrahydropyridine (MPTP). *N. Engl. J. Med.* **327:** 1556–1563.

60. Zawada, W. M., J. B. Cibelli, P. K. Choi, E. D. Clarkson, P. J. Golueke, S. E. Witta, K. P. Bell, J. Kane, A. P. Ponce de Leon, D. J. Jerry, J. M. Robl, C. R. Freed, and S. L. Stice. 1998. Somatic cell cloned transgenic bovine neurons for transplantation in parkinsonian rats. *Nature Med.* **4:** 569–574.

61. Zawada, W. M., D. L. Kirschman, J. J. Cohen, K. A. Heidenreich, and C. R. Freed. 1996. Growth factors rescue embryonic dopamine neurons from programmed cell death. *Exp. Neurol.* **140:** 60–67.

62. Zawada, W. M., D. J. Zastrow, E. D. Clarkson, F. S. Adams, K. P. Bell, and C. R. Freed. 1998. Growth factors improve immediate survival of embryonic dopamine neurons after transplantation into rats. *Brain Res.* **786:** 96–103.

63. Yayon, A., M. Klagsbrun, J. D. Esko, P. Leder, and D. M. Ornitz. 1991. Cell surface, heparin-like molecules are required for binding of basic fibroblast growth factor to its affinity receptor. *Cell* **64:** 841–848.

Appendix 5

SOCIETY FOR NEUROSCIENCE

SFN Support Team
1.888.348.2065
Click here for support
Forgot your ID numbe

Abstract Proof

Edit Menu (Click on these to edit the data in your abstract.)

Contact Info
Details
Themes and Topics
Institutions
Authors
Image Upload
Title
Key Words
Body
Disclaimers
Back to Menu

To see a sample of what your abstract will look like, click here.

- Total characters left: **0**
- When you are satisfied that all the information below is complete and accurate, you may press the Save Abstract button to save your abstract so that you may return and continue editing it at a later time. Remember that you must submit by the deadline for your abstract to be considered.
- If you are ready to submit your abstract, you may press the Submit Abstract butto to view the submission payment screen and enter your credit card information. You must pay the submission fee for your abstract to be considered.
- Submission of this abstract is final, like putting a paper abstract into the mailbox. Once you have submitted and paid for your abstract, you will not be able to revise it without submitting a replacement abstract and paying the replacement abstract fee of $50.00 USD.
- If you are going to submit this abstract, be sure to print this page for your records.
- After you have submitted your abstract, and received your control number, you must contact the SFN Program Department if you wish to have your abstract withdrawn.

Contact Info	Daniel Allan Linseman Denver VAMC 111H Denver CO 80220 USA Phone: 303-399-8020 5264 Fax: 303-393-5271 Dan.Linseman@UCHSC.edu
Date/Time Last Modified:	04/20/2001 at 12:30 am
Presentation Type:	Slide/Poster
Theme 1:	Neurological and Psychiatric Conditions
Subtheme 1:	Neurotoxicity
Topic 1:	Apoptosis
Abstract Title:	CONVERGENCE OF GSK-3BETA AND C-JUN SIGNALING IS REQUIRED DURING APOPTOSIS OF CEREBELLAR GRANULE NEURONS
Contributing Authors:	D.A. Linseman[1,2]; M. Li[1,2]; M.K. Meintzer[1,2]; T. Laessig[1,2]; K.A. Heidenreich

Authors: Heidenreich[1,2]

Institutions:

1. Pharmacology, University of Colorado Health Sciences Center, Denver, CO, USA

2. Research, Denver Veterans Affairs Medical Center, Denver, CO, USA

Key words: TRANSCRIPTION FACTOR, CASPASE, INSULIN, CELL DEATH

Abstract:

Primary rat cerebellar granule neurons (CGNs) require serum and depolarizing K+ for survival. Serum mimics growth factor survival signaling via a PI3K-mediated activation of AKT. Depolarization induces Ca2+ influx that promotes DNA binding of the pro-survival transcription factor MEF2D. Here, we examined if individual pro-apoptotic proteins act in concert to induce apoptosis of CGNs durin trophic factor withdrawal. Removal of serum elicited activation of glycogen synthase kinase-3beta (GSK-3beta). Whereas, lowering extracellular K+ induced phosphorylation of c-Jun. In CGNs deprived of both serum and K+, incubation with IGF-I selectively attenuated GSK-3beta activation without affecting c-Jun phosphorylation. In contrast, the p38/JNK inhibitor, SB203580, selectively blocked c-Jun phosphorylation but had no effect on GSK 3beta activation. Selective blockade of either pathway with IGF-I or SB203580 during trophic factor withdrawal suppressed caspase-3 activation and caspase-mediated degradation of MEF2D, suggestin that both GSK-3beta and c-Jun signals are required for apoptosis. Moreover, inclusion of either IGF-I or SB203580 during acute trophic factor withdrawal markedly enhanced recovery of MEF2D transcriptional activity achieved by re-addition of serum and K+. The results suggest that pro-apoptotic signals from GSK-3beta and c-Jun act in a coordinated fashion to promote CGN death by converging upstream of caspase-3 activation and MEF2D degradation in the apoptotic cascade.

Supported by: Department of Veterans Affairs Merit Award and Research Enhancement Award Program